Tapered Spiral Welding for US Offshore Wind Towers Project Summary Report

Draft Report – Deliverable 25.1

Prepared for:

New York State Energy Research and Development Authority

Albany, New York

Kori Groenveld
Program Manager; National Offshore Wind Research & Development Consortium

Prepared by:

Keystone Tower Systems

Denver, Colorado

Ed Whitnell
Chief Executive Officer; Keystone Tower Systems

Eric Sells
Senior Engineer, Offshore Programs; Keystone Tower Systems

NYSERDA Contract 116-165427 October 2025

Notice

This report was prepared by Eric Sells in the course of performing work contracted for and sponsored by the New York State Energy Research and Development Authority (hereafter "NYSERDA"). The opinions expressed in this report do not necessarily reflect those of NYSERDA or the State of New York, and reference to any specific product, service, process, or method does not constitute an implied or expressed recommendation or endorsement of it. Further, NYSERDA, the State of New York, and the contractor make no warranties or representations, expressed or implied, as to the fitness for particular purpose or merchantability of any product, apparatus, or service, or the usefulness, completeness, or accuracy of any processes, methods, or other information contained, described, disclosed, or referred to in this report. NYSERDA, the State of New York, and the contractor make no representation that the use of any product, apparatus, process, method, or other information will not infringe privately owned rights and will assume no liability for any loss, injury, or damage resulting from, or occurring in connection with, the use of information contained, described, disclosed, or referred to in this report.

NYSERDA makes every effort to provide accurate information about copyright owners and related matters in the reports we publish. Contractors are responsible for determining and satisfying copyright or other use restrictions regarding the content of reports that they write, in compliance with NYSERDA's policies and federal law. If you are the copyright owner and believe a NYSERDA report has not properly attributed your work to you or has used it without permission, please email print@nyserda.ny.gov

Information contained in this document, such as web page addresses, are current at the time of publication.

Table of Contents

List of Figures

List of Tables

1 Summary

This report is Keystone Tower Systems' comprehensive final report on the development, testing, and optimization of spiral-welded offshore wind tower. Key findings from the report are presented here. The report outlines coordinated efforts with partners including GE Vernova, Northeastern University, Johns Hopkins University, Edison Welding Institute (EWI), and BVG Associates. The work demonstrates Keystone's spiral-welded shell design capabilities (both tower and monopile), advancements in scalable manufacturing (whether multi-wrap or single-wrap), improvements in knowledge of multi-layers buckling and fatigue, advanced welding techniques with particular attention to Hybrid Laser Arc Welding (HLAW) and economic modelling for next-generation wind towers and monopiles.

Key activities and findings include:

1. Basic shell design:
    a. Collaboration with GE Vernova focused on the 12MW Haliade-X turbine platform
    b. Scaling designs up to 18MW
    c. Create monopile designs for 18MW contemporary and XXXL future designs
2. Tower Design Optimization:
    a. Consider multiple configurations – drop-in replacements, two-section minimum air clearance, single-section towers
    b. Optimize design with improved manufacturing Tolerance Quality Class
    c. Optimize tower – spiral-mill – factory with wide feedstock material
3. Multi-Wrap Innovation:
    a. Introduced layered shell structures using thinner materials to reduce bending forces and improve weld efficiency
    b. Conduct fundamental research in buckling and fatigue:
        i. Buckling models predicted critical buckling loads of multi-layered shells could achieve parity with monolithic shells.
        ii. Physical tests corroborated model predictions – there was no statistically significant difference between fully bonded test specimen and monolithic (single-wall) specimen.
        iii. Fatigue testing similarly showed multi-layer samples to exhibit behavior consistent with monolithic samples with identical surface detail categories
    c. Costs for multi-wrap towers showed minor savings with modest throughput loss when restricted to SAW for crosswelds
    d. Throughput losses were significant when permitting tower optimization for HLAW crosswelds
        i. This indicated the need for tower – spiral-mill – factory optimization

        ii. With HLAW, costs were near parity (<2% difference), but throughput was increased 170%.
4. Monopile Development:
    a. Multi-wrap designs were applied to monopile foundations up to 71.1 mm thick.
    b. HLAW welding improved fabrication throughput by 27% with <1% cost increase and reduced bending forces nearly fourfold
5. Hybrid Laser Arc Welding (HLAW):
    a. EWI developed procedures for 25mm plate joints combining GMAW and laser welding. Results met ASTM D1.1 standards for static loading
    b. Mechanical testing of welds were successful. The welds offered low hardness and high energy absorption and ductility
    c. HLAW cuts weld times dramatically, enabling 40mm welds in the same time of a single SAW pass using Keystone's current weld technology
6. Factory Design:
    a. Keystone presented an integrated factory economic model
    b. Keystone refined a robust throughput Model.
        i. Mass-flow models revealed HLAW achieves 80–220% higher productivity compared to optimized SAW welding for 24–44mm plate thicknesses
        ii. Wider (3.0m) feedstock further boosts efficiency
        iii. A drop in productivity for thicknesses 26-32mm was observed when using multi-wrap coil feedstock
    c. Keystone factory economics indicate:
        i. Up to 47% smaller factory footprint
        ii. Up to 55% lower staffing needs than traditional can-tower manufacturing
        iii. Resulting in up to 25% fabrication cost reduction – LCOE savings estimated at $0.62–$0.67/MWh (~1% total project savings)
7. Single-Section Towers:
    a. Potential savings of $12,500/MW by eliminating flanges and reducing crane picks for simplified installation
    b. Feasibility in the U.S. remains limited by Jones Act vessel constraints and port infrastructure

Each of these findings are discussed in significant detail in the following chapters.

2 Keystone Spiral-Welded Design Capabilities

This report section documents the coordinated design effort between Keystone Tower Systems and GE Vernova to advance offshore wind tower concepts for large turbines. The collaboration focused on the GE Haliade-X 12MW turbine platform. Keystone expanded the design investigations into larger monopiles, scaled up to 18MW turbine systems

The initial tower design phase centered on producing reference towers that adhered to GE's load data and geometry, meeting the structural demands of the Haliade-X platform. Variants explored configurations ranging from spiral-welded direct replacements of three-section traditional can towers to one- and two-section spiral-welded towers. Structural evaluations considered fatigue and buckling per EN 1993 standards, with buckling as the primary design constraint.

Multi-wrap tower designs are introduced, in which multiple thin steel layers replace a single thick plate. This approach offers notable advantages: (1) reduced bending forces, (2) improved weld efficiency, and (3) access to a large untapped steel supply chains using hot-rolled coil feedstock. Comparative cost analyses showed that two-layer towers can slightly reduce unit cost but lower throughput, while three-layer towers of the 12MW scale were inefficient.

The multi-wrap concept was also extended to offshore monopiles, where very thick shell sections make traditional single-wrap fabrication impractical. Using 3.0-m-wide plate feedstock, Keystone analyzed both single- and double-layer monopiles up to 71.1 mm equivalent wall thickness. Advanced welding techniques—particularly hybrid laser arc welding (HLAW)—proved transformative, cutting effective weld times dramatically. Modeling results showed that two-layer multi-wrap monopiles improved throughput by about 27% with minimal cost increase (<1%), while also lowering required bending forces by nearly fourfold.

These studies demonstrate that the relatively thin shell of the 12MW reference tower is best fabricated in a single-wrap whereas a higher duty 18MW monopile benefits from multi-wrap fabrication. Later sections of this report will better clarify when single-layer or multi-layer designs are preferable.

Overall, the study demonstrates that multi-wrap designs, combined with emerging weld technologies, can unlock scalable manufacturing of next-generation offshore towers and monopiles. The findings

underscore the importance of integrated design with manufacturing optimization to balance cost, efficiency, and material utilization across the full production system.

2.1 Tower Design

The following sub-sections of this report describe the coordination between GE and Keystone Tower Systems to design suitable offshore wind tower variants for GE's Haliade-X 12MW rated turbine platform. GE provided load sets and their traditional can tower design for a proposed wind farm off the North Atlantic coastline. Keystone utilized these input files, industry design codes, and Keystone's proprietary in-house design tool to quickly generate design alternatives. Keystone's design alternatives consider potential project constraints such as logistics for minimum height 2-section towers or single-section towers to maximize factory throughput and minimize overall tower costs.

2.1.1 Tower Design Considerations

Keystone collaborated with OEM partner GE to generate offshore wind design reference towers. The turbine used for these tower designs was the GE Haliade-X turbine, capable of 12, 13, and 14MW configurations. The rotor diameter is 220m (722ft) and has a nominal head mass of 800t (880tn). Design particulars used in this project are conveyed in Table 1.

Table 1. Turbine Design Particulars

Property	Design Value
Power Rating, MW	12
Nominal Head Mass, t (tn)	800 (880)
Hub Height (tower base), m (ft)	116.7 (382.8)
Turbine Interface Diameter, m (ft)	5.70 (18.7)
Tower Base Diameter, m (ft)	7.93 (26.0)
Blade-Passing Diameter, m (ft)	7.93 (26.0)
Excluded Frequencies[a], Hz	Not repeated here.

[a] Tower harmonic frequencies are excluded from bands of frequencies corresponding to blades passing the tower structure.

The turbine described in Table 1 is subject to environmental loads, as defined by IEC 61400-1[1] and IEC 61400-3[2]. GE has a proprietary controls loop to modify the turbine geometry, such as yaw or blade

[1] International Electrotechnical Commission (IEC). 2019. "IEC 61400-1: Wind energy generation systems – Part 1: Design requirements. 5th edition," Geneva: IEC.

[2] International Electrotechnical Commission (IEC). 2019. "IEC 61400-3-1: Wind energy generation systems – Part 3-1: Design requirements for fixed offshore wind turbines. 1st edition," Geneva: IEC.

angle of attack, as the environment changes. The environmental loads, combined with the simulations of the controls loop, yields a set of loads that are transmitted from the turbine, through the tower, to the foundation (whether onshore or offshore) and ultimately reacted and distributed through the earth. GE shared indicative loads for the Haliade-X 12MW turbine with Keystone for this tower design exercise.

Other design data include shell material comprised of EN 10025-2 S355, a structural steel with a Specified Minimum Yield Strength (SMYS) of 355MPa at 0.2% strain offset. The steel is approximate equivalent to Imperial Grade-50 (50ksi) steels available in North America. Design details provided by GE, which were undisclosed to protect commercial interests, included (1) intermediate flange geometries, (2) location and design details of internal equipment attachments, (3) stress concentration, load, and resistance factors, (4) misalignment and tower tilt magnitudes, and (5) door region design details.

The loads and gross geometry requirements shared in Table 1 were combined to evaluate the tower for fatigue and buckling resistance. Buckling and fatigue were evaluated according to European Standards EN 1993-1-6[3] and EN 1993-1-9[4], respectively. For the subject tower design and planned deployment location, the tower was totally governed by buckling considerations.

2.1.2 Tower Variants

Several design limits were considered when proposing tower variants. The starting point was GE's design of a (base case) 3-section tower fabricated from plate on a traditional can grow line; this tower is depicted as Figure 1(a). Keystone's proposed variants and their key features are shared in Table 2 and depicted in Figure 1 and Figure 2.

[3] European Committee for Standardization (CEN). 2007. "EN 1993-1-6: Eurocode 3 – Design of steel structures – Part 1-6: Strength and stability of shell structures, incorporating Amendment A1:2017," Brussels: CEN.

[4] European Committee for Standardization (CEN). 2005. "EN 1993-1-9: Eurocode 3 – Design of steel structures – Part 1-9: Fatigue, incorporating Amendment A1:2017," Brussels: CEN.

Table 2. Turbine Design Particulars

Variant	Depiction	Purpose	Benefit
3-section TQC-B	Figure 1 (b)	Drop-in Replacement	Interchangeable with can Suppliers
2-section TQC-B	Figure 1 (c)	Blade Clearance	Maintain blade tip clearance requirement
2-section TQC-B	Figure 1 (d)	Minimum Height	Consider US logistics obstacles
1-section TQC-B	Figure 1 (e)	Single-Section	Maximize productivity on spiral-mill
3-section TQC-A	Figure 2 (a)	Drop-in Replacement	Save mass & Interchangeable
2-section TQC-A	Figure 2 (b)	Blade Clearance	Save mass & Maintain blade tip clearance
2-section TQC-A	Figure 2 (c)	Minimum Height	Save mass & Consider US logistics obstacles

Figure 1. 12MW Reference Towers – Standard Design

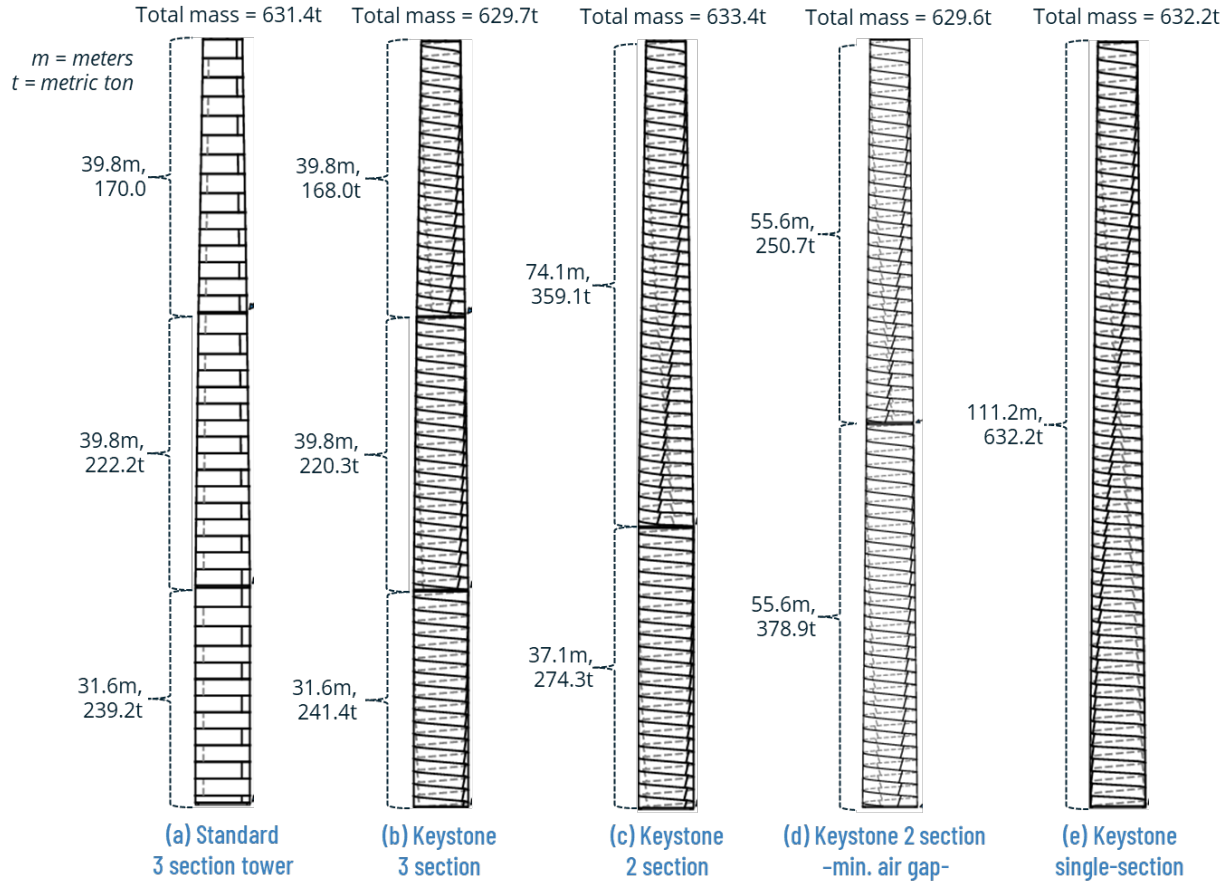

Figure 2. 12MW Reference Towers – Aggressive Design

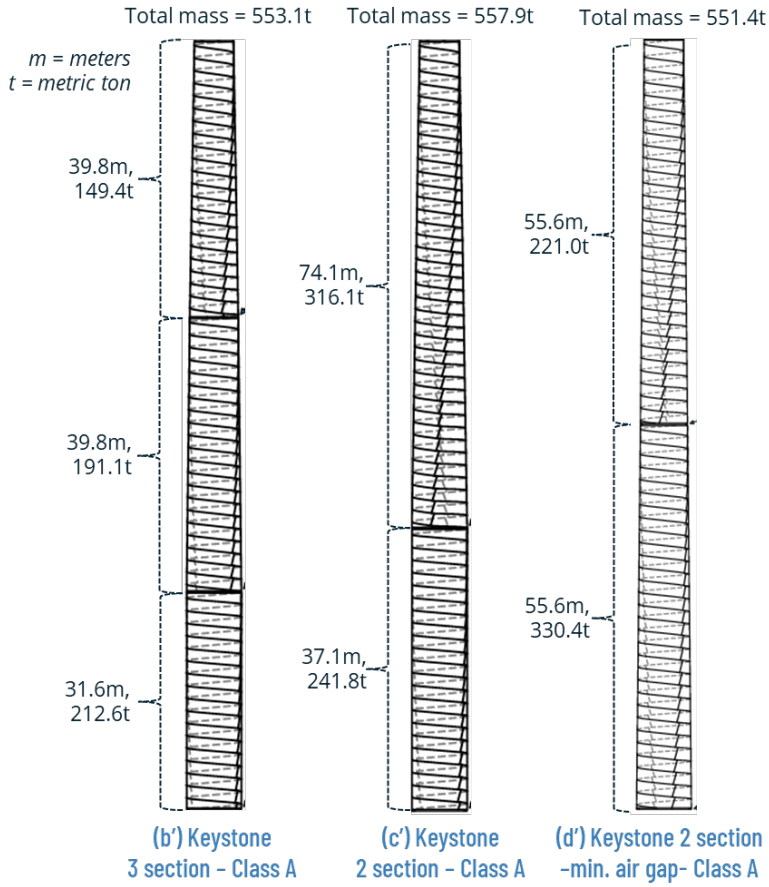

2.2 Multi-wrap Tower Design

An additional round of tower design effort was intended to focus on the evaluation of multi-wrap wind turbine towers as an alternative to traditional single-wrap towers. The study ultimately proceeded in two tracks. The first track developed towers optimized for monolithic steel plate feedstock, or "single-wrap" geometry. The second track investigated the "multi-wrap" tower concept.

Key advantages of the multi-wrap approach are (1) a maximum bend force is dictated by the maximum thickness material passing through the mill which can be limited by increasing layer count, (2) a linear relationship arises between wall thickness and weld passes: doubling thickness only requires doubling the number of weld passes, not a squared increase (4times), and (3) opening alternative feedstock supply chains such as cheaper HRC instead of plate steel.

Bills of Material (BoMs) paired with a new sub-arc weld (SAW) timing model revealed that while multi-wrap feedstock increases weld velocity, it also adds mill start-stops, lowering overall efficiency. Comparative cost analyses showed:

1. Single-wrap with plate (baseline): 100% throughput, 100% relative cost.
2. Two-layer coil multi-wrap: 84.7% throughput, 97.7% relative cost.
3. Three-layer coil multi-wrap: 58.6% throughput, 115.7% relative cost.

These results demonstrate trade-offs. Two-layer towers reduce fabrication costs but lower annual output. Three-layer towers increase costs and lower throughput and were clearly inefficient at the 12 MW reference scale.

A separate analysis demonstrated success with wider single-wrap feedstock plates (3.0 m vs. 1.8 m). Overall, Task 18 highlights that no universal preference exists between single-wrap and multi-wrap designs. Optimal solutions depend on the combined tower–spiral-mill–factory system analysis, balancing throughput with per-tower cost. This underscores the need for integrated design and manufacturing optimization in scaling future offshore wind turbine towers.

2.2.1 Additional Tower Variants

This project proceeded along two parallel tracks. In the first track, Keystone and OEM partner GE designed traditional single-layer (***single-wrap***) type wind turbine towers where the entire wall thickness is from a single monolithic steel plate. Several single-wrap tower variants were just shared in Section 2.1.1. The single-wrap reference tower(s) were analyzed by Northeastern University, Johns Hopkins University, and by Keystone for their buckling and fatigue resistance, manufacturability, handling and logistics insights, and for building baseline quayside factory throughput and economic models.

In the second track, Keystone continued collaborating with Northeastern and Johns Hopkins Universities to investigate fatigue and buckling resistance models and test results for ***multi-wrap*** towers. Different methods for bonding the layers were investigated physically and mathematically. Subsequent sections of this report (Sections 4.2through 4.4) indicate promising buckling and fatigue results and will be explored in more detail. The second track multi-wrap approach needs reference tower designs to also evaluate the throughput and economics of a multi-wrap spiral-welded quayside tower factory.

The promise of the multi-wrap concept is to make the relationship of shell thickness to the number of weld passes linear. For a doubling of a multi-wrap shell thickness, the number of wraps is doubled and the number of passes per wrap are held constant. The result is a 1:1 ratio of layer count and the total number of weld passes. Fewer weld passes mean the spiral mill can move faster and achieve an overall increase in mass flow velocity through the machine. Additional benefits include:

1. Bend forces are limited.
    a. Machine bend capacity no longer needs to increase with increasing thickness.
    b. Saves capex and thousands of engineering hours per spiral mill generation.
2. Multi-wrap towers unlock the use of a separate steel material supply chain.
    a. Hot-rolled coil is produced in the US in thicknesses up to 25mm.
    b. Offshore scale towers with two to three coil layers (50-75mm) encompass shell thickness requirements expected for the next generation of offshore towers.

Additional tower variants were introduced into the project to evaluate factory throughput and economics for the multi-wrap tower concept. The multi-wrap tower is presented in Figure 3(d) alongside a wide trapezoid single-wrap concept (c). The additional tower variant benefits are addressed in Table 3.

Table 3. Additional Turbine Design Particulars

Variant	Depiction	Purpose	Benefit
3-section TQC-B	Figure 3 (b)	Drop-in Replacement	Interchangeable with can Suppliers
3-section TQC-B	Figure 3 (c)	Drop-in Replacement	Interchangeable. Plate feedstock available with wider dimensions.
3-section TQC-B	Figure 3 (d)	Drop-in Replacement	Interchangeable. Multi-wrap and relatively cheap coil feedstock.

Figure 3. Additional 12MW Reference Towers – Wide Single-Wrap & Multi-Wrap

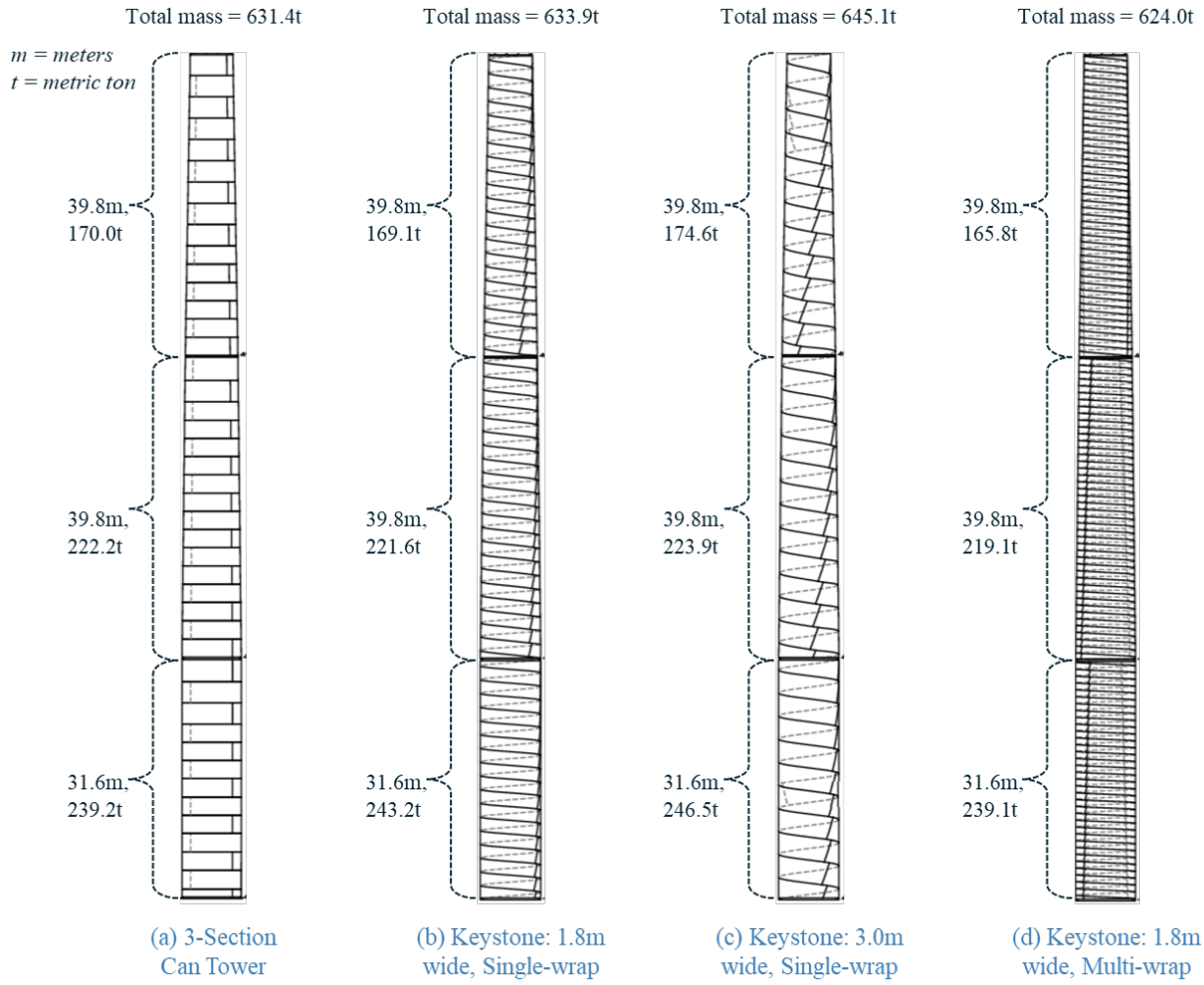

2.2.2 Layer Agnostic Optimization

A Bill of Materials (BoM) for the single-wrap and multi-wrap tower concepts presented in Figure 3 were used in conjunction with a new SAW weld timing model. The model allowed Keystone to anticipate the time it takes to form a spiral-welded tower shell on the spiral-mill as a function of thickness of the feedstock material. A BoM comprised of thicker single-wrap feedstock requires more SAW weld passes and moves through the spiral-mill relatively slowly.

Alternatively, a BoM comprised of relatively thin multi-wrap feedstock requires fewer weld passes and has high spiral-mill velocity. The multi-layer BoM does; however, require additional handling and mill start-stops which lowers the overall operations efficiency. A simple tabulation of the spiral-mill

throughput and subsequent factory operational costs and labor requirements is captured in Table 4. A three-layer variant of the 3-section multi-wrap tower was created solely for this analysis.

Table 4. Full Production Cost Comparison of Single, Double, and Triple-wrap Tower

Comparison Parameters		SAW-1.8m (Single [b])	SAW-1.8m (2-layer [d])	SAW-1.8m (3-layer)
Rel. Throughput (#towers/yr)		100.0%	84.7%	58.6%
Constituent Tower Costs	Capex	6.5%	7.7%	11.1%
	Material - shell	56.8%	47.2%	47.2%
	Material - other	20.1%	20.1%	20.1%
	Labor	10.1%	15.0%	26.2%
	Overhead	6.5%	7.7%	11.1%
Rel. Tower Costs ($/tower)		100.0%	**97.7%**	**115.7%**

Clearly, at the low thicknesses of the 12MW reference tower BoM, the three-layer option is too inefficient, and throughput suffers while costs start to climb. Between the single-wrap and two-layer variants, it is unclear which tower is preferred. The two-layer tower costs slightly less (-2.3%) to fabricate; however, the additional handling requirements reduces annual throughput by about 15%, relative to the single-wrap option.

This is a good place to also point out that the baseline single-wrap variant (Figure 3 [b]) is formed from plate feedstock, yet is restricted to 1.8m wide sheets – consistent with coil feedstock width limits. Plate is readily available with widths of 3m and beyond. A quick check confirmed a wider plate feedstock option permitted higher throughput, as is shared in Table 5.

Table 5. 1.8m vs 3.0m Wide Feedstock Single-Wrap Weld Speed and Fabrication Time Comparison

Configuration	Rel. VHW-Avg (%)	Rel. Fab. Time (%)
SAW-1.8m (Single [b])	100%	100%
SAW-3.0m (Single [c])	72%	88%

It's sufficient to point out that it is not always readily apparent whether a single-wrap or multi-wrap tower is preferred. There is a balance between spiral-mill throughput and the unit cost of each tower. What

should become evident is that a tower – spiral-mill – factory *system* analysis should be undertaken to optimize the geometry of planned towers and to find the likely annual number of towers produced by the factory and the tower unit costs. Keystone explores the details of the weld timing model more extensively in Section 6 and demonstrates the tower – spiral-mill – factory design optimization process.

2.3 Multi-wrap Monopile Design

Keystone extended the multi-wrap design concept from wind turbine towers to offshore monopiles. While monopiles present unique challenges due to growing shell thickness requirements, Keystone recognized the ability to leverage the spiral-forming method's advantage for long and uniform geometries. Here, Keystone examined both the manufacturing feasibility and cost-benefit impacts of multi-wrap construction for a monopile with shell thickness up to 71.1mm.

Single-wrap and multi-wrap variants were designed using 3.0 m wide plate feedstock. Standard submerged arc welding (SAW) is impractical at thicknesses above 70mm; therefore, multi-wrap offers a natural solution by distributing thickness across multiple layers. To further address thick shell fabrication, Keystone investigated advanced welding technologies. Hybrid laser arc welding (HLAW) emerged as a breakthrough candidate, capable of completing a 40mm weld in the time of a single SAW pass. A combined HLAW joint and subsequent SAW fill passes, developed with Edison Welding Institute, significantly reduces weld times and opens commercial feasibility for large monopiles.

Analysis showed that the single-wrap 71.1mm monopile required up to 12 tandem SAW passes per joint. In contrast, a two-layer multi-wrap monopile divided the thickness into 40mm and 31.1mm layers, each welded as single-pass equivalents (2 passes). This reduced effective weld passes by 10. The two monopiles were modeled with Keystone's crossweld timing tool, which indicated that multi-wrap increased fabrication throughput by ~27% with only a marginal cost increase (<1%).

Additionally, bending forces scale disproportionately with thickness (at a rate of $t^{\sim 2.3}$). Thus, bending a 71.1mm plate requires approximately 3.8 times the force of a 40mm plate, further reinforcing the advantages of multi-wrap designs for very thick monopiles.

In conclusion, Keystone demonstrated that multi-wrap fabrication, paired with advanced welding methods such as HLAW, offers a clear pathway to producing monopiles for next-generation offshore turbines. The approach balances manufacturability, throughput, and cost.

2.3.1 Monopile Design Variants

The single-wrap and multi-wrap tower design efforts demonstrated in the previous report sections were repeated by Keystone, but for monopile designs. Keystone's spiral-forming technique excels at continuous operations; therefore, the long and consistent geometry of monopiles is readily appealing. Keystone can also easily accommodate increases to shell diameters. The remaining concern, then, is the increasing demand on monopile will thicknesses and the ability of Keystone to roll these thicker plates.

Keystone conducted research to establish reasonable contemporary monopile designs. An obvious choice of a reference design came from the technical staff from the National Renewables Energy Laboratory (NREL) and the Technical University of Denmark (DTU). The team published their reference offshore wind turbine in early 2020[5]. The 15MW offshore wind reference turbine was intended to represent a conservative estimate of the industry capabilities in the near- and medium-term future.

In the intervening years; however, turbine OEMs have continued the arms race in nameplate rating growth of their machines. By 2023 most OEMs were advertising prototypes with nameplate ratings of approximately 18MW. Siemens Gamesa is in the process of erecting and commissioning a gigantic 21MW test turbine[6]. Chinese OEMs are advertising nameplate ratings even higher. Given these developments, Keystone Tower Systems chose to scale the monopile associated with the 15MW reference offshore turbine to be more reflective of a contemporary 18MW monopile. Scaling the monopile up from the 12MW reference tower to an 18MW reference monopile also gave Keystone the opportunity to examine the cost/benefit analysis of the multi-wrap concept at a rather different design point from that of previously examined tower.

The 15MW reference monopile, and Keystone's scaled 18MW variant, have overall length of 90m. Of the total length, 45m is considered embedded in soil, there is a 30m mean sea level water column, and a 15m stick-up. The outside diameter of the monopile is a uniform 10m from top to bottom. Scaling the design only modified wall thickness; the length and diameter was held constant. KTS used a wall thickness scaling factor of 128.5% to account for the combination of a larger swept area and higher hub height of a

---

[5] Gaertner, Evan, Jennifer Rinker, Latha Sethuraman, Frederik Zahle, Benjamin Anderson, Garrett Barter, Nikhar Abbas, Fanzhong Meng, Pietro Bortolotti, Witold Skrzypinski, George Scott, Roland Feil, Henrik Bredmose, Katherine Dykes, Matt Shields, Christopher Allen, and Anthony Viselli. 2020. "Definition of the IEA 15-Megawatt Offshore Reference Wind,". Golden, CO: National Renewable Energy Laboratory. NREL/TP-5000-75698.

[6] Munguía, Sergio Fdez, Dec. 10, 2024, "Data and images of Siemens Gamesa's 21 MW offshore wind turbine," Reve, www.evwind.es/2024/12/10/data-and-images-of-siemens-gamesas-21-mw-offshore-wind-turbine/103183.

18MW turbine atop a similar monopile. The 15MW reference monopile and Keystone's 18MW scaled reference monopile overall geometry are provided in Table 1.

Table 6. Reference Monopile Design Particulars

Region	$Elev_{Top}$ (m)	$Elev_{Bot}$ (m)	OD (m)	t_{15MW} (mm)	t_{18MW} (mm)
Stickup	90	85	10	41.1	52.8
	85	80		42.2	54.2
	80	75		43.5	55.9
Water Column	75	70		45.5	58.5
	70	65		47.5	61
	65	60		49.5	63.6
	60	55		51.5	66.2
	55	50		53.5	68.6
	50	45		55.3	71.1
Embedded	45	0		55.3	71.1

Blueprints for Keystone's scaled 18MW reference monopiles are shared in Figure 4 and Figure 5 for the single-wrap and multi-wrap variants, respectively. Note that both designs use 3.0m wide plate as the feedstock material. The material thickness reached up to 71.1mm, so even a two-layer variant (35.6mm) exceeds coil supply availability in North America. The designs also reflect length limitations for steel plate in the North American supply chain.

Figure 4. 18MW Monopile – Single-Wrap, 3.0m Wide Trapezoid Blueprint

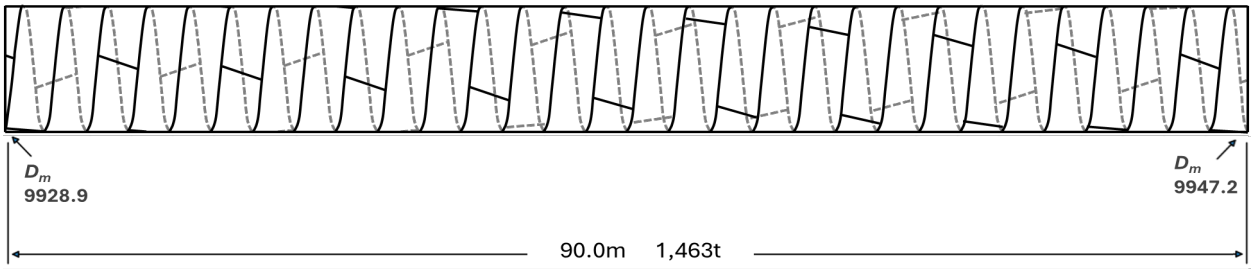

Figure 5. 18MW Monopile – Multi-Wrap, 3.0m Wide Trapezoid Blueprint

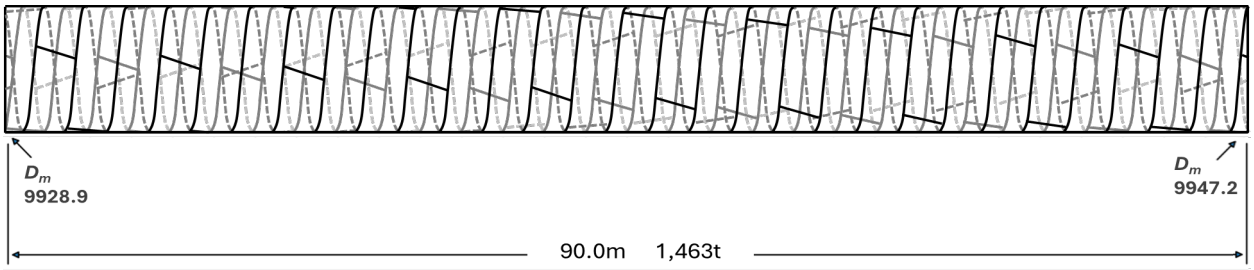

2.3.2 Thick Shell Optimization

Standard sub-arc welding at thicknesses beyond 70mm is not tenable. The multi-wrap concept clearly becomes the preferred path as shell thickness and the number of weld passes balloons.

In addition to the multi-wrap concept, Keystone considered weld technology alternative such as (1) friction stir welding, (2) electron beam welding, (3) multi-head long-stick-out SAW, and (4) Hybrid laser arc welding (HLAW). Of these options, HLAW was selected for further investigation. HLAW investigation details will be shared in 5.1. For this section, it is sufficient to consider HLAW is capable of completing a 40mm weld in the same time as a single-pass SAW weld. For thickness increments beyond 40mm, SAW will complete all subsequent joint fill passes.

For successful commercial fabrication of monopiles, Keystone assumes a weld technology breakthrough in the form of HLAW weld procedures is accomplished. Then, single-wrap and multi-wrap design variants can compete. The HLAW joint geometry created in collaboration with Edison Welding Institute (EWI) is depicted in Figure 6. The joint land (dimension Y) is up to 34mm deep with a U-groove above the joint. The U-groove portion of the joint is filled with SAW passes. The first SAW pass initiates immediately behind the HLAW passes; thus, a 40mm joint can effectively be welded in the time of a single-pass SAW weld.

Figure 6. HLAW Joint Geometry

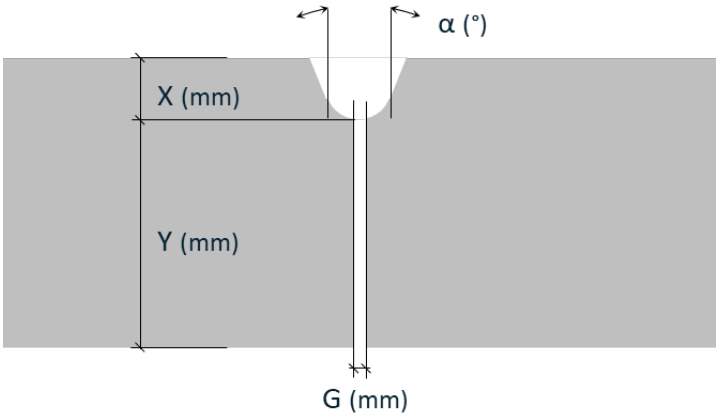

The thickest wall of the single-wrap monopile, 71.1mm, requires up to 12 tandem SAW passes. In contrast, a multi-wrap design can use 40mm and 31.1mm joints on the mandrel and over-wrap layers, respectively. Each such joint can be welded in the equivalent time of a single SAW weld (2-pass equivalent). In this scenario, the multi-wrap monopile saves the equivalent of 10 weld passes.

The BoM of the two 18MW reference towers were fed into the crossweld timing model developed by Keystone. The result, shared in Table 7, indicated the multi-wrap monopile design *increased* throughput by approximately 27%. Fabrication costs only raised modestly at less than 1%. Inefficiencies of double-handling the two-wrap design were more than offset by the vast increase in helical weld velocity.

Table 7. Full Production Cost Comparison of Single and Double-wrap Monopile

Comparison Parameters		**HLAW-3.0m (Single [b])**	**HLAW-3.0m (2-layer [c])**
Rel. Throughput (#monopiles/yr)		100.0%	127.2%
Constituent Monopile Costs	Capex	4.4%	3.9%
	Material - shell	83.2%	84.9%
	Material - other	1.1%	1.1%
	Labor	6.3%	6.7%
	Overhead	5.0%	4.3%
Rel. Costs ($/monopile)		100.0%	**100.8%**

Further, bend forces increase somewhere in the elastic-plastic range; approximately to the 2.3 power of thickness. This means a 71.1mm plate, as compared to a 40mm plate, requires approximately 3.8 times more bending force. For the 18MW monopile case, the winning scenario is clearly to select multi-wrap operations with 3.0m wide plate feedstock.

3 State of the Industry and Baseline Definitions

This section of the report summarizes Keystone Tower Systems' collaboration with BVG-Associates in the cost-savings analysis of single-wrap spiral-welded tower designs, as well as subsequent logistics studies for single-section tower deployment. The findings highlight both the market advantages of Keystone's manufacturing approach and the practical considerations for implementing these innovative tower configurations in the U.S. offshore wind sector.

BVG-Associates conducted an independent market impact assessment comparing Keystone's spiral-welded single-wrap towers with conventional can tower manufacturing. The results demonstrated substantial benefits in factory efficiency, staffing, and cost reduction. Keystone's automated spiral-forming process enables annual production of 1,500 MW of towers using roughly 55% fewer employees and 47% less factory space compared to traditional methods. These efficiencies yield a 25% overall cost reduction, saving approximately $34,658/MW of rated turbine capacity. Material savings stem from Keystone's high Tolerance Quality Class fabrication, reducing steel mass by 12% while maintaining structural integrity. BVG also estimated a ~1% decrease in Levelized Cost of Energy (LCOE) of the entire wind farm development, equivalent to $0.62–$0.67 per MWh, for offshore developers using Keystone towers.

Keystone also focused on the logistics and potential cost savings of manufacturing continuous single-section towers—structures formed as one uninterrupted piece to maximize spiral-mill throughput. This approach eliminates intermediate flanges, reduces crane picks, and simplifies handling and installation. Keystone estimated additional savings of about $12,500/MW of turbine rated capacity, from reduced material and installation complexity. Practical challenges remain; however, for U.S. offshore projects, primarily due to: (1) limited Jones Act–compliant installation vessels, (2) small and draft-limited ports, and (3) inland port locations often obstructed by bridge infrastructure, limiting vertical air clearance. Only the Jones Act compliant Charybdis vessel, commissioned in 2025, can load such large, single-section towers directly from US ports for direct offshore installation.

These studies confirm that Keystone's spiral-welded technology can deliver major cost and efficiency advantages over conventional methods, while innovations such as single-section towers could further transform the economics of offshore wind manufacturing—pending the resolution of key logistical and infrastructure constraints in the U.S. market.

3.1 BVG Analysis for Single-wrap Tower

Keystone consulted with BVG-Associates to characterize the market impact derived from Keystone's single-wrap spiral-welded tower designs (those discussed in Section 2.1.1). BVG-Associates is a UK-based strategy consulting firm with deep expertise in the local and global offshore wind sector – a perfect partner for understanding the market and assessing impacts.

BVG-A reviewed Keystone's single-wrap tower designs drew comparisons to conventional can tower suppliers with whom they have worked. BVG-A and Keystone formulated a means of comparing the tower plant characteristics between conventional and spiral-welded forming techniques, how those differences affect tower costs and factory location, possible impacts to logistics, and ultimately an estimate of cost savings to Developers in the form of Levelized Cost of Energy (LCOE).

BVG-Associates demonstrated, for Keystone's single-wrap drop-in replacement tower, the following findings and conclusions:

1. Keystone can produce approximately 1,500MW of spiral-welded towers per year with far fewer resources compared to conventional can factories.
    a. High quality class enables Keystone to save roughly 12% of overall material mass.
    b. Automation enables production capacity with as much as a 55% reduction in staff.
    c. Spiral forming efficiency reduces the factory footprint by about 47%
2. A reduced factory footprint enables Keystone to select quayside locations that competitors cannot use; this presents some value that is not readily quantified, such as:
    a. Keystone may select plots more strategically located near marshalling/storage ports.
    b. Fewer competitors for the small plots should give Keystone a stronger negotiating position.
3. Keystone's fabrication cost savings are estimated as $34,658/MW – estimated as 25.2% of a conventional can tower supplied from the United States.

3.1.1 Characteristics of Conventional vs. KTS Tower Factories

BVG-Associates presented a high-level comparison of the characteristics a conventional tower manufacturing facility compared to a Keystone Tower Systems facility. These characteristics are shown in Table 8. In both cases, the annual tower production is approximately 1,500MW worth of towers – 125towers with 12MW nameplate ratings.

Table 8. Conventional and Keystone Facility Characteristics

Element	Conventional	Keystone
Staffing (#)	400	180
Facility footprint – buildings (acres)	9.4	5
Approx. storage area (acres)	6.0	6.0
Facility overall site (acres)	15.4	11.0
Maximum production rate (MW/yr)	1500	1500

Keystone's early models indicated they could achieve the 125tower throughput with 180 Full-Time Equivalent (FTE) employees instead of the conventional 400FTE; this indicates a 55% reduction is staff requirements. Automation of the spiral-welded forming process requires fewer employees than staffing numerous can grow lines. Additionally, weld defect rates with the automated welding process are reduced and require fewer hours spent my Non-Destructive Test (NDT) inspection and weld repair staff. Staffing levels for other processes in the factory (bevel, internals, blast, and paint) are similar to requirements for a conventional tower manufacturing facility.

Replacing the can grow lines with the more efficient spiral-mill also reduced Keystone's required facility footprint from an estimated 9.4acres to 5.0acres – a roughly 47% decrease. Costs associated with heavy civil infrastructure at these port locations is very costly. Decreasing the factory footprint directly reduces the site costs and time associated with the build-out. Additionally, a less directly tangible benefit of a smaller quayside area requirement is the possibility of acquiring plots that are not appealing to other suppliers. This can benefit Keystone in either (1) directly decreasing demand – and cost – for the land lease and (2) enable Keystone to strategically locate their facility near larger marshalling ports or storage/transportation hubs.

3.1.2 Key Cost Savings of KTS Towers

BVG-Associates used their expertise in the wind industry to determine the approximate cost of a conventionally manufactured offshore wind turbine tower supplied from within the United States. BVG-A then collated the differences between a conventional can tower and a Keystone supplied drop-in replacement tower; specifically, the reference Keystone tower comes from Figure 2(b'). Keystone's reference tower is a 3-section tower with identical gross dimensions as a conventional can tower; however, KTS' spiral-welded tower is assumed to be manufactured to Tolerance Quality Class – A and have material mass savings of approximately 80tonnes (12% overall mass savings).

BVG-A performed their comparison calculations as shown in Table 9. The masses stated in Table 9 include scrap. BVG-Associates estimated a conventional 12MW US supplied can tower to cost $137,170/MW whereas a Keystone supplied drop-in replacement tower costs just $102,512/MW. The total cost savings is estimated at $34,658/MW and is an approximate 25.2% savings over conventionally manufactured towers.

Table 9. Conventional and Keystone Tower Manufacturing Costs

Element	Sub-element	Conventional Cost		Conversion Explanation		KTS Cost	
		Cost ($/MW)	Cost ($/tower)	Factor	Description	Cost ($/MW)	Cost ($/tower)
Labor	Employment cost	$20,000	$240,000	0.45	- KTS factory has 45% of the staff - Equal throughput	$9,000	$108,000
Materials	Primary steel	$77,050	$924,600	0.75	- According to KTS, coil $1,175/t in 2028, plate $1,380 - KTS 590t vs 670t	$57,771	$693,250
	Rest of materials	$20,482	$245,780	1	- No further differences	$20,482	$245,780
Facilities/ Equipment	Factory/ Equipment	$11,092	$133,100	0.72	- KTS factory cost 72% of conventional - Equal throughput	$8,000	$96,000
	Port space lease	$2,717	$32,604	0.53	- Equal throughput	$1,430	$17,160
	Tower storage	$1,716	$20,592	1.00	- Equal throughput	$1,716	$20,592
	Factory overheads	$4,114	$49,364	1	- No further differences	$4,114	$49,364
Total	-	**$137,170**	**$1,646,040**	-	-	**$102,512**	**$1,230,146**

BVG-Associates used these cost savings to predict savings for project Developers in terms of Levelized Cost of Energy (LCOE), as conveyed in Table 10. BVG-A predicted Keystone could impact the offshore development costs by $0.62 to $0.67 per Megawatt-hour. BVG-A assumed a baseline cost of $63/Mwh. Thus, the savings Keystone can accomplish represent approximately 1% of project development costs. The LCOE savings are accomplished primarily through (1) Keystone's ability to fabricate tower shells to a higher Tolerance Quality Class and thereby use less steel in each tower and (2) through significant automation and reduced labor costs. Some additional minor savings can be realized by deploying a smaller factory and strategically co-locating it near marshalling ports to reduce logistics costs.

Table 10. Summary LCOE Savings Achieved with Keystone Spiral-welded Towers

Component Cost	LCOE Saving ($/Mwh)	
	2-Sxn Tower at own Port	2-Sxn Tower at Marshalling Port
Materials	$0.33	$0.33
Labor	$0.19	$0.19
Factory & Equipment	$0.08	$0.08
Shipping & Handling	$0.03	$0.07
Total	**$0.62**	**$0.67**

3.2 Single-Section Logistics

Keystone, with a desire to maximize spiral-mill productivity, seeks to fabricate continuous single-taper single-section towers. Other obvious advantages are readily apparent; however, Keystone wanted to (1) quantify the advantages and (2) surveil the state-of-the-industry to understand if hard limits may prevent deploying single-section offshore towers.

In answer to those basic questions: (1) Keystone conservatively estimated combined savings of ±$12,500/MW when using single-section towers and that (2) there were no firm reasons why handling equipment commonly encountered in the offshore wind sector could not accommodate a single-section tower. Monopiles are commonly handled and have diameter, length, and mass dimensions that far exceed typical tower section dimensions. Ultimately, the limitations to using single-section towers may be unique to the US offshore market. Protectionism necessitates the use of Jones Act compliant WTIVs whereas the US shipbuilding industry has been sluggish to address demand. A single Jones Act compliant WTIV, the Charybdis, may enable load-out and installation of single-section offshore wind towers.

3.2.1 Single-Section Logistics Details

Keystone's continuous spiral-welded manufacturing technique is most efficient when interruptions to the forming process are avoided or minimized. One way to optimize the forming process, then, is to manufacture very long single-taper continuous tower sections. Taken to the extreme, this means single-section towers without any intermediate section-breaks or flanges. Such a tower variant was previously shared and was presented in Figure 1(e). Beyond Keystone increasing spiral-mill throughput, additional apparent benefits of a single-section tower include:

1. elimination of costly flange material and the cumbersome section flanging operation,
2. simplified site logistics with fewer sections to track, handle, and re-mate with a tower kit,
3. a single crane pick to tip-up and stage the tower in the marshalling yard,
4. a single crane pick to load the Wind Turbine Installation Vessel (WTIV),

5. a single crane pick during turbine installation at sea,
6. lower Operations and Maintenance (O&M) bolt inspection costs throughout the life of the tower.

Keystone analyzed scenarios presented by the single-section tower design to arrive at plausible cost-savings. The findings are summarized in Table 11. Overall cost savings are approximated as $12,500/MW. These valuations are rather conservative and expect zero value when the trade-offs do not have a clear value proposition. For instance, simplifying site logistics has a value associated with fewer instances of handling Work In Progress (WIP) tower sections; however, the net storage area is assumed to be equal in the 3-section vs. 1-section scenarios. Labor and equipment savings are difficult to predict and are given zero value. Clear and large costs, such as pricey land storage, are not credited or expensed.

Table 11. Summary of Cost Savings with Single-Section Tower

Benefit	Description	Value ($/MW)
Material savings	Remove costly flanges	4,500
Simplify site logistics	Less WIP and section shuffling	0
Reduce marshalling crane picks	Co-locate small factory at marshalling port	5,000
Reduce installation crane picks	WTIV vs. feeder barge installation is project-specific	0
Reduce bolt inspection	Reduce inspection time/trips	3,000
	Total	**12,500**

3.2.2 Limits to Single-Section Logistics

There are clear limits to using very long tower sections in the US offshore market. The largest barriers that exist in the US market are:

1. A single Jones Act compliant WTIV
2. Existing ports are relatively small
3. Draft barriers at existing ports and sail distances

Delivery and installation orientations of the tower, nacelle, and blades are depicted in Figure 7. A single-section tower can be utilized with installation orientations 2, 3, 4, or 6. In all such cases, a Wind Turbine Installation Vessel (WTIV) shall perform the lift and installation from its own deck. Executing that pick from an adjacent vessel is not currently technically feasible. The Charybdis, the sole Jones Act compliant (US built, flagged, and crewed vessel) WTIV, was placed in service in September 2025.

For all projects planned without the use of the Charybdis WTIV, the single-section tower orientations can not be accomplished. Instead, those projects plan to use foreign flagged WTIVs which necessitate a fleet of US flagged feeder vessels to transport the wind turbine components from US ports to the offshore wind

project location. The much smaller feeder vessels cannot accommodate the tall center of gravity of vertically oriented single-section towers. A horizontally oriented single-section tower has never been picked and tipped-up from a feeder vessel by a WTIV. The installation method must be orientation 1.

Lastly, many US ports are located up-river of bridges or have narrow or shallow shipping channels. Even if Jones Act compliant WTIVs were readily available, it's not obvious that the installation strategy in the US would shift away from feeder vessels. Feeder fleets are capable of fully supplying WTIVs to continuously work in the field. Projects located far from ports may have higher overall productivity when using the feedering strategy.

Figure 7. Offshore Wind Turbine Installation Methods (credit: Ahn et. Al.[7])

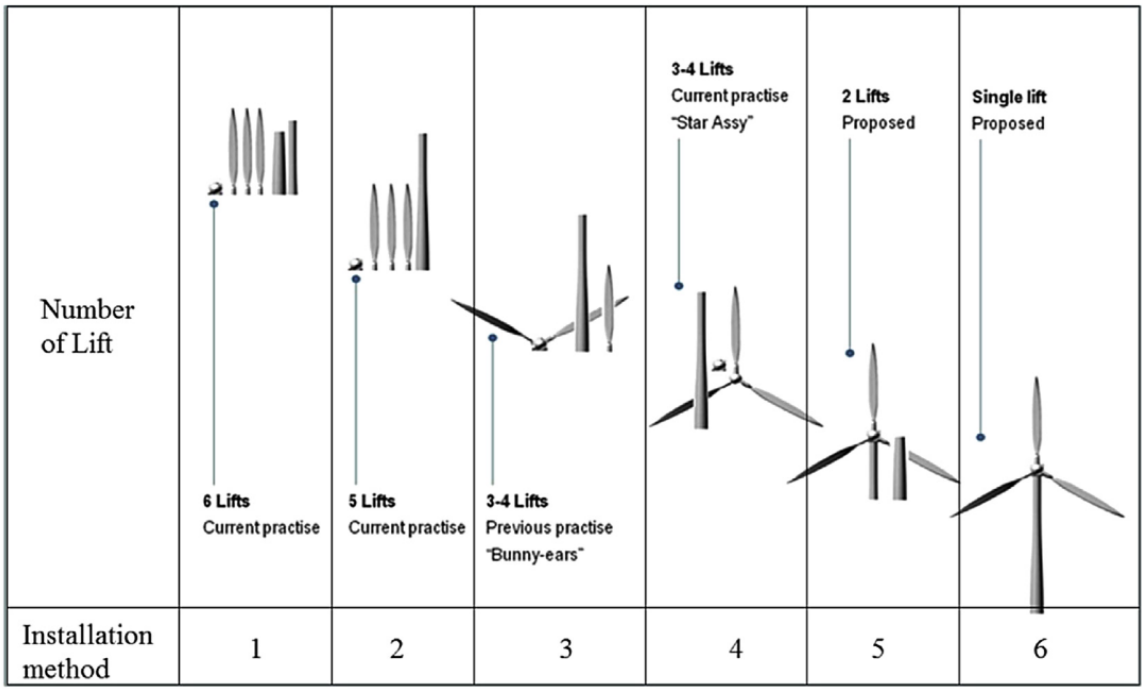

[7] D. Ahn et. al. 2016. "Comparative evaluation of different offshore wind turbine installation vessels for korean west-south wind farm," *International Journal of Naval Architecture and Ocean Engineering* vol. 9, no. 1, pp. 45-54, Jan. 2017. Accessed: Jan 17, 2023. Available: doi.org/10.1016/j.ijnaoe.2016.07.004

4 Multi-wrap Investigations

The NOWRD project investigation proceeded along two main tracks: (1) a single-wrap investigation that can act as a baseline for comparison and explore the requirements for forming thick material, and (2) a multi-wrap tower shell structure. This report section gives a detailed assessment of the various investigations and findings regarding the latter multi-wrap structure.

Firstly, a thorough review of the literature regarding multi-layered panel structures with bonding and/or periodic tensile fasteners was conducted. There appeared to be a dearth of studies for compressively loaded multi-layer panels and/or cylindrical shell structures. The lack of previous studies caused the researchers to recommend down-scaling the physical buckling specimen to allow for simpler and quicker test specimen prototyping. This proved insightful as several iterations of specimen design were required before testing proceeded successfully.

Multi-wrap shell structures were investigated computationally, with the analyses led by Johns Hopkins University. In parallel, small "benchtop scale" specimens were subjected to physical testing by Northeastern University. The analytical models and physical tests showed strong agreement with each other. Ultimately, the critical buckling loads of fully bonded multi-wrap structures were expected to meet or exceed those of monolithic single-wrap shells of equivalent thickness. The difference in capacity of single-wrap and fully bonded multi-wrap tests were not statistically significant.

Seminal testing of unique layered structures in fatigue were performed. The three-layer fatigue samples also showed equivalent or superior fatigue capacity when compared to monolithic single-wrap expectations. Non-destructive ultrasonic inspections were performed on the three-layer sample. All known machined flaws were found.

4.1 Literature Review

Northeastern University performed an extensive literature review in the topic area of buckling of thin-walled structures. Northeastern cited 29 references, as provided in Table 12. The references ranged from course notes, research or journal papers, and even academic textbooks. Three main topic areas, and their intended impact on the research, were covered:

1. General buckling of thin-walled cylinders with single layer walls,

How might flat panel research inform cylindrical structure understanding – with or without ring or axial stiffeners?

2. Buckling of cylinders (and finite-width flat panels) with two-layer walls having compression-only or tension-compression interlayer contact,
   What is the buckling strength of classic multi-wall panels and how has interface delamination of bonded walls been treated?
3. Buckling of flat panels with two-layer walls including periodic tensile fasteners.
   What design guidance is given for spacing of bolts, rivets, or spotwelds for meaningful buckling resistance?

Northwestern stated, importantly, that a key finding is that no significant literature was discovered on the subject of buckling of either flat panels or cylinders, consisting of walls with two or more layers and periodic connection. Important mechanistic understandings of multi-layered panels or cylinders remain unanswered, such as important design considerations of (1) the strength of the shear connection between layers, and (2) the influence of length free span between layers on composite buckling of the tube wall.

In the absence of previous research in the area, Northeastern recommended that the project accommodate preliminary "benchtop-scale" buckling tests of two-layer cylinders. The plan was to use the small and relatively cheap and easily fabricated specimen to guide subsequent sample design decisions.

Table 12. Buckling Literature Review Reference List

Name	Year	Title	Publishing Organization	Source Link	Source Type
G. Gerard	1957	*Handbook of Structural Stability Part V – Compressive Strength of Flat Stiffened Panels*	National Advisory Committee for Aeronautics (NACA)	abbottaerospace.com	Technical Note
P. Seide	1958	*Compressive Buckling of a Long Simply Supported Plate on an Elastic Foundation*	AIAA	arc.aiaa.org	Journal Paper
E. Bruhn	1973	*Analysis and Design of Flight Vehicle Structures*	Purdue University Press (Manual)	ihpa.ie	Engineering Textbook
NASA	1975	*Astronautics Structures Manual, Vol. II*	NASA	abbottaerospace.com / ntrs.nasa.gov	NASA Technical Manual
H. Chai et al.	1981	*One Dimensional Modeling of Failure in Laminated Plates by Delamination Buckling*	Caltech	library.caltech.edu	Research Paper
C. Calladine	1989	*Theory of Shell Structures*	Cambridge University Press	—	Academic Textbook
G. Kardomateas	1991	*Spot Weld Failure from Buckling-Induced Stressing of Beams under Cyclic Bending and Torsion*	Georgia Tech	gatech.edu	Journal Paper
H. Gu & A. Chattopadhyay	1996	*Delamination Buckling and Postbuckling of Composite Cylindrical Shells*	Arizona State University	aims.asu.edu	Research Paper
K. Shahwan & A. Waas	1998	*Buckling of Unilaterally Constrained Infinite Plates*	ASCE	ascelibrary.org	Journal Paper
X. Ma et al.	2007	*Compressive Buckling Analysis of Plates in Unilateral Contact*	Elsevier	sciencedirect.com	Research Paper
C. Kassapoglou	—	*AE4509 Energy Methods for Buckling of Skin-Stiffened Plates, Inter-Rivet Buckling*	TU Delft	ocw.tudelft.nl	Course Notes
M. Elso	2012	*Finite Element Method Studies on the Stability Behavior of Cylindrical Shells under Axial and Radial Uniform and Non-Uniform Loads*	Universidad Pública de Navarra	academica-e.unavarra.es	Research Thesis
X. Lin et al.	2017	*Bolted Built-Up Columns Constructed of High-Strength Steel under Combined Flexure and Compression*	ASCE	ascelibrary.org	Journal Paper
R. Michele	2022	*Inter-Rivet Buckling*	Aerospace Engineering.net	aerospacengineering.net	Technical Article
A. Lindström	2007	*Strength of Sandwich Panels Loaded in In-Plane Compression*	Luleå University of Technology	diva-portal.org	Thesis
N. Fleck & I. Sridhar	2001	*End Compression of Sandwich Columns*	University of Cambridge	cam.ac.uk	Journal Paper
ASTM International	2016	*ASTM C364/C364M-16: Standard Test Method for Edgewise Compressive Strength of Sandwich Constructions*	ASTM International	ansi.org	Standard
M. Yasaswi & P. Naveen	2014	*Mechanical Evaluation with Finite Element Analysis of Truss Core Sandwich Panels*	ResearchGate	researchgate.net	Research Paper
J. Jelovica & J. Romanoff	2018	*Buckling of Sandwich Panels with Transversely Flexible Core*	SAGE Journals	journals.sagepub.com	Journal Paper

Name	Year	Title	Publishing Organization	Source Link	Source Type
Z. Bazant & A. Beghini	2005	*Constant Shear Modulus for Small-Strain Buckling of Soft-Core Sandwich Structures*	ASME	asmedigitalcollection.asme.org	Journal Paper
M. Schultz et al.	2011	*Compression Behavior of Fluted-Core Composite Panels*	NASA	ntrs.nasa.gov	Technical Report
J. Romanoff et al.	2020	*Design Space for Bifurcation Buckling of Laser-Welded Web-Core Sandwich Plates*	Springer	springer.com	Journal Paper
P. Schaumann & C. Kleindorf	2008	*Sandwich Towers for Wind-Energy Converters*	Leibniz University Hannover	stahlbau.uni-hannover.de	Research Paper
K. Yadav & S. Gerasimidis	2020	*Imperfection Insensitive Thin Cylindrical Shells for Next Generation Wind Turbine Towers*	Elsevier	sciencedirect.com	Research Paper
McDermott International	2019	*Hydropillar Elevated Water Storage*	McDermott	mcdermott.com	Technical Brochure
D. Bushnell & M. Jacoby	2014	*Minimum Weight Design of an Axially Compressed Isotropic Prismatic Panel*	ResearchGate / ShellBuckling.com	researchgate.net	Journal / Report
T. Han et al.	2015	*Design Feasibility of Double-Skinned Composite Tubular Wind Turbine Tower*	International Association for Structural Engineering and Mechanics (IASEM)	i-asem.org	Conference Paper
S. Vernardos et al.	2021	*Experimental and Numerical Investigation of Steel-Grout-Steel Sandwich Shells for Wind Turbine Towers*	Elsevier	sciencedirect.com	Journal Paper
A. Patnaik et al.	2005	*Compression Buckling Behavior of 7075-T6 Aluminum Skin Stiffened Panels Fabricated by Friction Stir Welding*	ResearchGate	researchgate.net	Research Paper

4.2 Multi-wrap Analyses

This section of the report presents a comprehensive buckling analysis of Keystone's spiral-welded offshore wind tower design, with emphasis on the structural behavior of multi-wrap configurations under critical load conditions and how they compare to single-wrap configurations. Finite Element Analysis (FEA) models were developed by Johns Hopkins University to evaluate buckling performance, material response, and the impact of bonding techniques and weld imperfections.

The tower models were configured as cantilevered systems fixed at the base, replicating offshore boundary conditions, and subjected to torsion- and bending-dominated load cases (LC3 and LC8, respectively). Using S355-grade structural steel, analyses incorporated elastic-plastic and strain-hardening material models. For multi-wrap designs, bonding between layers was modeled as (1) partially-bonded with only mechanical connection between layers through the helical weld and (2) fully-bonded with mechanical helical weld connection and structural adhesive of varying stiffnesses. Structural adhesive materials considered ranged from rather soft epoxy, stiff epoxy, brass brazing, or perfectly bonded steel (infinitely stiff). Manufacturing imperfections were introduced per EN 1993-1-6 tolerance classes (A–C) to assess real-world variability.

Results from Linear Bifurcation Analysis (LBA) showed that fully bonded multi-wrap shells achieved equivalent or higher buckling resistance compared to single-layer shells, while partially bonded models (bonded only along helical welds) exhibited approximately 50% capacity loss. Notably, even weak adhesive bonding significantly improved performance over partially bonded cases. For torsion (LC3) load cases, weld imperfections provided a modest reinforcing effect (acting as corrugations). For bending loads (LC8), larger imperfections reduced strength, as expected.

Advanced Geometric and Material Nonlinear Imperfection Analyses (GMNIA) further confirmed that fully bonded two-layer shells can match the load capacity of a monolithic shell even with low shear stiffness adhesives. Overall capacity reductions of GMNIA analyses relative to LBA analyses (due to combined imperfections) ranged from 40–60%, consistent with expectations for thin-walled structures. The study concludes that properly bonded multi-wrap tower shells perform *structurally equivalent* to conventional single-thickness shells. These findings validate multi-wrap concepts as a viable path toward scalable, high-strength spiral-welded offshore wind towers.

4.2.1 Basic Tower Model, Boundary Conditions, and Loads

The analytical models were built for Keystone's spiral-welded tower design previously presented in Figure 1(b). A Finite Element Analysis (FEA) model was constructed for the wind tower with realistic geometries assigned, as conveyed in Figure 8. Focus was placed on the heavier wall base sections.

Figure 8. Haliade-X 12MW – Base Thickness Assignment (Left) & R/t Ratio along Tower (Right)

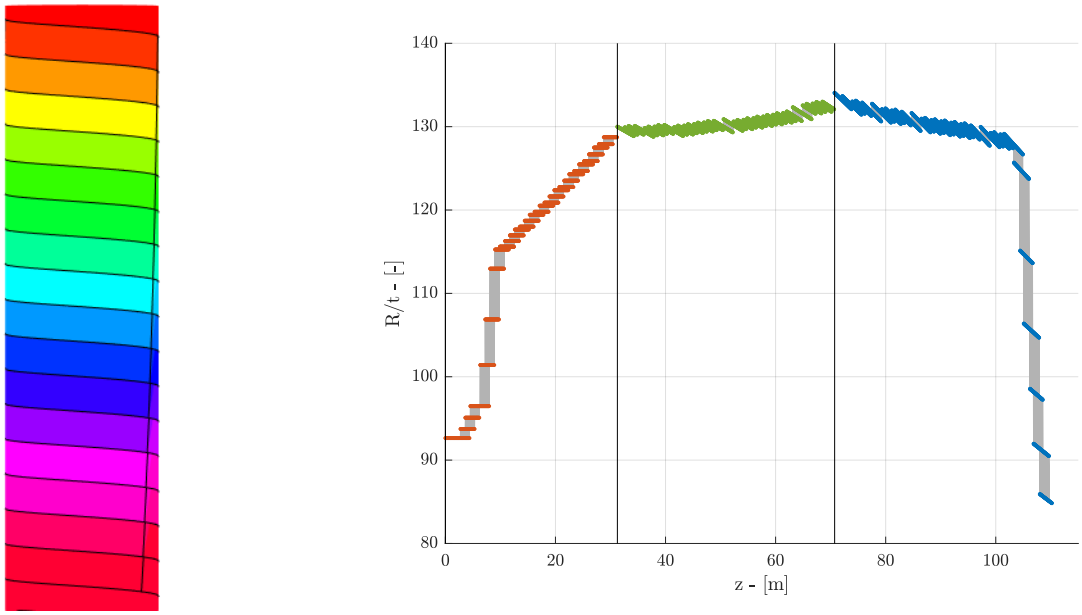

All nodes at the top or bottom of each section of tower were tied to coupling constraints, so that all nodes move as a single rigid body. The coupling constraint is depicted in Figure 9. The bottom constraint of the base section was not allowed to rotate or translate; thus, it acts as though it is fixed with infinite stiffness. The top constraint was allowed to rotate and translate. The result is a base (and remaining sections of tower above) that retains a rigid and circular cross-section at the flanged connections, is fixed at the bottom, and is allowed to deflect like a vertically oriented cantilever beam.

Figure 9. Demonstration of Coupling Constraint Boundary Condition

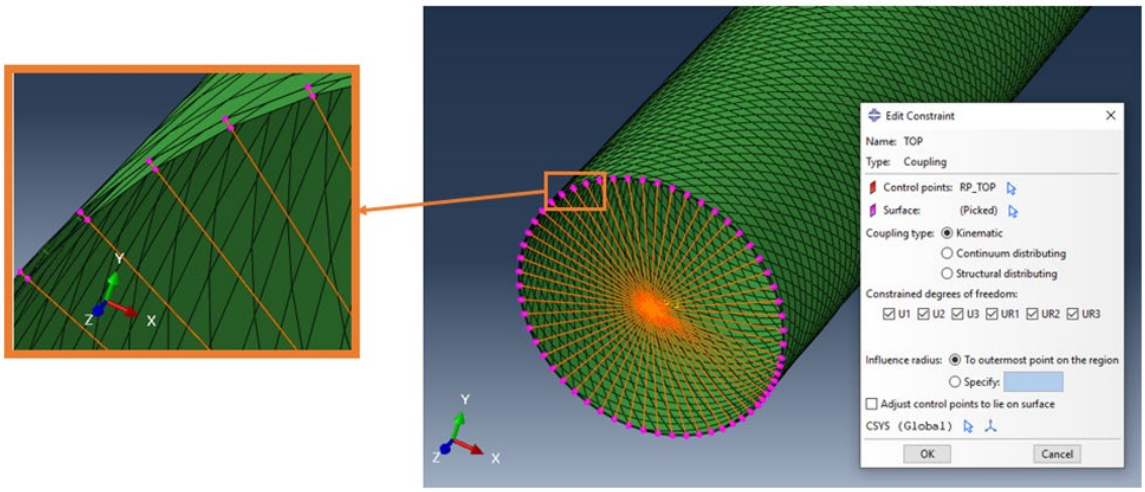

The loads were consistent with typical offshore wind ultimate load cases. Load case three (LC3) was torsion dominated and my govern capacity at certain regions of the top section. Load case eight (LC8) was bending dominated and governs in most regions of the tower, especially the lower base section.

4.2.2 Mesh Details and Investigations

The helical spiral of trapezoid shape feedstock material underwent significant scrutiny to appropriately setup and mesh the FEA. Figure 10 and Figure 11 each show the single-wrap and multi-wrap FEA of the base section which is unrolled from the cylindrical geometry into a flat space. Special care in the meshing was taken at the section ends and at the nip edges, adjacent to the crosswelds. Note that the two layers of the multi-wrap section are clocked by an offset of 180° - that is, if a feature on the inner layer is clocked at 0°, the same feature on the outer layer would exist at 180°. This is depicted in the flat space in Figure 11 as the outer layer being laterally displaced ½ the circumference along the involute shape of the section.

Figure 10. Base Section in Flat Space – Single-Wrap Mesh

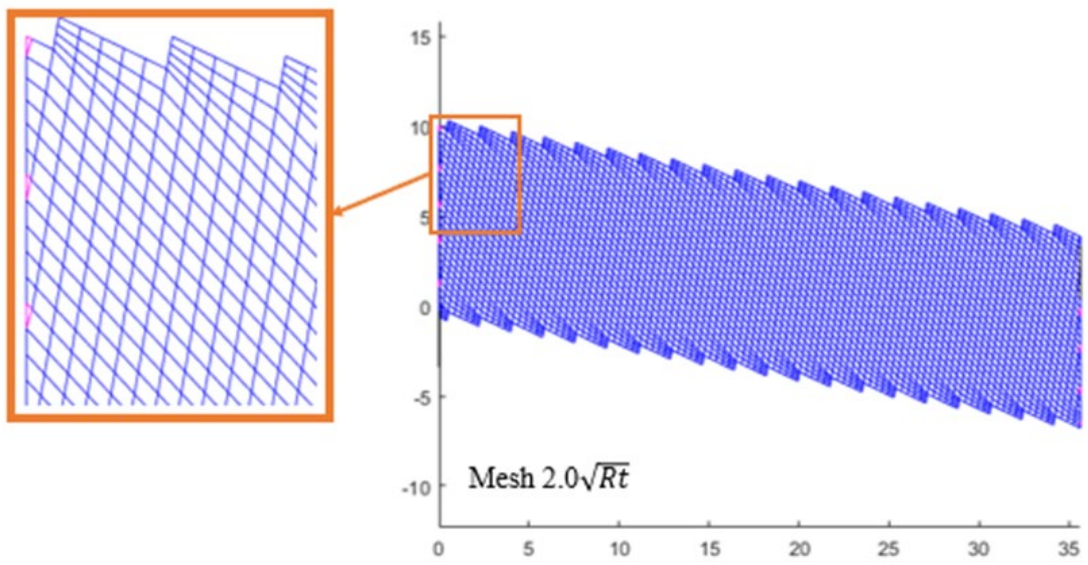

Figure 11. Base Section in Flat Space – Multi-Wrap Mesh

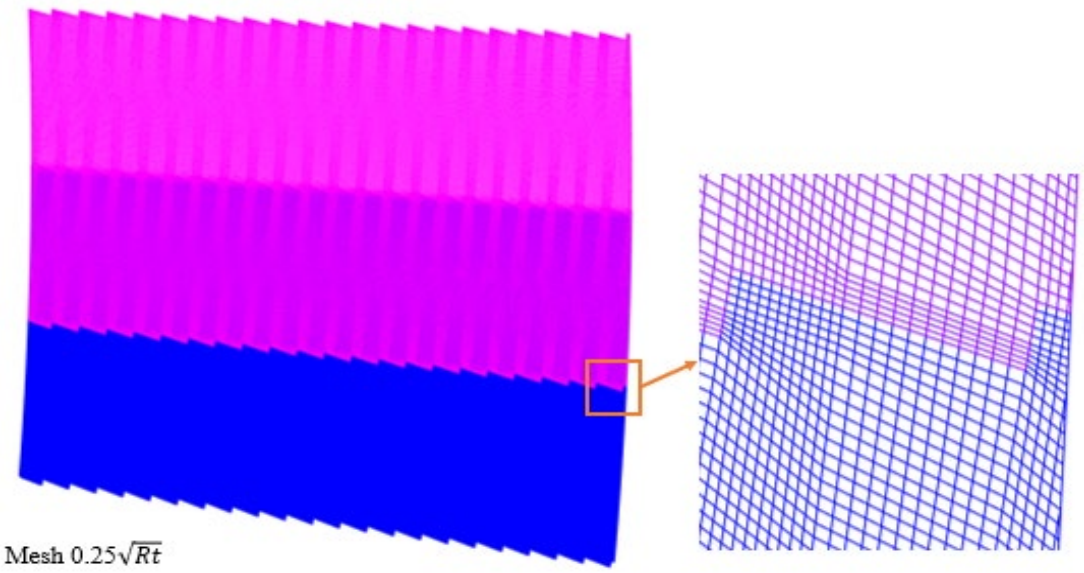

Johns Hopkins investigated mesh size while establishing their models. The aim is to enlarge the mesh as much as possible to minimize computational resources and time of each analysis; however, this is limited to stability of the model behavior when loaded. Smaller meshes are more stable. Mesh size stability is shared in Figure 12.

Figure 12. Mesh Size Depiction (Left) and Resulting Model Behavior (Right)

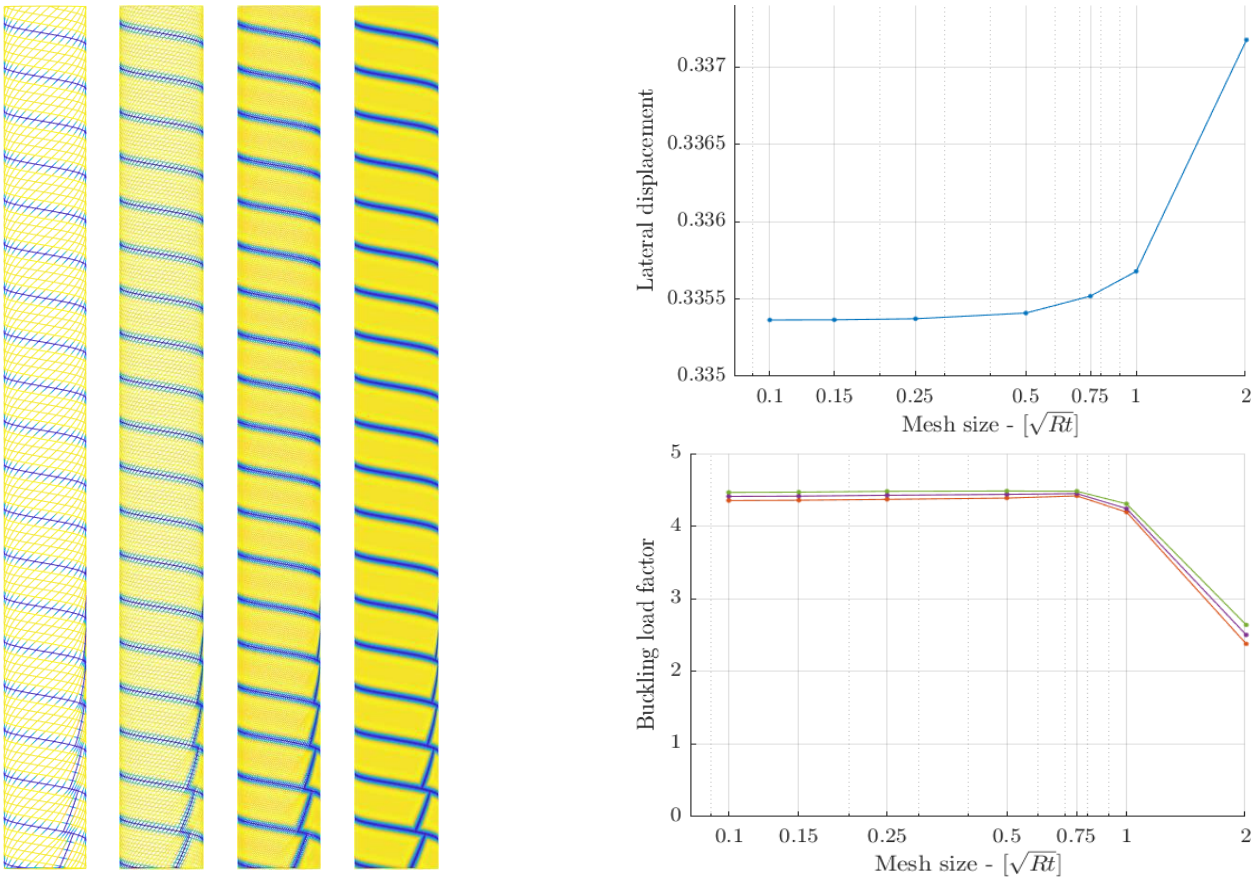

4.2.3 Materials

A typical structural steel was used for the trapezoid feedstock that is formed into the spiral-welded tower. The metric standard S355 material has yield strength of 355MPa and is similar to Grade 50 materials (σ_y = 51.5ksi) if using North American standards. Other basic material parameters assumed were: (1) Youngs Modulus, E = 210GPa, (2) Poisson's Ratio, ν = 0.3, and (3) Shear Modulus, G = 80.8GPa. For Linear Bifurcation Analyses (LBA) the material was considered elastic-perfectly plastic. For non-linear analyses (MNA, GMN(I)A), the material was considered strain-hardening. The strain-hardening curve assumed for the shell steel is provided in Figure 13.

Figure 13. True Stress-Strain Curve used for Non-linear Material Models

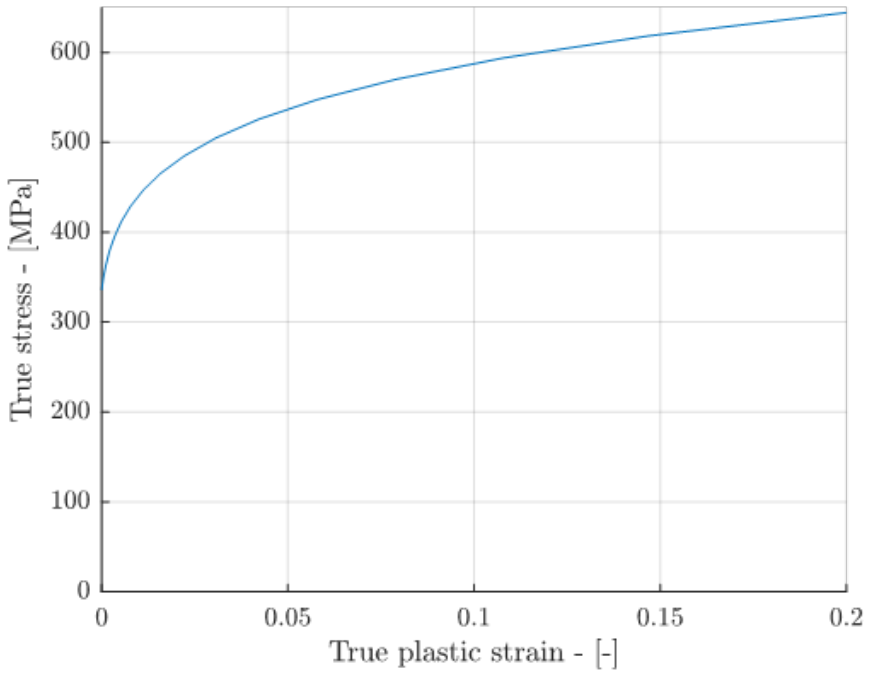

For multi-wrap analyses, connectors were created between nodes of the inner and outer wraps. The node connectors consist of either (1) a Multi-Point Constraint (MPC) BEAM or (2) a combined (a) beam element and (b) spring element. The MPC BEAM connector are rigid links to the inner and outer layers, akin to a an indeterminate fixed-fixed beam connector. The alternative, beam plus spring, connector relies upon the beam to carry shear load and the spring to transmit appropriate axial (normal to shell surface) load. The combined beam and spring stiffnesses can be varied to mimic different bonding materials. The bonding materials investigated have material characteristics as given in Table 13.

Table 13. Material Properties of Structural Bonding Agents

Bonding Material	Shear Stiffness (GPa)	Young's Modulus (GPa)	Poisson's Ratio	Shear Str. (MPa)	Tensile Str. (MPa)
Brass brazing	39	117	0.34	270	360
3M™ Epoxy 2214	1.78	5.171	0.45	17.24	69
3M™ Epoxy 2216 Gray	0.342	---	0.45	---	---

4.2.4 Imperfections and Weld Details

Imperfections were added to the most complex FEA – the Geometric Material Non-linear Imperfection Analysis (GMNIA). Shell imperfections are allowed in the form of dimples or relatively small variations

in bending curvature. Shell imperfections fall into manufacturing Tolerance Quality Classes (TQC) and range from A (best) to C (worst). The shell imperfection magnitudes are taken from European standard EN 1993-1-6 (2021), as recounted in Table 14.

Table 14. Dimple Tolerance Parameters

Tolerance Quality Class (TQC)	Description	$U_{ox,max}$	$U_{o\theta,ref}$
Class A	Excellent	0.006	0.008
Class B	High	0.010	0.017
Class C	Normal	0.016	0.036

Weld imperfections are treated differently from the shell imperfections in the FEA model. Rapid cooling in the vicinity of welds results in relatively concentrated local deformations. The weld seems to pull itself into the shell and drags surrounding material in with it. Researchers have found that the sharpness of the modelled shape of the weld has an impact on the load bearing capacity of the structure. The weld imperfections were modelled with the "Type A" shape, as defined by Rotter and Teng[8], since they most accurately reflect the actual profile of measured weld depressions. A depiction of the weld shape imperfections is provided in Figure 14.

Figure 14. Weld Depression Shape Profiles

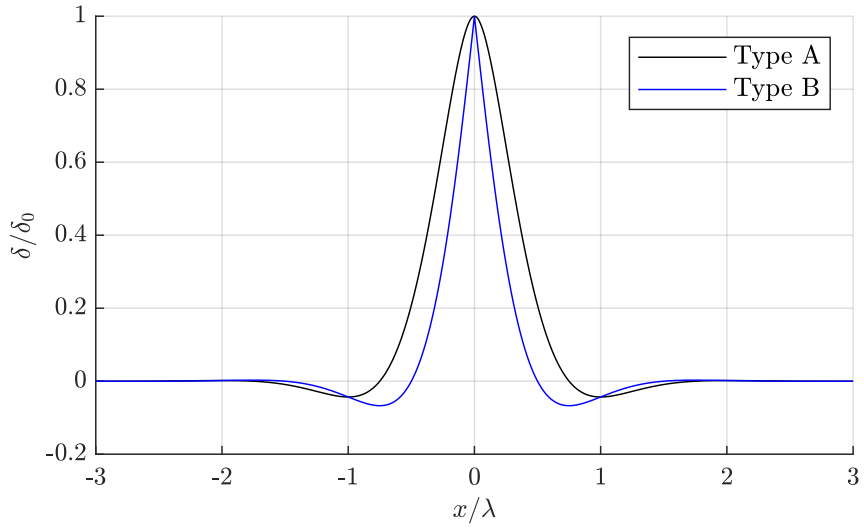

[8] J. M. Rotter and J.-G. Teng, "Elastic Stability of Cylindrcal Shells with Weld Depressions," *Structural Engineering,* vol. 155, no. 5, pp. 1244-1263, 1989.

An additional caveat of the weld imperfections for Keystone's multi-wrap concept is that helical welds of the inner and outer shell layers are offset by 180°, or ½ the trapezoid width. The inner welds are performed when fabricating the inner mandrel tower shell. The outer welds are performed later when over-wrapping the outer tower shell layer and butt welding the over-wrap to the mandrel as a permanent backing plate. The result of this process is that the inner and outer layers have different frequency of weld deformations, as indicated by Figure 15.

Figure 15. Helical Weld Depression Profiles of Multi-wrap Shell Structure

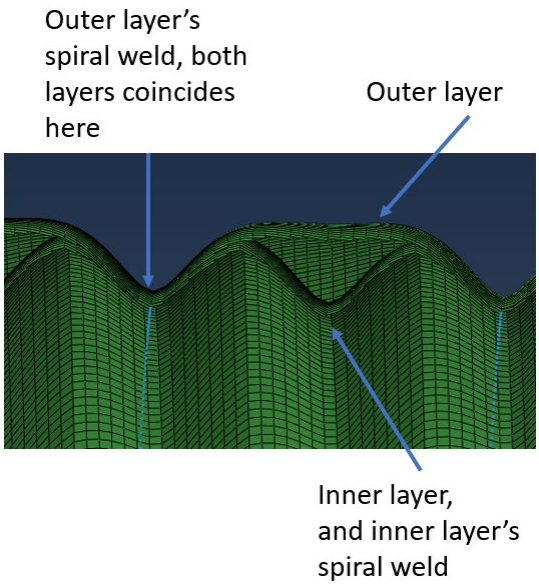

4.2.5 Analysis Results

Northeastern University completed Linear Bifurcation Analysis (LBA) to study the relative loads of the various models and to obtain the eigenmodes, or deflected shapes, to apply in later more complex collapse models. The first eigenmode buckling load factors are given in Table 15. These load factors are multiples of an arbitrarily selected load applied to the model that result in rapid and catastrophic failure of the shell – the load-response curve has a point at which increasing loads are steadily resisted until reaching a point at which the curve bifurcates and no load resistance remains.

Note in Table 15 that the partially bonded cases (layers bonded only at helical weld) have approximately half the load carrying capacity of all other scenarios. Even the weakest bonding agent, paired with helical welds, is sufficient to keep the layers bonded and working together to resist collapse. It seems that the partial bonding at the helical weld does much of the work to force compatibility of deformations between the layers whereas the bond agent must carry much less shear between helical weld spans.

To test that the model can show separation of layers with a bonding agent, an extremely weak bonding material was tested in a model with weld imperfection A. The bond agent had stiffness equal to G=1kPa ($3*10^{-6}$ the weakest epoxy adhesive expected). The result of this test showed capacity within 0.3% to the partially bonded scenario; thus, this demonstrated that very weak bonding agents can fail.

Table 15. LBA Load Factors

Orientation	LC 3 Weld Imperfection Class				LC 8 Weld Imperfection Class			
	0	A	B	C	0	A	B	C
Single	7.35	7.26	7.10	6.76	3.12	3.02	2.81	2.50
2-layer, partial, gap=0.1mm	4.10	4.01	3.83	3.49	1.55	1.44	1.31	1.14
2-layer, partial, gap=0.5mm	4.14	4.01	3.84	3.50	1.55	1.43	1.30	1.14
2-layer, fully, gap=0.1mm	7.38	7.63	7.75	7.85	3.14	3.17	3.05	2.84
2-layer, fully, gap=0.5mm	7.54	7.76	7.88	7.99	3.20	3.23	3.11	2.90
2-layer, adhesive G=39GPa, gap=0.1	7.39	7.63	7.75	7.86	3.14	3.18	3.05	2.84
2-layer, adhesive G=1.74GPa, gap=0.1	7.39	7.63	7.75	7.86	3.14	3.17	3.05	2.84
2-layer, adhesive G=0.342GPa, gap=0.1	7.38	7.63	7.75	7.85	3.13	3.16	3.04	2.83

The LBA results are more easily read graphically from Figure 16. First, consider the increase in load factor for LC3 (high torsion load) with increasing weld imperfections. This indicates that the helical weld imperfections act as reinforcing corrugations in this scenario. For LC8 (high bending moment) load factors decrease with increasing weld imperfection size, as expected. It is also readily apparent that the multi-wrap bonded models have higher load factors than the single-wrap model. Shear is transferred through the gap between layers and acts to increase the effective shell wall thickness. The partially bonded scenario, only bonding layers at the helical weld, has lower load factors in all cases.

Figure 16. First Buckling Load for LBA

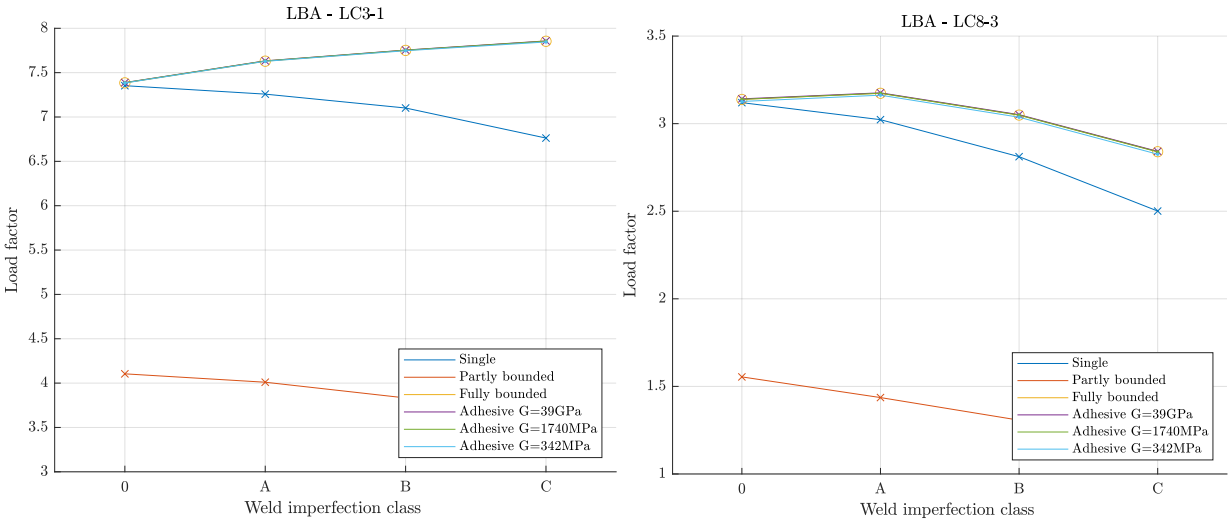

The full collapse models include (1) geometric non-linearities (eigenmode initial deformations), (2) material non-linearities (true stress-strain material curves), and (3) local imperfections (at welds, in this case). Each of these imperfections and non-linearities knock-down the capacity of the shell structure. The result is load factors that decrease in the range of ±40% for LC3 and ±60% for LC8. The load factors, normalized to the two-layer fully bonded scenario with weld and eigenmode imperfection class A, are collated in Table 16.

The GMNIA results clearly show:

4. A loss of capacity for the partially bonded (helical weld only) cases.
5. Slight loss of capacity as the bonded layer shear stiffness decreases
6. Similar capacity between the "single" monolithic shell model and all 2-layer fully bonded models, even when the weakest bonding agent (G=340MPa) is used.

Table 16. Normalized GMNIA Load Factors

Orientation		Shell Imp.	LC 3 Weld Imperfection Class			LC 8 Weld Imperfection Class		
			A	**B**	**C**	**A**	**B**	**C**
Single		A	0.95	0.92	0.87	0.95	0.90	0.87
		B	0.90	0.86	0.81	0.90	0.88	0.84
		C	0.82	0.78	0.73	0.88	0.85	0.82
2-layer Partially Bonded		A	0.68	0.63	0.57	0.73	0.71	0.68
		B	0.62	0.58	0.54	0.71	0.70	0.67
		C	0.57	0.55	0.52	0.68	0.68	0.65
2-layer Fully Bonded		A	**1.00***	0.98	0.94	**1.00***	0.98	0.94
		B	0.96	0.94	0.91	0.97	0.96	0.90
		C	0.91	0.89	0.85	0.95	0.94	0.88
2-layer with structural adhesive	G=39GPA	A	1.00	0.98	0.95	0.98	0.96	0.94
		B	0.97	0.95	0.92	0.91	0.90	0.89
		C	0.92	0.90	0.87	0.90	0.89	0.88
	G=1740MPa	A	1.00	0.98	0.95	0.97	0.96	0.94
		B	0.97	0.95	0.92	0.91	---	0.89
		C	0.92	0.90	0.87	0.90	---	0.88
	G=340MPa	A	1.00	0.98	0.95	0.96	0.94	0.92
		B	0.97	0.95	0.92	0.91	0.90	0.89
		C	0.92	0.90	0.87	0.90	0.89	0.88

4.3 Buckling Specimen Design and Testing

This section summarizes the design, fabrication, and testing of small-scale multi-wrap buckling specimens conducted to validate analytical models developed for Keystone's spiral-welded tower concept. Because limited research existed on multi-wrap cylinders, the team at Northeastern University designed benchtop-scale specimens to experimentally assess buckling performance, bonding impacts to

buckling capacity, and agreement with finite element model predictions.

The specimens consisted of nested sheet-metal layers—an inner ‘pipe’ and outer ‘sleeve’—joined with structural adhesive or left unbonded. Early attempts using thin-walled welded configurations resulted in unacceptably large weld defects and premature failures, prompting a transition to fully bonded designs. Subsequent iterations of specimen design introduced (1) end-ring stiffeners to prevent local crushing and (2) intentionally manufactured dimples representing EN 1993-1-6 Tolerance Quality Class C imperfections. These refinements produced stable, repeatable buckling behavior.

Triplicate tests of three configurations—single-layer, two-layer unbonded, and two-layer adhesive bonded—revealed clear performance trends. The unbonded two-layer specimens carried approximately 76% of the single-layer capacity, while fully bonded specimens reached 95%, indicating that adhesive bonding effectively restores the structural integrity to be in-line with that of a monolithic shell. Statistical analysis showed no significant difference between the bonded multi-layer and single-layer results. Failure consistently initiated at the pre-fabricated dimples, validating their function as a means of controlling manufactured quality.

FEA simulations from Johns Hopkins reproduced the physical tests with exceptional accuracy. When realistic adhesive properties (E = 200 MPa, Fy = 10 MPa) were used, the model predicted a critical buckling load of 73.8 kips—98% of the measured average (75.2 kips). This close correlation confirms the reliability of the analytical methods used to predict multi-wrap shell performance. The results validate both (1) the modeling framework and (2) the structural viability of adhesive-bonded multi-wrap tower shells as efficient, high-performance alternatives to traditional single-thickness designs.

4.3.1 Multi-Wrap Buckling Specimen Plan & Anatomy

A major finding from the literature review, summarized in Section 4.1, is that there did not exist much research in the area of multi-wrap cylinders. The research was basically devoid of examples of physical tests and lacked recommendations for specimen construction techniques. Because of this lack of background or experience, a major recommendation from the literature review was to use small “benchtop” scale specimens that could be relatively easily tested and iterated upon. In other words, the test plan and how to execute it was expected to evolve throughout this project.

Given that the details would evolve, there was a general concept of the final appearance of the multi-wrap buckling test specimen. The basic geometry of the planned samples is shared in Figure 17. Two layers

(inner “pipe” and outer “sleeve”) of sheet metal were to be nested between end rings. The two layers may or may not be bonded with structural adhesive. The number of outer sleeves, and the associated weld spacing, could also be varied.

Figure 17. Planned Multi-Wrap Buckling Test Configuration

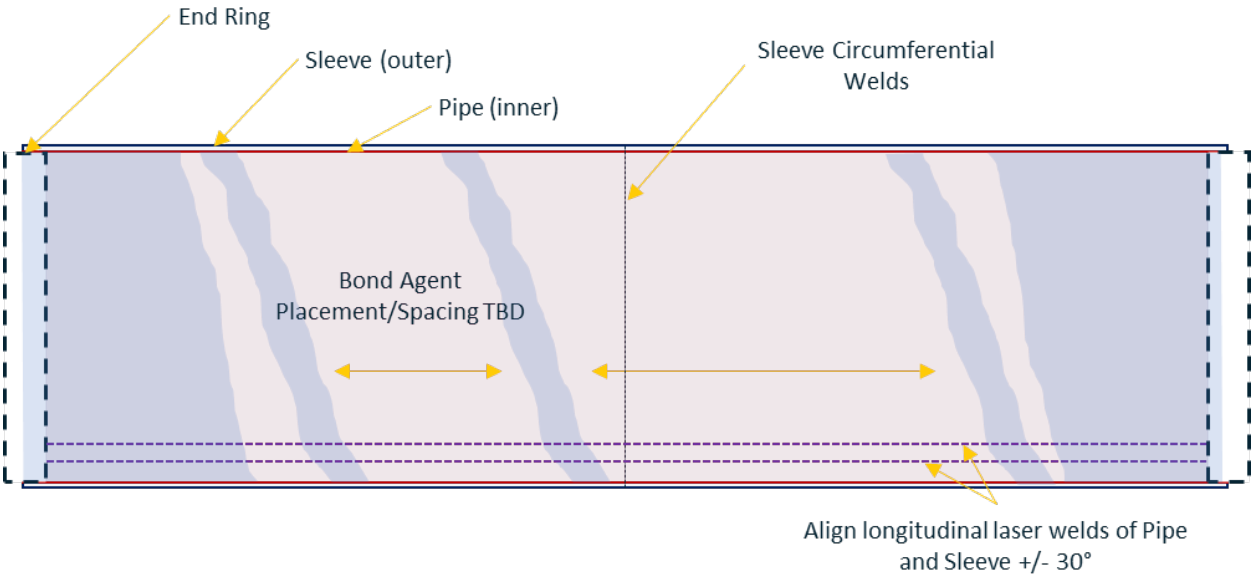

Luckily, a suitable test material was discovered to be readily available. Nordfab™ manufactures and distributes air ventilation ducting. They have standard off-the-shelf geometries that nest in exactly the way this project team planned for our test specimens. Nordfab™ graciously agreed, when we contacted them, to customize the end-finishes of their materials and ship them directly to our project team to avoid handling damage. An image of the tall inner “pipe” materials and shorter outer “sleeve” materials unpacked in a Northeastern University classroom is provided in Figure 18.

Figure 18. Benchtop Scale “Pipes” and “Sleeves” for Multi-Wrap Buckling Tests

These raw materials were assembled with end-rings to ensure the load imposed by the compressive test machine was uniformly distributed to the shell. Cantrell Quality, located in Boston, custom fabricated the end rings and collaborated with the several iterations of custom specimen assembly. A final specimen cut-out revealing the specimen anatomy is shared in Figure 19. The end rings, outer sleeve, inner pipe, and circumferential welds are identified. The inner and outer layers are both welded circumferentially to the end rings with a shared circumferential weld.

Figure 19. Benchtop Scale Test Specimen Anatomy

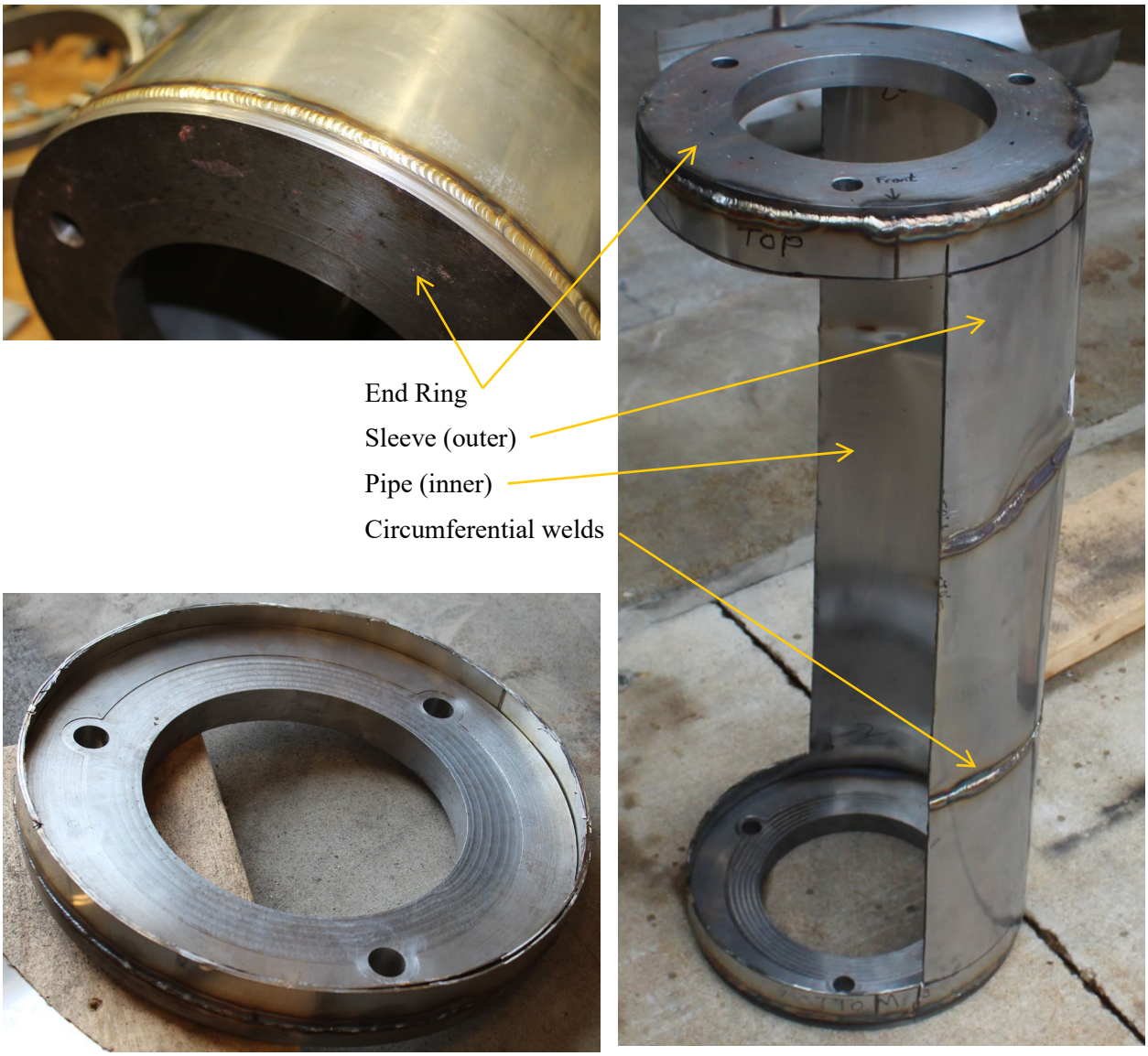

4.3.2 Pre-test Trials & Specimen Development

Several test specimen configurations were tested with poor results before testing could reliably proceed. So future researchers may avoid some of the same mistakes, these failed attempts are shared here.

Initially, a test configuration of interest was the use of a prismatic inner pipe with outer sleeves welded with butt welds into the inner pipe as a permanent backer. This configuration would closely mimic the "partially bonded" model configurations previously discussed in Section 4.2. The physical test samples ultimately proved impossible to fabricate. Observe in Figure 20 that significant weld defects were imposed on the test specimen. The act of welding very thin sheet meant that the weld energy was not

appropriately absorbed and distributed into the shell material. The scale of the defects far exceeded what would be achieved with scales typical of wind towers wherein the ratio of wire fill metal is much smaller relative to the volume of shell absorbing the weld heat.

Figure 20. Visible Flaw (Left), Premature Buckle (Center), Cross-Section of Weld Flaw (Right)

Attempts at improving welds were abandoned. Next, fully bonded specimen were attempted. The external surface of the inner pipe and internal surface of the outer sleeve were both fully coated in epoxy. The epoxy was applied and brushed into a uniform thickness coat, as can be observed in Figure 21. The sleeve was then telescoped over the pipe before the end ring circumferential weld was applied.

Figure 21. Structural Adhesive Uniformly Applied to Trial Specimen

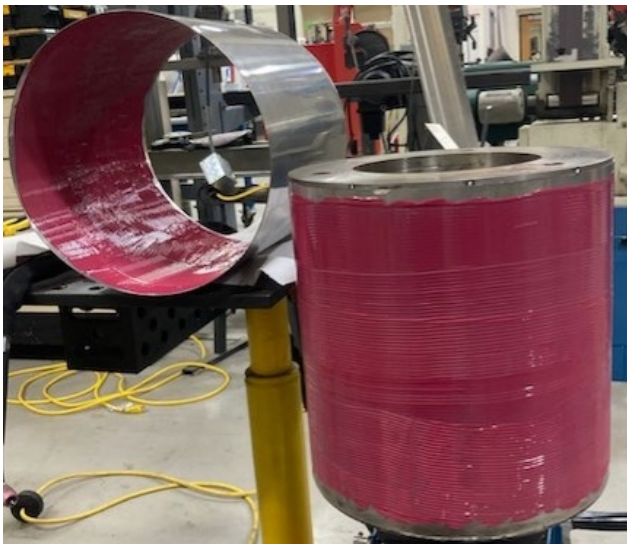

Preliminary test with fully bonded specimen were more promising. Failure loads were more consistent with expectations. Instead of dramatically premature failures, as with the welded samples, it was instead observed that buckling failure initiated somewhat prematurely and always near the end rings. This indicated that the compressive load was not getting uniformly distributed into the specimen shell. To combat the premature end buckling, end stiffening restraints were added to the specimen. The ring stiffeners were placed inside and outside the specimen at the ends. Premature end buckling and the improvement made with ring stiffeners is shown in Figure 22.

Figure 22. Bonded Specimen – End Crushing (Left) and Ring Stiffener (Right)

At this point, the tests were giving expected results; however, the variability was rather high and was largely dependent upon the as-fabricated quality of the steel tubes used for each specimen. To remove the impact of mixing higher and lower quality tubes, we decided to manufacture in a known dimple at the midspan of each test sample. The manufactured dimple was sized to represent a Tolerance Quality Class (TQC) “C” dimple, as defined by EN 1993-1-6. The dimple was formed by a Hammer and Dolly technique, as shown in Figure 23.

To form the dimple, two machined surfaces were held around the shell of the specimen. One surface (on the specimen ID) acts as an anvil. The anvil surface convexity matches the inner radius of the shell. In the center of the anvil, a concave circle was machine. The concavity of the circle matches the radius of the test specimen. The dolly is placed on the outer surface, perpendicular to the anvil, so that the convex surface will fit the machined circle of the anvil. The dolly side is repeatedly hammered until the specimen shell deforms into the machined dimple shape of the anvil. A resulting dimple is shown in Figure 24.

Figure 23. Anvil on ID (Left) and Dolly on OD (Right) to Form Dimple of Specified Size

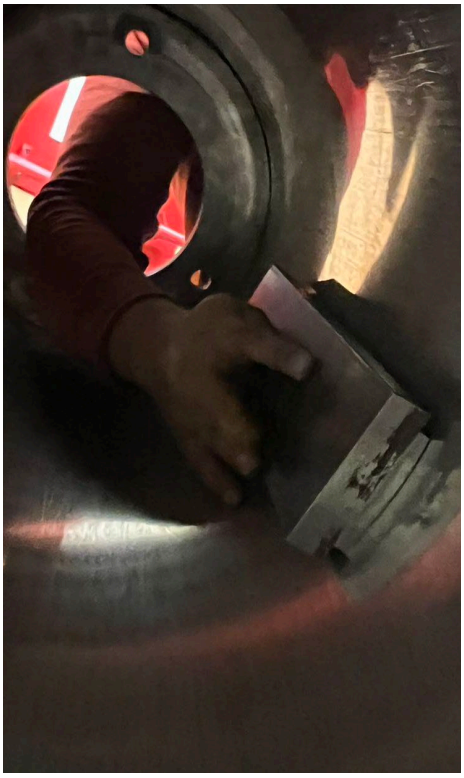

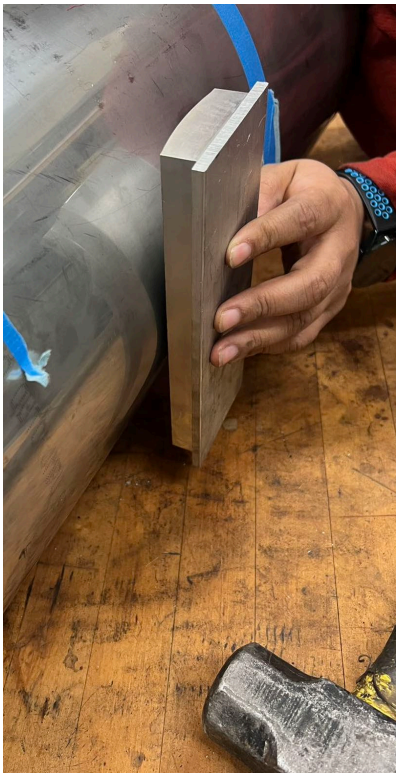

Figure 24. Manufactured Dimple of Known Size and Shape

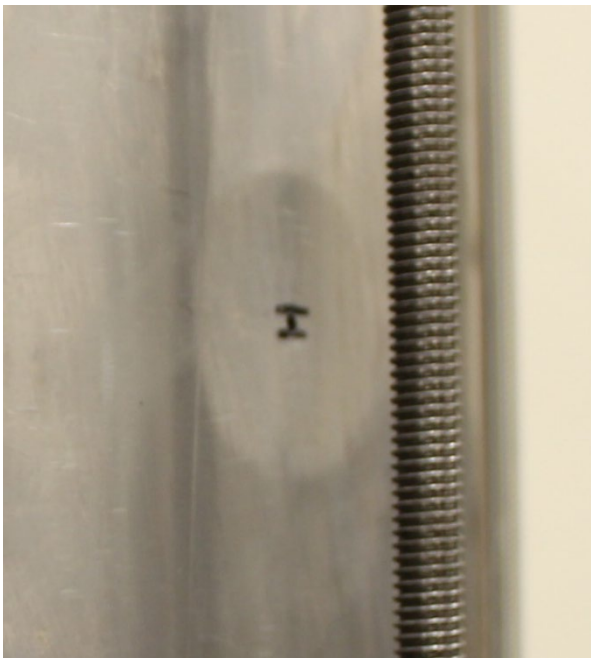

By eliminating large welded flaws, forcing failure away from the ends with ring stiffeners, and enforcing known fabrication quality of the specimen with manufactured dimples, the specimen test behavior was steady and predictable. The specimen design complete and ready for testing.

4.3.3 Multi-Wrap Buckling Tests

Triplicate buckling tests were performed on three specimen designs:

1. 2-layer, fully bonded.
2. 2-layer, unbonded.
3. 1-layer

The specimen were measured, instrumented, and tested in a way to capture several pieces of data. Major pieces of data included: (1) dimple geometry, (2) force-displacement read-outs, and (3) critical buckling load from the MTS machine, and (4) Force-strain from strain gauges spaced in even intervals around the circumference of each specimen.

Northeastern University attempted to gather surface point clouds as the specimen deformed. The attempt to gather surface point clouds failed because the surface of the steel was too reflective and the laser sensing equipment could not accurately locate the surface of the specimen. Attempts were made to reduce

the reflectivity of the surface – clear epoxy spray and black matte spray paint both failed to render a surface that could be detected for generating point clouds.

An example test setup and progression is depicted in Figure 25. The TQC-C dimple is placed mid-height on the specimen and is the location of buckle nucleation. The tests continued past critical buckling load to continue gathering force-displacement and force-strain data. The buckle wave progressed in a sinusoidal shape around the circumference of the specimen. The strain gauges are also visible in Figure 25.

Figure 25. Example Buckling Test Setup and Progression

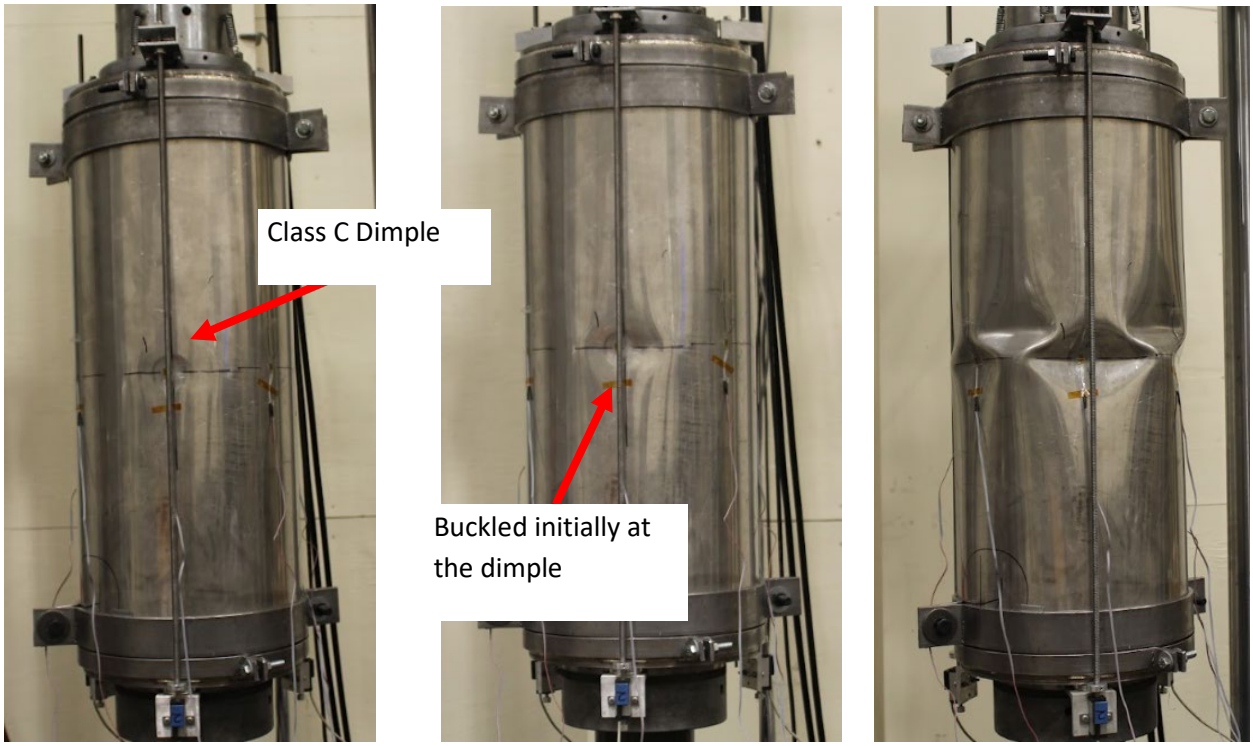

4.3.4 Multi-Wrap Buckling Test Results

Test results for nine (9) specimen are collated in Table 17. The specimen description and details about the test geometry are noted. The critical buckling load for each test is reported along with the average critical buckling load of the triplicate test. Consider the single-layer specimen as baseline; the unbonded specimen buckled at roughly 76% capacity and the adhesive bonded specimen buckled at 95% capacity. The single-layer and two-layer adhesive bonded test specimen results are close enough that a student t-test indicated that there is no statistically significant difference between the two data sets.

Table 17. Buckling Test Description and Results

Specimen No.	Layer Connection	Dimple Class	Boundary Conditions	Failure Location	F_{cr} (kips)	Avg. F_{cr} (kips)
Specimen-7	Adhesive	A	1” end collar	Failed near bottom end collar	69.5	---
Specimen-8		C	3” end collar	Failed top quadrant, seam weld	77.5	75.2
Specimen-9				Buckled simultaneously at the dimple and at top end collar	72.8	
Specimen-10	None			Buckled at midspan	52.4	60.3
Specimen-11				Buckled at midspan	66.7	
Specimen-12				Buckled at top end collar	61.7	
Specimen-13	Single Layer			Buckled at midspan	84.6	79.4
Specimen-14				Buckled at midspan	74	
Specimen-15				Buckled at top end collar	79.5	

The average force-strain curve for each specimen (except specimen-7, not collected) was graphed together in Figure 26. The average of each triplicate series is indicated by a star of the same color as the test series. One take-away is that each test demonstrated similar stiffness. The single-layer tests seemed to climb higher on the knee of the material curve before instability finally took-over and buckled the specimen.

Figure 26. Force-Strain Curve of Each Test

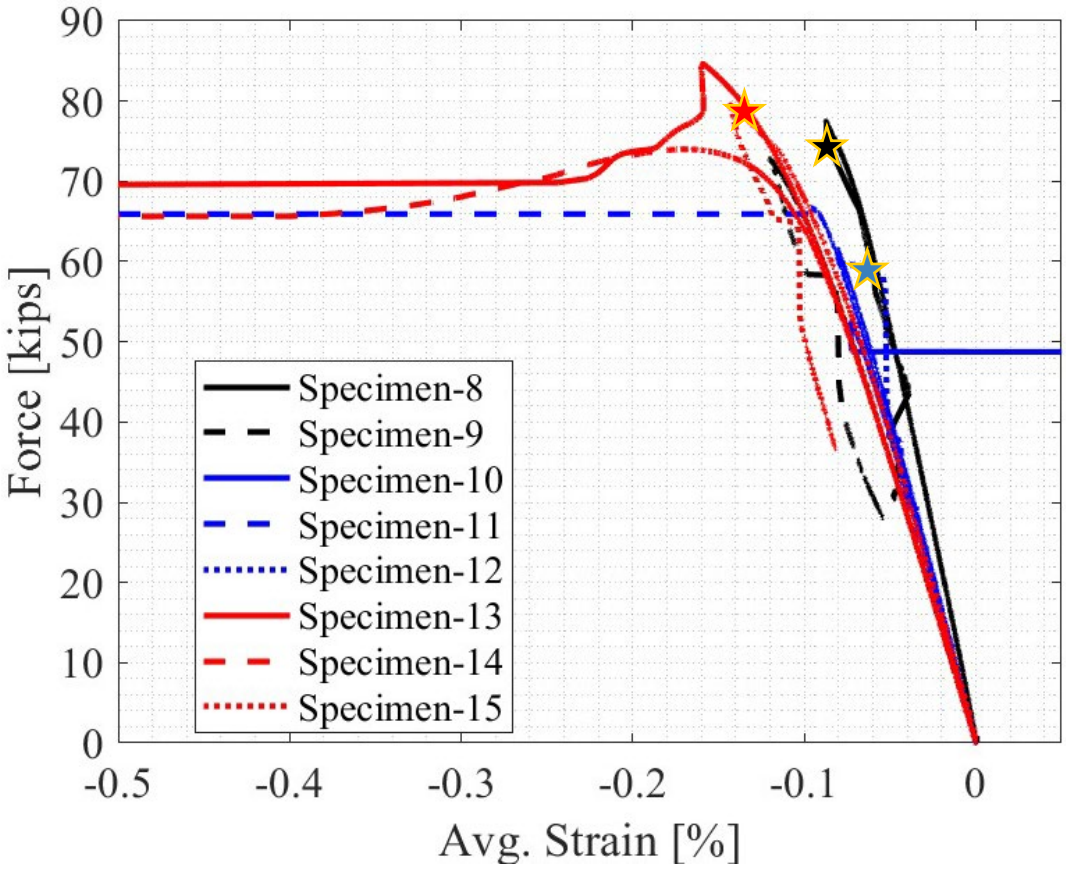

4.3.5 Matching Analytical & Test Results

Finally, Professors B. Schafer and S. Ádány from Johns Hopkins University modeled the "benchtop scale" specimens using true geometry and material characteristics to see how much agreement would be observed between models and actual test results.

The initial TQC-C dimple that was placed on the physical tests was replicated with a lateral force in the model space. The deflected shape of the cross-section in the model is depicted in Figure 27. The steel shell material curve was tested by Northeastern University and is shown in Figure 28. The material was modelled as a simplified tri-linear curve.

Figure 27. TQC-C Dimple Created in Model with Initial Lateral Loads

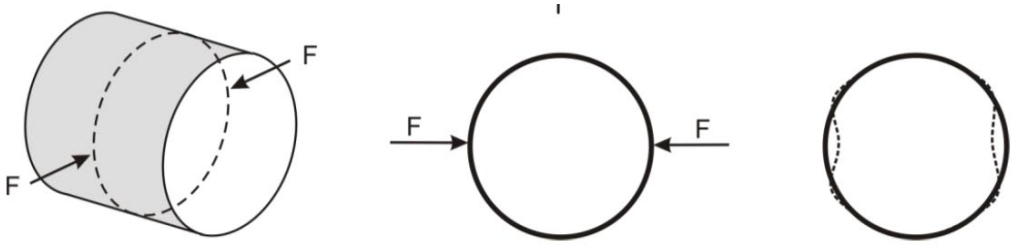

Figure 28. As-Measured Shell Material (Left) and Simplified Model Material (Right)

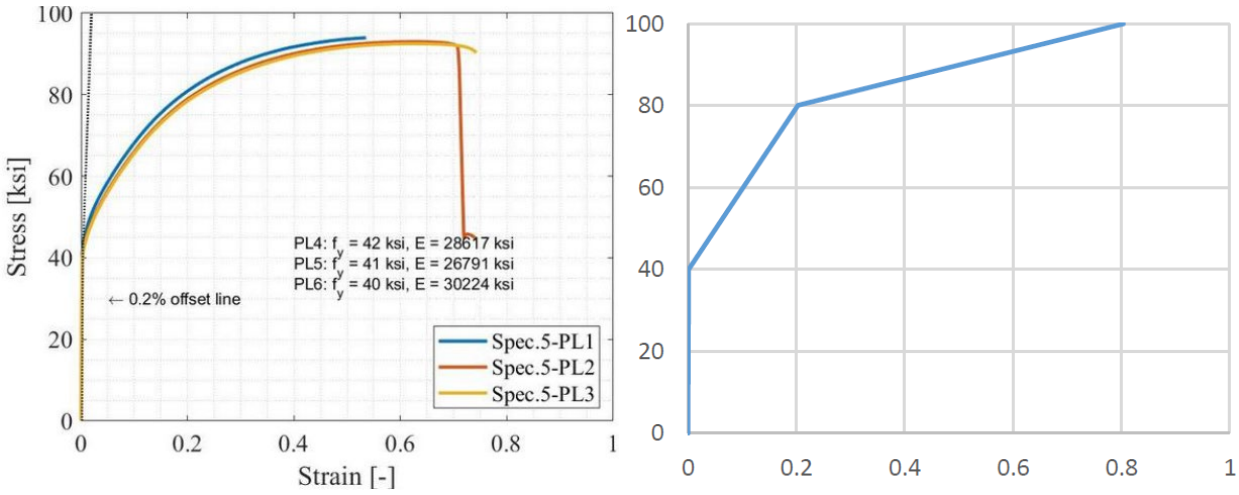

Two versions of the 2-layer fully adhesive bonded specimens were modelled:

1. Case 1: Ideal structural adhesive. Assuming narrow gap = 0.1mm, ideal thermal conditions while setting, and no environmental contamination.
    a. Young's Modulus, E = 2,000MPa

b. Yield Strength, F_y = 20MPa
c. Critical Buckling Load, F_{cr} = 87.1kips

2. Case 2: Realistically de-rated bond characteristics. Gaps up to 1mm likely occurred. Specimens were fabricated in humid and cold conditions.
   a. Young's Modulus, E = 200MPa
   b. Yield Strength, F_y = 10MPa
   c. Critical Buckling Load, F_{cr} = ***73.8kips***

The force-strain data for specimen-9 are plotted next to the Case 2 FEA model results in Figure 29. There is remarkable agreement between these two cases. The two-layer fully bonded model with realistic adhesive properties (***73.8kips***) very closely matched the physical test results for the same specimen design; as previously reported (Table 17), the average critical buckling load expected is ***75.2kips***. The model results achieve a critical buckling load that is 98.1% of the average test results. The model results are not different from the test results with statistical significance.

Figure 29. Physical Test Results (Left) and Model Results (Right)

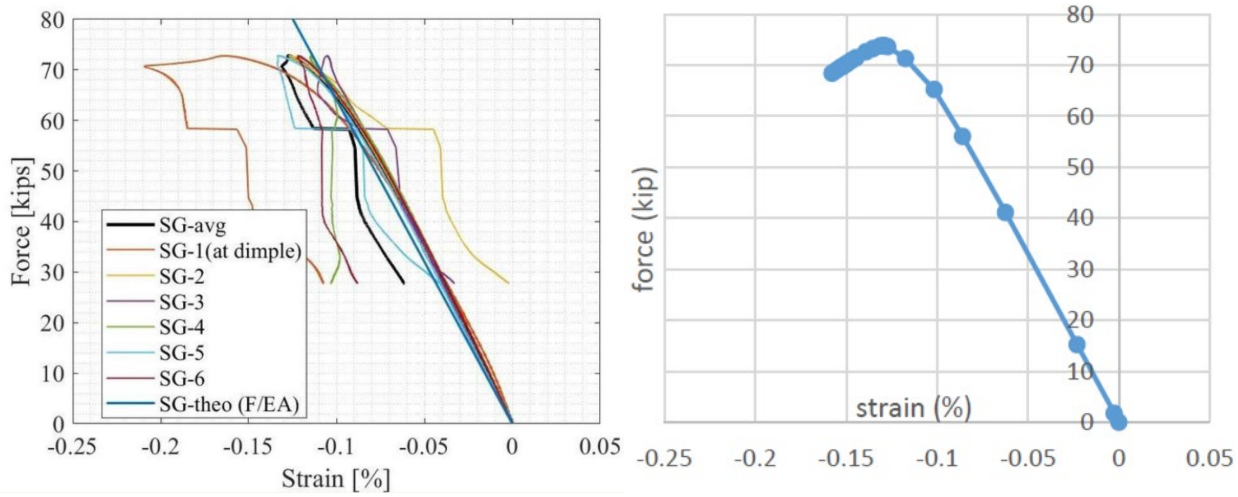

4.4 UT and Fatigue Testing

The buckling models and physical testing indicated that 2-layer shell structures that are fully bonded can likely achieve critical buckling loads consistent with single-layer, monolithic, shell structures. Fatigue is the other major failure mode checked for wind tower structures and is being investigated in this section.

Keystone fabricated 3-layer panels using weld procedures typical of their SAW helical weld procedures. The 3-layer panels were fabricated to investigate the weld quality, destructively and non-destructively, and to establish seminal research in a unique weld detail for multi-layered shell structures. The general

layout of the physical test panels is depicted in Figure 30. The test panels were made of flat plates and were created layer-by layer, from (bottom-to-top) in a fashion that represents the planned spiral-welded fabrication technique for a multi-layer wind tower (inside-to-outside).

Figure 30. Test Panel Geometry Viewed Through-Wall Slice (Left) and Outside Surface (Right)

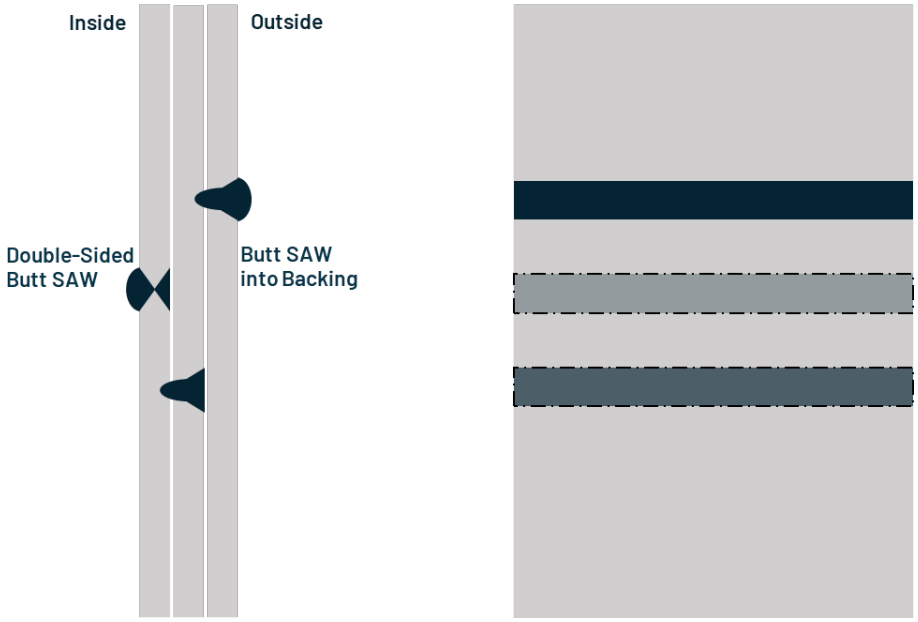

The test panels were sized such that up to six (6) fatigue dogbone specimen may be cut and retrieved from each panel. The three-layer test panel gross dimensions and fatigue specimen cut plan are shown in Figure 31. The fatigue dogbone specimen geometry is detailed in Figure 32.

Figure 31. Dogbone Specimen Layout on Test Panel

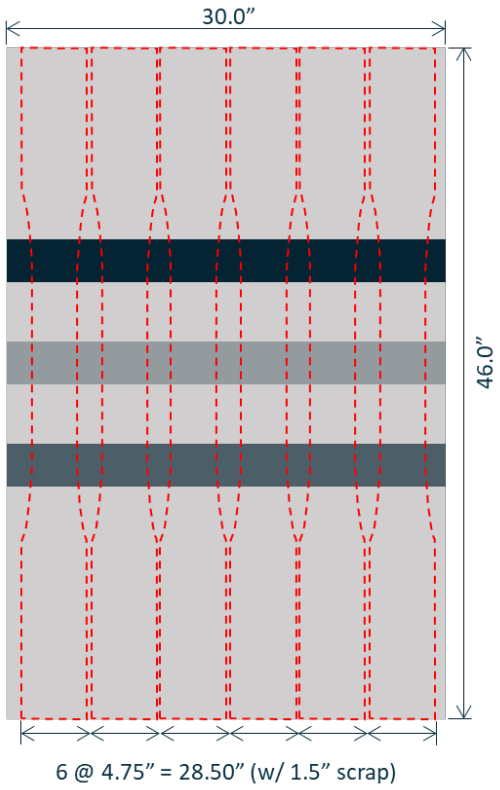

Figure 32. Dogbone Specimen Dimensional Details

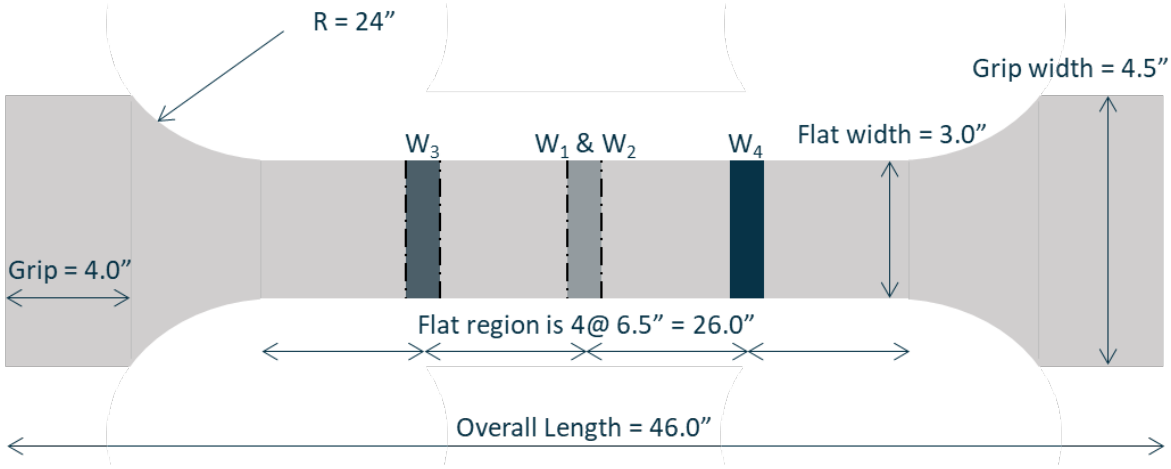

The following sub-sections provide more details in the fabrication, testing, and fatigue life results of these 3-layer test specimen. In short, the weld procedures were successful and the panels allowed the successful retrieval of a sufficient number of multi-layer dogbone specimen. The welds appeared ductile and tough and even sharply bending the welds did not induce tearing at the layer boundary. Phased Array Ultrasonic

Testing (PAUT) inspections were performed on known flaws machined into the welds of each layer; all flaws were visualized and appropriately sized.

Fatigue testing indicated that the weak point of this unique multi-layer specimen was at the weld toe of surface-breaking welds. Ten welds were tested in fatigue and one survived runout of 10million cycles. Of the nine (9) failed specimen, eight (8) occurred at an exterior surface weld toe. The observed behavior was consistent with expectations. The theory, and the results of the fatigue testing, indicate that a shell formed from multiple layers will exhibit fatigue resistance consistent with single-layer, monolithic, shell structures. In this case, the surface butt welds were fabricated to detail category 80 (DC80), as defined by Table 8.3 if the European Code[9] and the multi-layers sample results indicated at least DC80 performance.

4.4.1 Three-Layer Panel Fabrication

The designed test panels were fabricated in Keystone's shop in Denver, Colorado. Keystone's existing tower manufacturing procedures were used or mimicked as closely as practicable in a shop setting. Detailed test panel fabrication steps are given below and reference layer and weld numbers, as depicted in Figure 33. Weld procedure instructions reference Table 18. Pictures follows the manufacturing steps to assist the understanding of the reader.

Figure 33. Test Panel Fabrication Sequence

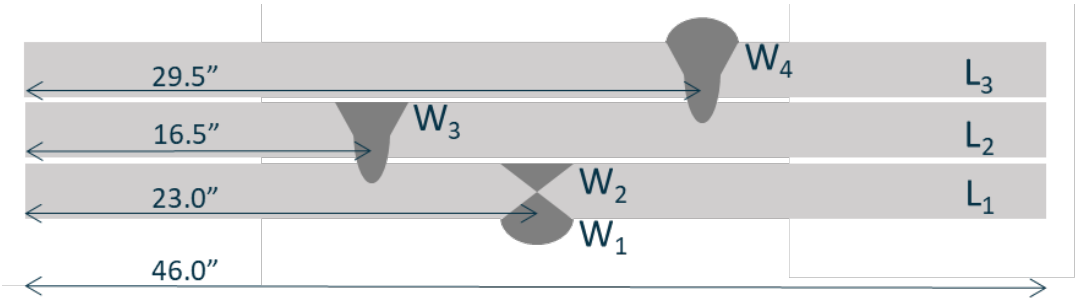

[9] European Committee for Standardization (CEN). 2005. "EN 1993-1-9: Eurocode 3 – Design of steel structures – Part 1-9: Fatigue, incorporating Amendment A1:2017," Brussels: CEN.

Table 18. Weld Parameter Settings

Weld			Lead Wire Settings				Trail Wire Settings			
ID	Pass	Travel (mm/s)	Angle	Feed Mode	Amps	Volts	Angle	Feed Mode	Amps	Volts
W_1	Single	7.5	2° drag	50 IPM CV DC+	---	34.0	---	---	---	---
W_2	Single	7.5	2° drag	60 IPM CV DC+	---	31.5	---	---	---	---
W_{3-1}	First	15	2° drag	CC DC+	880	30.0	12° Push	CC AC	800	34.0
W_{3-2}	Second	15	2° drag	CC DC+	600	34.0	12° Push	CC AC	650	36.0
W_{4-1}	First	15	2° drag	CC DC+	880	30.0	12° Push	CC AC	800	34.0
W_{4-2}	Second	15	2° drag	CC DC+	600	34.0	12° Push	CC AC	650	36.0

Fabricate test panel:

1. At a fabrication worktable, align two 46” X 23” X 0.5” plates for a SAW butt weld to form the first layer, L_1. Tack together at ends for handling. See Figure 34 below.
    a. Joint detail = 60° included bevel, 5mm land, no in-plane gap.
2. Position L_1 on the weld gantry and clamp same to worktable. Perform the first weld, W_1:
    a. Set weld head start and stop positions.
    b. Input weld parameters according to Table 18 above.
    c. Execute the weld. Monitor for flux deposition and intervention in case of blowthrough or other deviations. See Figure 35 below.
    d. Stop the weld when complete. Clean and remove flux.
    e. Visually inspect the completed weld. Make note of flaws, as necessary.
3. Immediately, while warm, unclamp and remove L_1 from the weld gantry worktable. Flip L_1 so that W_1 is positioned on the bottom surface, facing the floor.
4. Position L_1 on the weld gantry and clamp same to worktable. Perform the second weld, W_2:
    a. Set weld head start and stop positions.
    b. Input weld parameters according to Table 18 above.
    c. Execute the weld. Monitor flux deposition and intervene in case of deviations.
    d. Stop the weld when complete. Clean and remove flux. See Figure 36 below.
    e. Visually inspect the completed weld. Make note of flaws, as necessary.
5. Let W_2 cool to room temperature while clamped to the weld gantry worktable.
6. Unclamp and remove L_1 from the weld gantry worktable. Transport to fabrication worktable.
7. Grind W_2 weld cap flush to L_1 plate surface.
8. Measure the deflection of L_1 in the direction perpendicular to welds W_1 and W_2.
    a. If deflection exceeds ¼” over the 46” span, cold work until under ¼” limit. Execute cold work procedure which is omitted from this final report.
9. Align 46” X 16.5” X 0.5” and 46” X 29.5” X 0.5” plates for a SAW butt weld to form the second layer, L_2. Fix L_2 into place by tacking to L_1 periodically around the shared perimeter.
    a. Joint detail = 60° included bevel, no land / knife edge, 2mm in-plane gap.
10. Position panel on the weld gantry and clamp same to worktable. Perform the third weld, W_3:
    a. Set weld head start and stop positions.
    b. Input weld parameters according to Table 18 above for W_{3-1}.

c. Execute the weld. Monitor flux deposition and intervene in case of deviations.
d. Stop the weld when complete. Clean and remove flux.
e. Visually inspect the completed weld. Make note of flaws, as necessary. See Figure 37 below.
f. While warm, input weld parameters according to Table 18 above for $W_{3\text{-}2}$.
g. Execute the weld. Monitor flux deposition and intervene in case of deviations.
h. Stop the weld when complete. Clean and remove flux.
i. Visually inspect the completed weld. Make note of flaws, as necessary.

11. Let W_3 cool to room temperature while clamped to the weld gantry worktable.
12. Unclamp and remove panel consisting of L_1 and L_2 from the weld gantry worktable. Transport to fabrication worktable.
13. Grind W_3 weld cap flush to L_2 plate surface. See Figure 38 below.
14. Measure the deflection of the panel in the direction perpendicular to welds W_1 through $W_{3\text{-}2}$
    a. If deflection exceeds ¼" over the 46" span, cold work until under ¼" limit. Execute cold work procedure which is omitted from this final report.
15. Align 46" X 29.5" X 0.5" and 46" X 16.5" X 0.5" plates for a SAW butt weld to form the third and final layer, L_3. Fix L_3 into place by tacking to L_2 periodically around the shared perimeter.
    a. Joint detail = 60° included bevel, no land / knife edge, 2mm in-plane gap.
16. Position panel on the weld gantry and clamp same to worktable. Perform the fourth and final weld, W_4:
    a. Set weld head start and stop positions.
    b. Input weld parameters according to Table 18 above for $W_{4\text{-}1}$.
    c. Execute the weld. Monitor flux deposition and intervene in case of deviations.
    d. Stop the weld when complete. Clean and remove flux.
    e. Visually inspect the completed weld. Make note of flaws, as necessary.
    f. While warm, input weld parameters according to Table 18 above for $W_{4\text{-}2}$.
    g. Execute the weld. Monitor flux deposition and intervene in case of deviations.
    h. Stop the weld when complete. Clean and remove flux.
    i. Visually inspect the completed weld. Make note of flaws, as necessary.
17. Let W_4 cool to room temperature while clamped to the weld gantry worktable.
18. Unclamp and remove panel consisting of L_1 through L_3 from the weld gantry worktable. Transport to plasma cut table.
19. Cut approximately 8" from each edge of the completed panels to remove flawed lead-in and run-out portions of welds W_1 through W_4. See Figure 39 below.
20. Measure the deflection of the panel in the direction perpendicular to welds W_1 through W_4.
    a. If deflection exceeds ¼" over the 46" span, cold work until under ¼" limit. Execute cold work procedure which is omitted from this final report
21. Repeat steps 1 through 20 for panels P_2 and P_3.

Figure 34. First Layer Butt Weld Joint Profile and Handling Tack Weld

Figure 35. Execute SAW Weld and Observe for Deviations

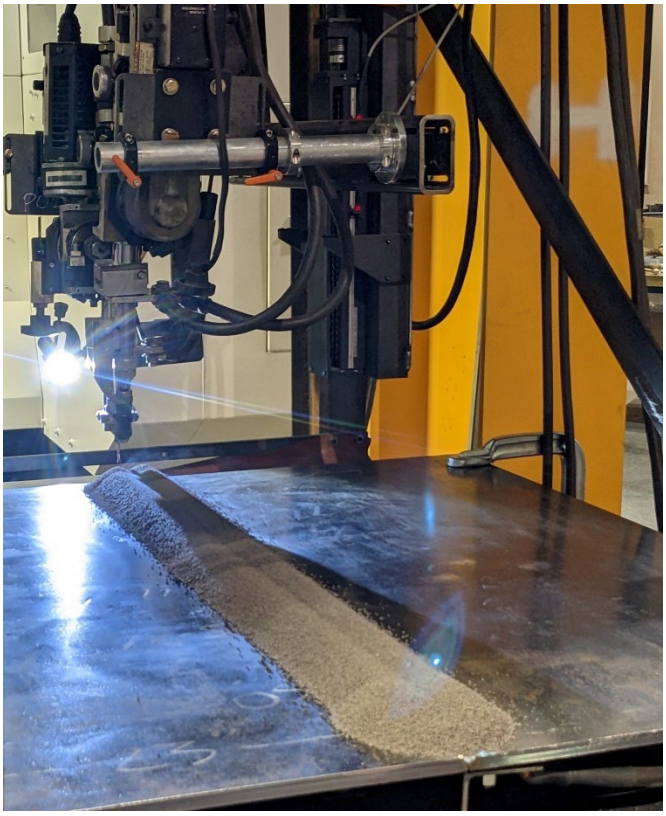

Figure 36. Clean Unspent Flux and Remove Flux Cap

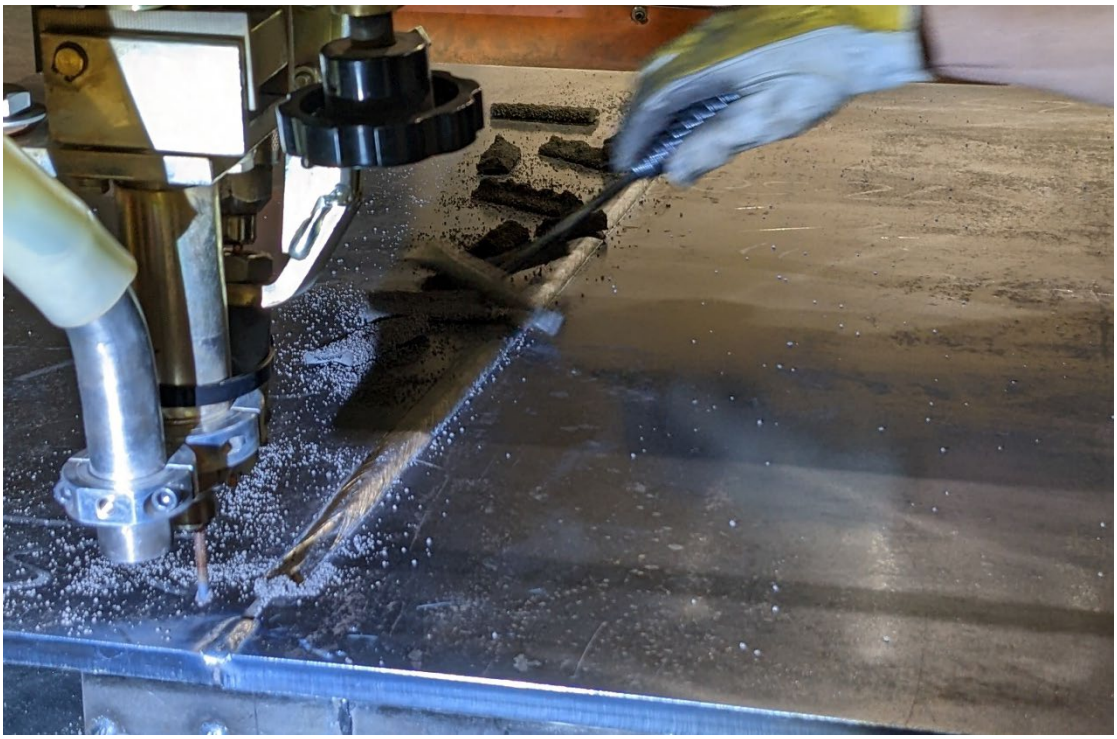

Figure 37. Visually Inspect Cleaned Welds (Left) First Pass (Right) Second Pass

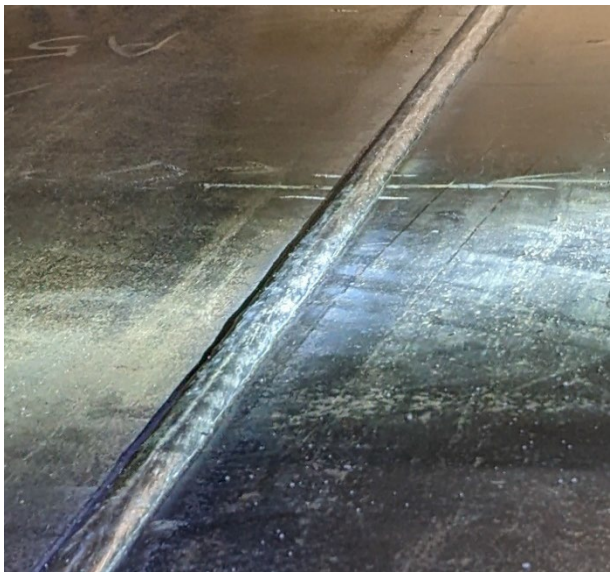

Figure 38. Remove Cap by Grinding

Figure 39. Plasma Cut Lead-in & Run-out of Completed Panels (Left) During Cut (Right) Complete

Cooling shrinkage of the welds was minimized by clamping the panels to the weld gantry worktable and allowing the panel to cool slowly to room temperature. Some shrinkage induced deflection of the various

layers still occurred. Keystone determined that it would be preferable to cold work the test panels straight rather than allow large inter-layer deflections and gaps to develop. Keystone determined “straight” was a deflection of less than ¼” over the 46” dogbone speciemen length. Note that a multi-wrap tower would cool in such a way as to tighten the outermost layer around the mandrel tower thereby minimizing deflections and locking in residual tensile weld stresses. A cold working procedure was developed and executed, but is not detailed here in this final report.

4.4.2 Three-Layer Panel Destructive and Non-Destructive Testing

Upon completing three test panels, they were examined to ensure no obvious and significant flaws existed. Several cross-sections were taken and examine. Observe in Figure 40 that two weld passes and their heat-affected zones are readily visible. The root of the first weld pass penetrates a backing plate. The lower and upper plates are held snug together, and the plate layer is only visible as a dark horizontal line.

Figure 40. Etched Weld Prepared for Side Bend Test

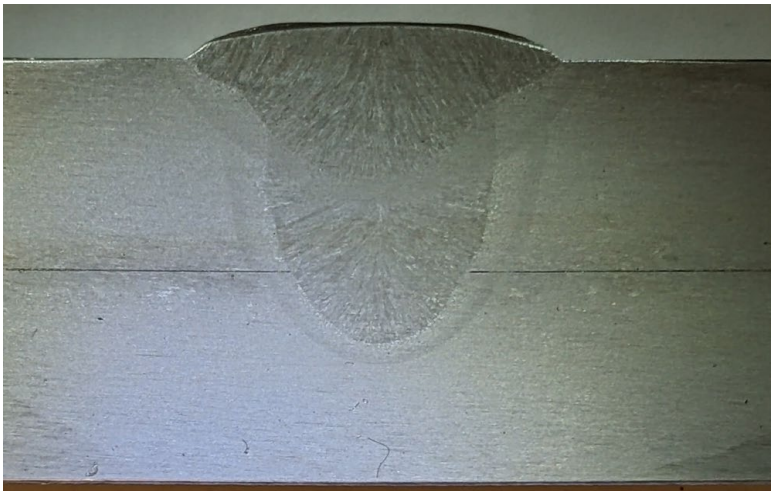

The weld cross-sections were then bent around a 2” diameter die. The highly deformed face of the weld cross-section samples is shown in Figure 41. No specimens ruptured, so the welds appear ductile. The layers held together with the penetrating first weld pass appear to separate due to anticlastic bending. Where the two layers intersect the weld are sharply notched; however, the weld did not tear or fracture, so the welds appear tough.

Figure 41. Weld Post-Bend

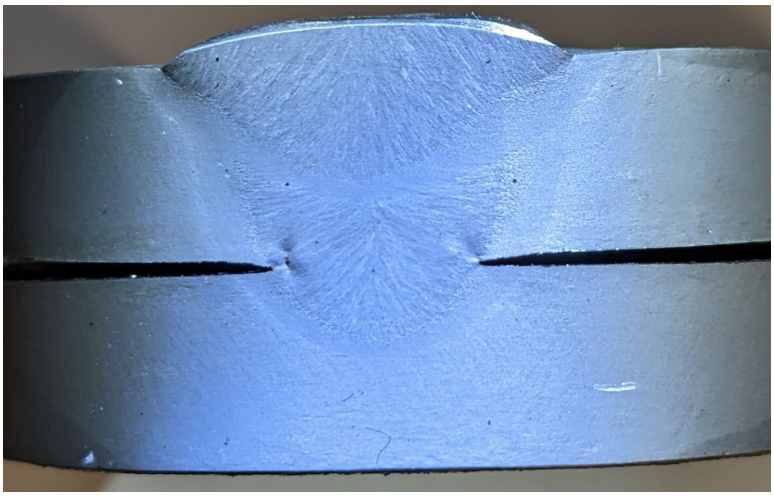

The panels were shipped to Edison Welding Institute (EWI). EWI was contracted to perform non-destructive PAUT testing of the multi-layer panels. EWI cut dogbone specimen from the panels and machined flaws into two of them for PAUT inspection. The flaws were planted as side-drilled holes. The PAUT inspection sample flaws and geometry details were manufactured by EWI from the three-layer panels and are detailed in Figure 42 and Figure 43.

Figure 42. PAUT Inspection Test Specimen & Machined Flaws

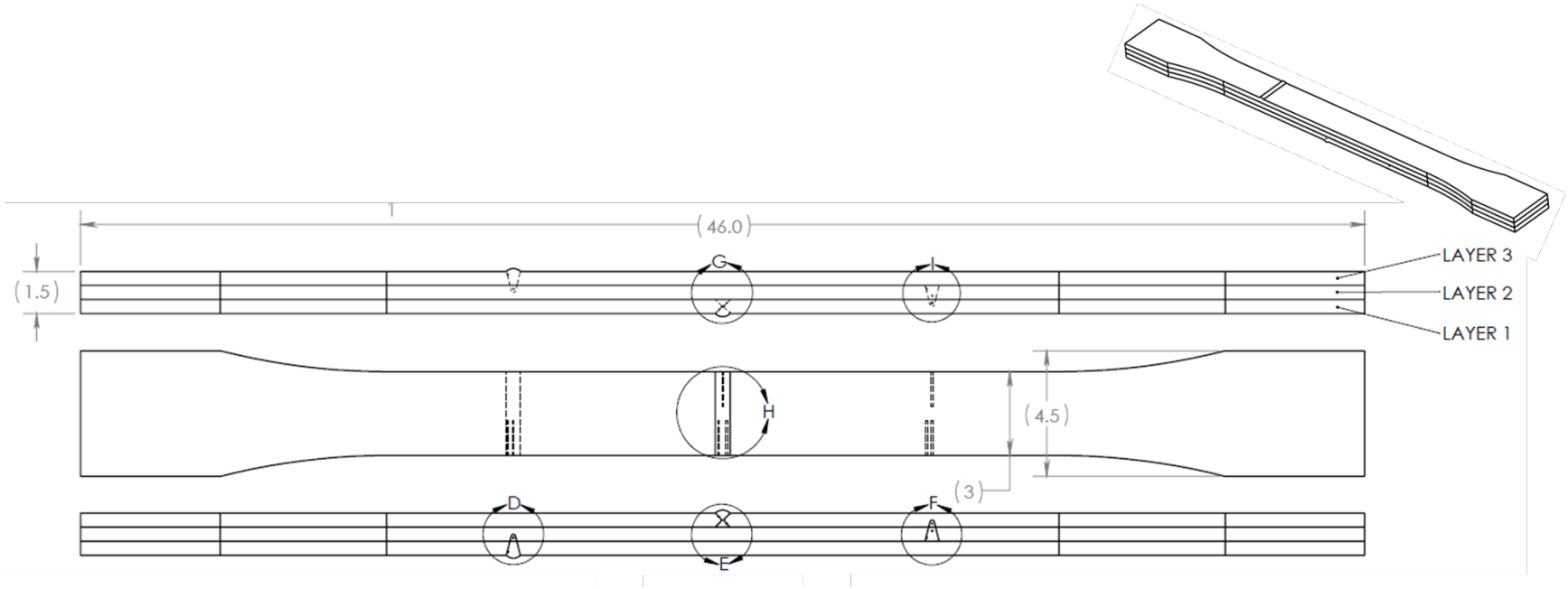

Image credit: Edison Welding Institute (EWI)

Figure 43. PAUT Machined Flaws Details

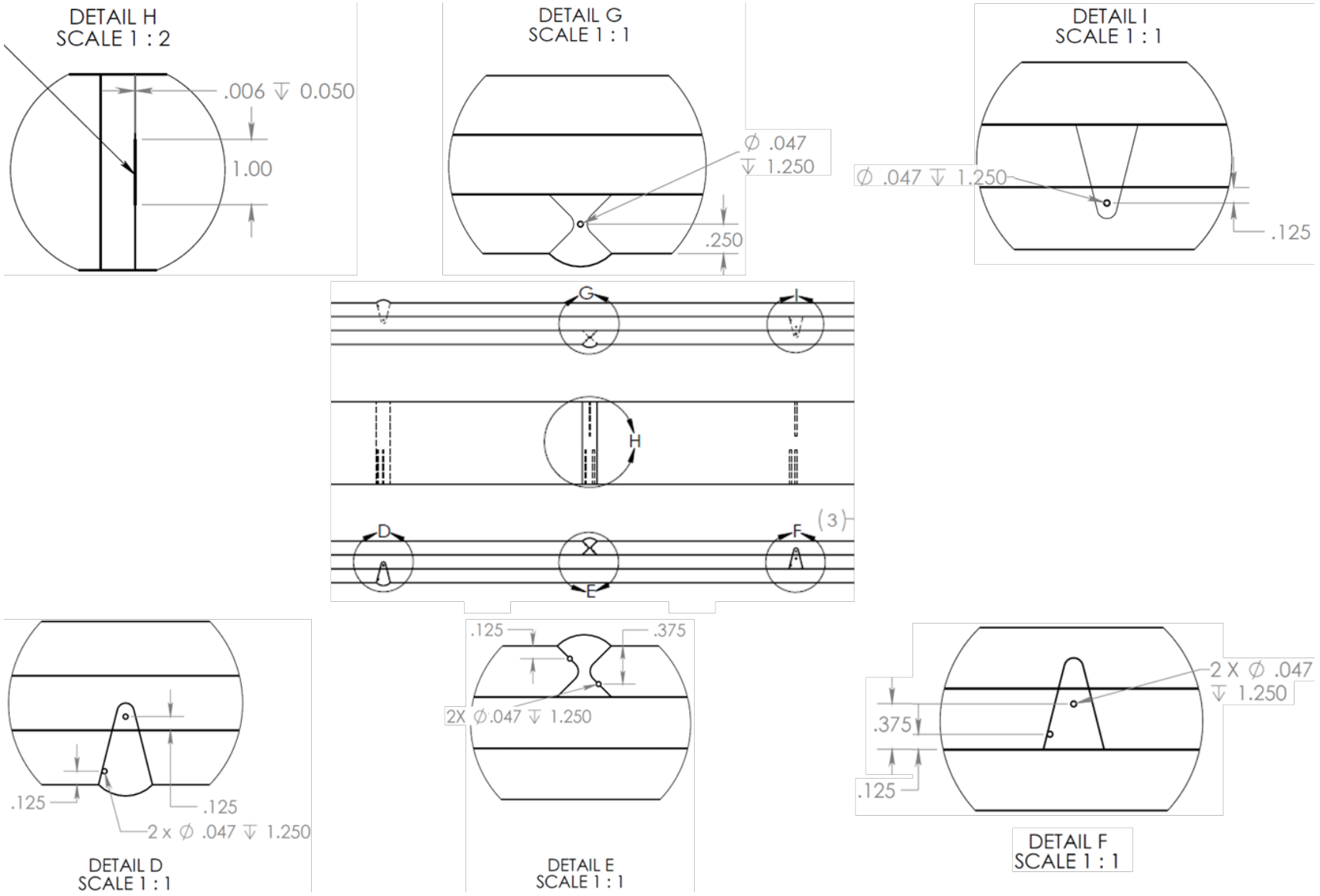

Image credit: Edison Welding Institute (EWI)

For butt joints, several angled beam inspection techniques are available, as depicted in Figure 44. The self-tandem (a) technique is good at detecting near-surface planar flaws such as delamination. Sector pulse-echo (b) uses all elements to send and receive signal across a broad range of angles and is a good technique for broadly viewing weld volumes and fusion zones. The creeping wave (c) technique is specialized to inspect the near surface. Time-of-flight diffraction (d) uses two separate signal and receiver probes. EWI was able to detect *all flaws*, even the surface "crack" type machined flaw, while only using the sector pulse-echo, (b), inspection technique. Further, all flaws were detected without needing to adjust amplitude of the sound waves.

The success of the initial inspections at discovering all flaws and accurately locating them meant that there was no need for development of a unique mulit-layer inspection methodology. The TPAC Explorer 60element probe with Prelude software appears highly robust at finding and characterizing flaws. Note; however, that certain flaws are only observable from one side of the weld or from either the top or bottom of the plate. Thus, a field weld inspection procedure would require double inspection of the concealed (mid-layer) helical weld when scanning through the root of W_3.

Figure 44. PAUT Inspection Techniques

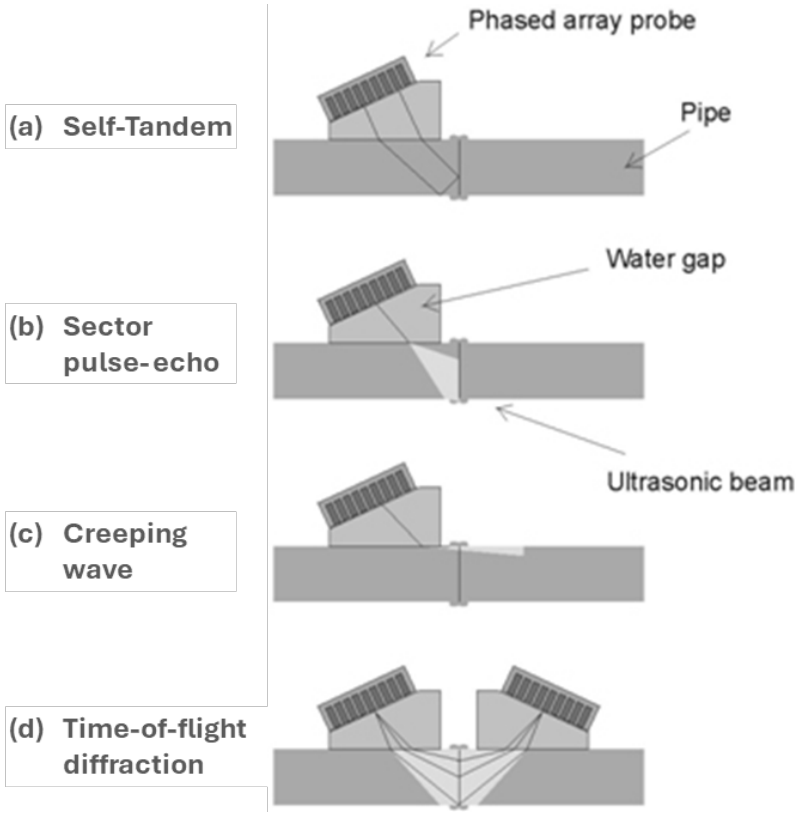

Image credit: The Welding Institute (TWI)

This final report will not belabor the inspection technique or results for each flaw; however Detail H observation is depicted to give the reader an understanding of the findings and how they were interpreted. Refer to Figure 43 to see that the detected flaw was a surface-breaking crack-like flaw. The PAUT inspector observed the results, captured in a screenshot, which is shared in Figure 45, below. The blue field represents all sound waves sent out by the inspection probe. One region of sound waves were returned to the receiver, indicating a flaw that reflected the sound waves. The flaws are measured as approximately 1" deep on the ½" thick test layer – indicating a flaw on the same surface as the probe.

Figure 45. Detail H Inspection Results

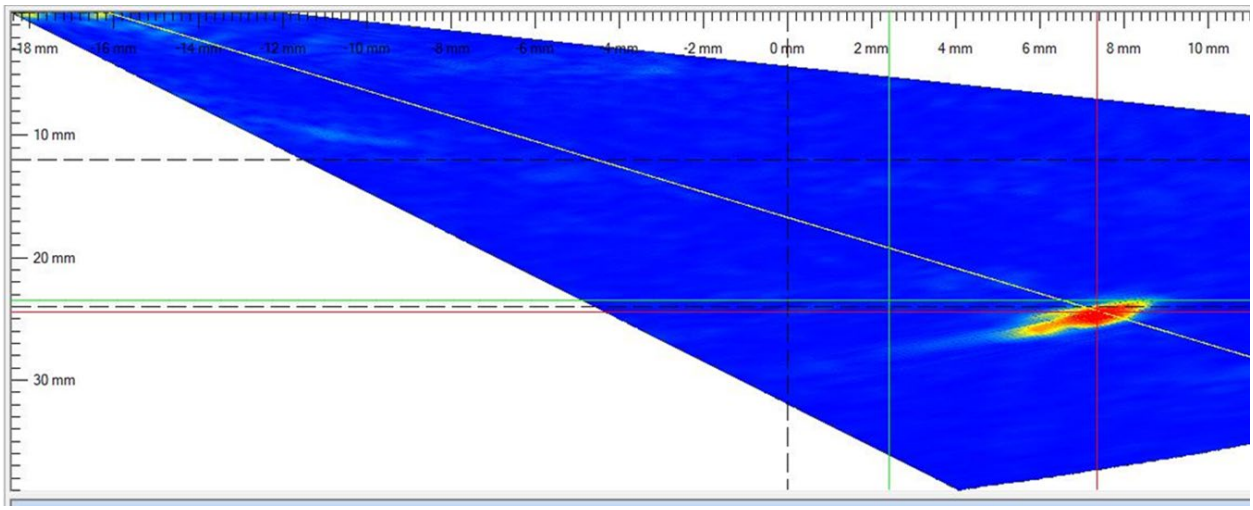

A depiction of this observation is provided in Figure 46. The blue arrows indicate a number of sound waves that are sent out by the probe in many directions. The red solid line indicates a sound wave that happens to encounter a flaw. The red dashed line is the reflected sound wave of that flaw that is returned to the receiver.

Figure 46. Explanation of Detail H Observation

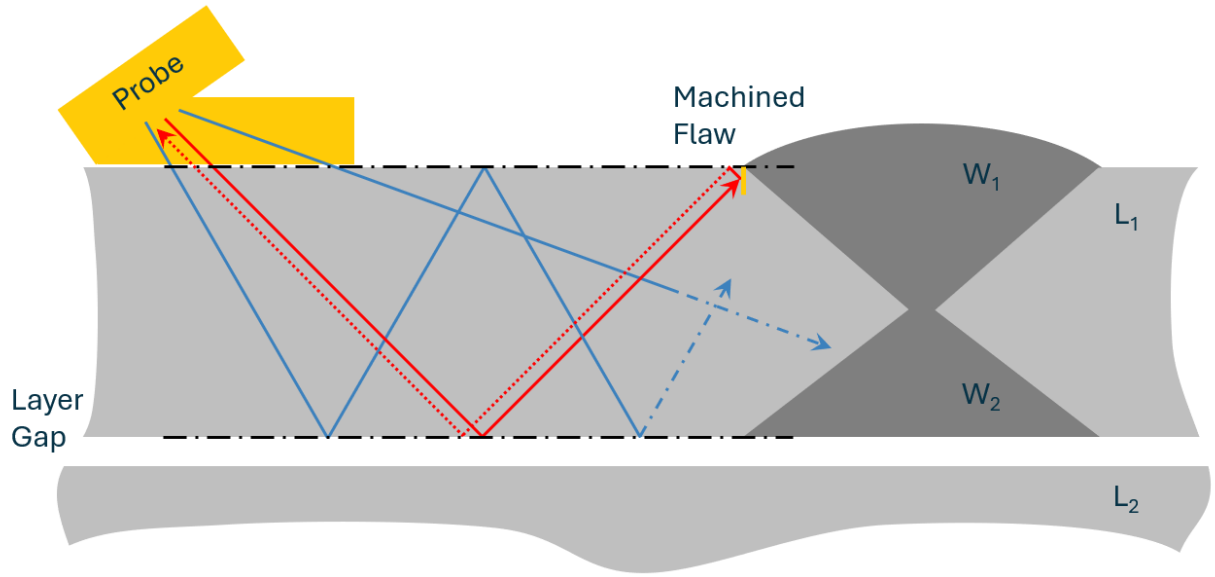

All planted flaws were observed by EWI. The details of each flaw are not repeated here. Limits to the success of this technique were considered. It is possible that some configurations may conceal flaws, such scenarios may include:

- Layers without surface connection after manufacture, such as shells with four or more layers.
- Vertical cracks, rather than planted drilled holes, may reflect inspection waves away from the receiver. Such an example is depicted in Figure 47.

Figure 47. Detail I-Type Flaw – Vertical Crack

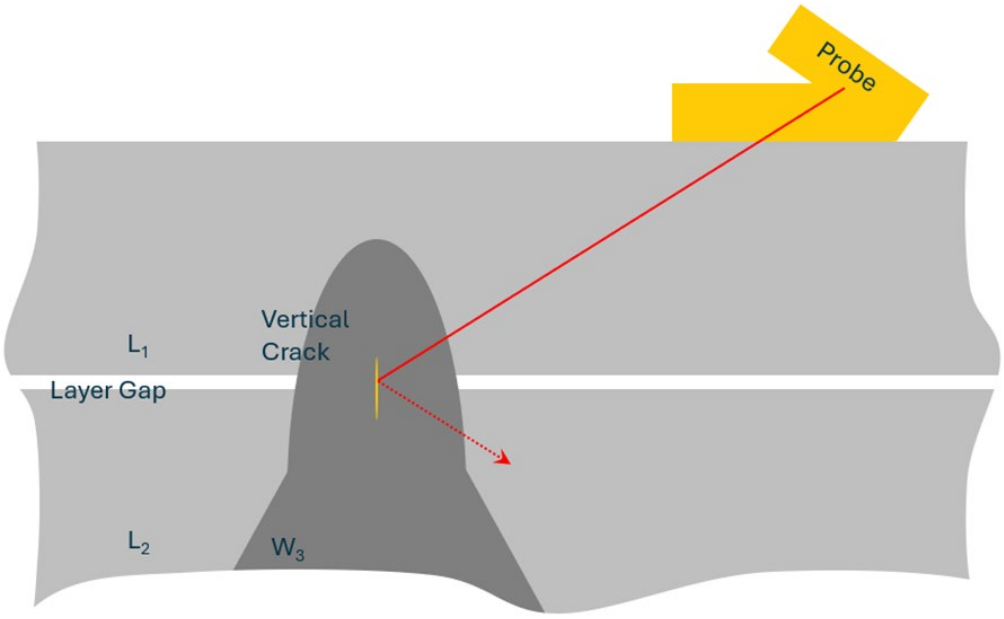

4.4.3 Three-Layer Panel Fatigue Testing & Results

EWI also performed fatigue testing on the three-layer dogbone samples they cut from the test panels. They cut the dogbone samples with a water jet. EWI removed hard edges and cut-induced flaws by grinding the edges of the samples with a high grit flapper wheel. They then instrumented each layer of the samples and loaded them into a 220kip servo-hydraulic fatigue testing machine, as shown in Figure 48. Each test was performed at a frequency of 2-3Hz.

Figure 48. Fatigue Sample Instrumented and Loaded in the Test Frame

All tests were conducted with a cyclic stress ratio, defined as the ratio of minimum stress to maximum stress, of R=0.5. R=0.5 indicates that the fatigue stress remains tensile throughout the test and is considered conservative. The actual applied stress range of a wind tower in service is likely to correspond to a lower R-ratio throughout it's service life.

Each layer was instrumented with strain gauges to monitor specimen failure progression. Three events in the fatigue life were recorded for each specimen: (1) Fatigue crack initiation, (2) complete failure of the first layer, and (3) complete failure of the second layer. The number of cycles to each event was recorded. The test stresses were high enough that the test was halted immediately following rupture of the second layer. The third layer would fail in a typical yield to rupture fashion on the next cycles if the test were allowed to continue. Example images of the failure progression are shared in Figure 49 through Figure 51.

Figure 49. Specimen 2-A – Fatigue Crack Initiation

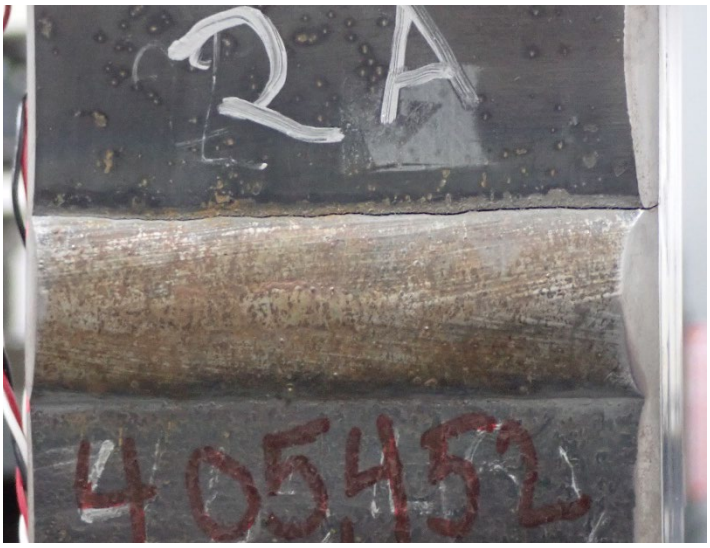

Figure 50. Specimen 2-A – Failure of 1st Layer (Left & Right Views)

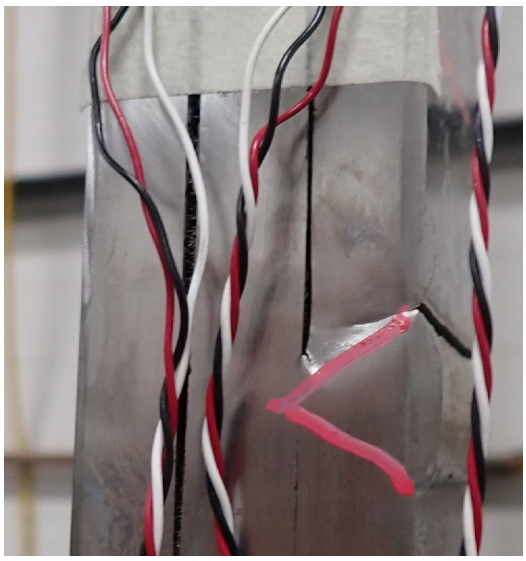

Figure 51. Specimen 2-A – Failure of 2nd Layer (Test Completion)

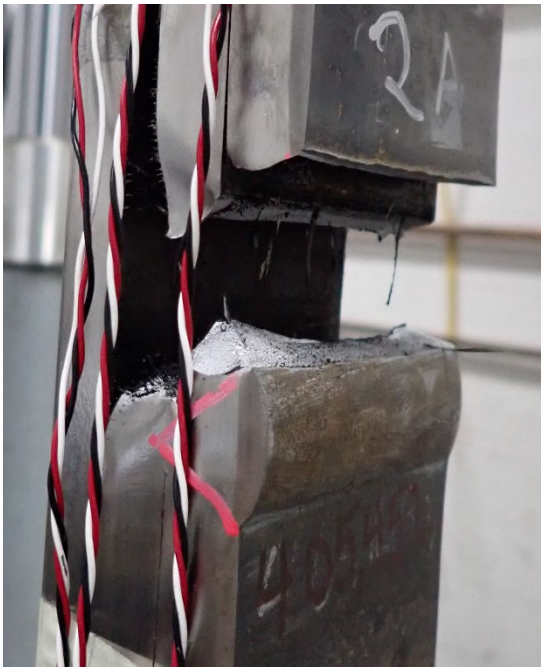

Results for all tests are reported in Table 19. The failure points (cycles to 2nd rupture) plotted on a stress-log(cycle) graph in Figure 52 are placed relative to standard EN1993-1-9 design curves. Observe that two statistical outliers (high) were identified (Samples 1-D and 3-A) and removed from the analytical results. By selecting a slope of m=(-)3, curves were plotted for (1) mean (black dashed) and (2) lower bound 5th percentile (red dashed) which defines the data design category. The test results indicate the tested multi-layer panels achieved *DC80.4*. The total wall thickness is 1.5" (38.1mm) – if thickness derating is considered, the tested multi-layer panels achieved *DC87.4*.

Table 19. Fatigue Test Results – All Tests at R=0.5

ID	Stress Range, MPa	Mean Stress, MPa	Weld Initial Crack	Cycles to Initial Crack	Cycles to 1st Rupture	Cycles to 2nd Rupture (End)
1-A	131.0	196.6	W1 - Toe	909,406	914,849	1,077,120
2-A	144.8	217.3	W4 – Toe	405,452	415,000	435,320
3-B	158.6	237.9	W4 – Toe	333,738	339,350	349,906
1-C	151.7	227.6	W4 – Toe	751,800	753,200	770,199
2-B	137.9	206.9	W4 – Toe	641,306	648,500	662,597
3-C	124.1	186.2	W4 – Toe	811,588	817,700	856,456
1-D	117.2	175.9	N/A - Runout	10,000,000	---	---
3-D	117.2	175.9	W4 – Toe	1,188,548	1,203,300	1,214,459
2-D	113.8	170.7	W4 – Toe	1,006,932	1,009,000	1,059,554
3-A	95.2	142.8	W3 - Root	5,473,143	5,473,143	5,475,308

Figure 52. Fatigue Test Results & Analysis – 2 Outliers Identified & Removed

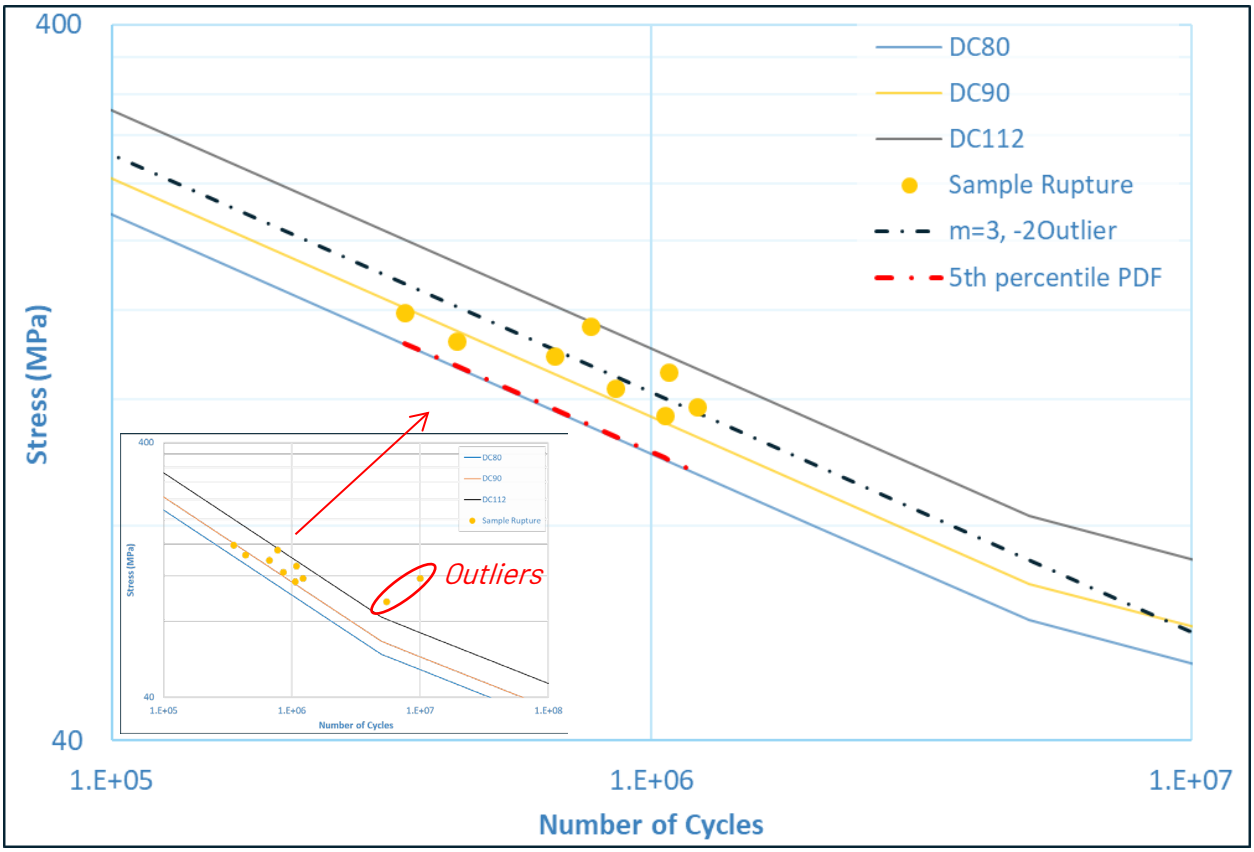

Some important observations from the testing are as follows:

1. Seven of ten failures occurred at the toe of Weld #4
    a. Post-test measurements of weld caps corroborated failure expectations:
        i. The one failure at W_1 had taller weld reinforcement than W_4 at that location.
        ii. Weld W_4 otherwise tended to have taller reinforcement than W_1.
    b. One test reached 10,000,000 cycles (runout) and did not fail.
    c. Test 3-A failed at mid-layer porosity – would be identified in production setting.
2. This test regimen is too small to conclusively state whether W4 tended to fail because of (1) weld cap geometry, (2) welding into backing layer, (3) or slight weld-cooled sample concavity
    a. More testing is needed to parse the impact of each factor.
3. The 3-layer sample test results behaved similar to a monolithic test sample and achieved *DC80.4* (or *DC87.4* if including thickness derating).
    a. The governing weld details appear to be as if the sample were monolithic and welded to EN1993-1-9 Table 8.3 weld detail 11.
4. These tests should be repeated with DC90 weld caps.

5 Single-Wrap Investigations

This section summarizes Keystone Tower Systems' investigation into Hybrid Laser Arc Welding (HLAW) technology as a means to expand the applicability of single-wrap designs into offshore tower scales. A transition in focus to single-wrap designs was driven by factory throughput analyses showing that coil-based feedstock thickness limitations sometimes reduced productivity and by the opportunity to improve weld efficiency for all tower shells.

Keystone collaborated with the Edison Welding Institute (EWI) to develop, test, and qualify an HLAW procedure for 25mm-thick plate steel, aiming to improve production rates for thick material relative to conventional Submerged Arc Welding (SAW). The HLAW process integrates Gas Metal Arc Welding (GMAW) with a focused laser beam, producing deep, narrow welds at high travel speeds while maintaining joint integrity. EWI performed extensive parameter optimization by varying: laser power, beam-to-wire distance, travel speed, and gas composition. After multiple iterations, EWI consistently achieved clean welds with quality back-bead formation and minimal internal and surface defects. EWI developed weld procedures for two joint configurations (1) a 19mm square land with 6mm U-groove GMAW capping pass and (2) a two-sided HLAW 25mm square joint; Keystone believes these could be extended, relatively simple, to a third joint design (3) a two-sided HLAW 34m square land with 6mm GMAW/SAW capping pass.

Non-destructive and mechanical testing confirmed the success of the developed procedure. X-ray and visual inspections showed few discontinuities, meeting ASTM D1.1 acceptance criteria for statically loaded non-tubular joints. Hardness tests indicated average values of 204 gf/mm^2—well below Keystone's 380 gf/mm^2 limit—while tensile and toughness tests demonstrated compliance with ASTM A572 Grade 50 requirements. Charpy impact testing revealed high energy absorption in both the HLAW root and heat-affected zones, and bend ductility tests showed no visual defects after 180° bends.

Overall, EWI's work validated HLAW as a robust, industrially viable welding solution for large-diameter, thick-walled spiral-welded towers. The developed single- and double-sided HLAW joints achieved high quality and performance, reducing weld time dramatically. The findings suggest the potential to complete 40mm joints in the same time as a single-pass SAW weld. These findings represent a key step toward scalable, high-throughput manufacturing of next-generation wind turbine towers.

5.1 HLAW Investigations

The multi-wrap track of this research project showed promise in that the fundamental buckling and fatigue behavior of the multi-layer shell structure appears to exhibit behavior consistent with monolithic or single-wrap shell structures. Two primary factors; however, swayed the researchers to shift effort and project resources to further exploring the single-wrap track. The primary factors against further multi-wrap research were:

1. Factory throughput models (discussed later in Section 6) indicated that limiting feedstock to coil thicknesses (< 25mm) artificially throttled productivity and reduced the multi-layer value proposition.
2. The value of getting Keystone's prototype scale spiral-welding mill capable of forming multi-wrap shells was not as high since benchtop scale buckling specimens were formed and tested with a different technique. More value for the effort was achievable elsewhere.

One of the largest and earliest hurdles to expanding single-layer thicknesses is weld technology; thus, the single-wrap investigation focuses on weld technology. Keystone currently uses traditional Submerged Arc Weld (SAW) technology which is stable in industrial environments; however, weld volume capabilities are modest. This means several weld passes are required, even for relatively thin parts. As thicknesses increase, weld volumes increase exponentially and throughput rates plummet. Alternative weld techniques were identified, as in Table 20, with Hybrid Laser Arc Welding (HLAW) identified for further investigation in this project.

Table 20. Weld Technology Alternatives Considered

Weld Technology	Technical Maturity	Industrial Stability	Initial Setup Time	Weld Pass Time	Inter-Pass Time	Reduce Pass Number
Hybrid Laser Arc Welding (HLAW)	High	Moderate	Same	Decrease	Decrease	Yes
Multi-Head (3+) SAW	High	High	Same	Same	Same	Yes
Electron Beam Welding (EBW)	High	Low	Increase	Increase	Decrease	Yes
Friction Stir Welding (FSW)	Moderate	Low	Increase	Increase	Increase	Yes

5.1.1 HLAW Weld Development

Keystone collaborated with EWI to develop a HLAW weld procedure, perform weld trials, and test the resulting welds. The basic weld joint was selected as a 19mm (0.75") square land with a 6mm U-groove

bevel for a total 25mm (1.0”) welded joint. The plan was to weld the 19mm land with HLAW with a following 6mm GMAW capping pass. The weld joint is shown in Figure 53.

Figure 53. HLAW Joint – Plan (Left) and Actual Sample (Right)

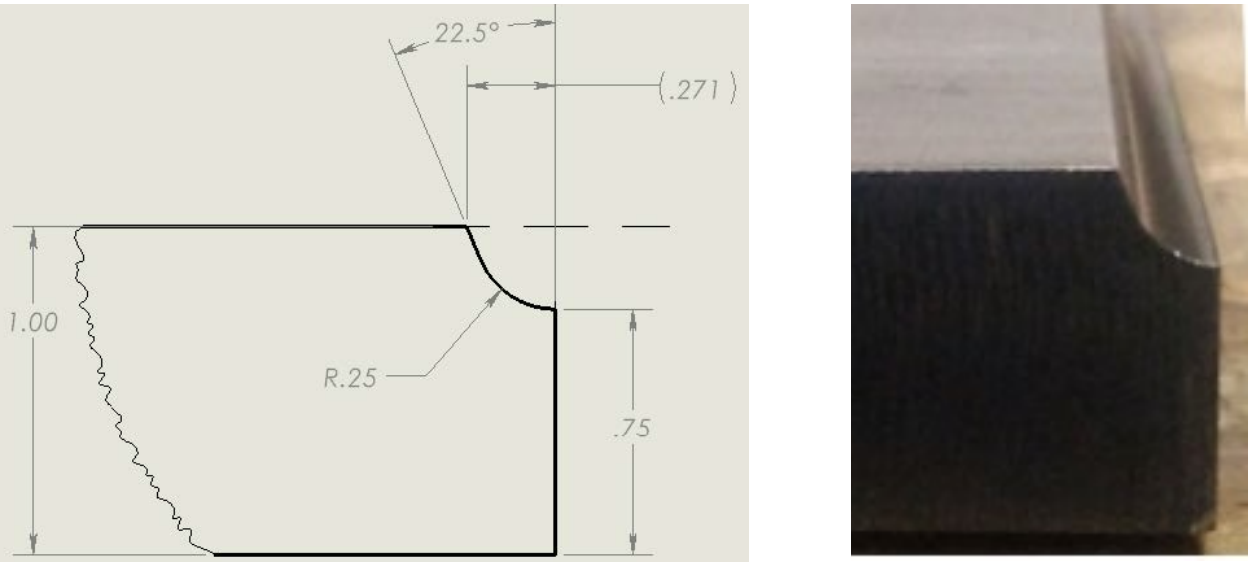

The Hybrid Laser Arc Welding system combines elements of Gas Metal Arc Welding (GMAW) and laser welding. An arc is passed through a filler metal to the base metal being welded. The arc is intense enough to establish and maintain a molten mixture of the filler and base metals. Trailing shortly behind the arc wire (3-4mm), a precisely focused laser beam is shot through the weld pool and into the square weld joint. The weld pool heat, along with the intensity of the laser beam, is sufficient to fuse to the base metal within the deep (19mm in our case) square joint. An inert gas cushions the weld from oxidation throughout the process from above and below the plate. EWI’s HLAW setup and controls interface are provided in Figure 54 and Figure 55.

Figure 54. HLAW Setup with Callouts and GMAW Power Supply Shown

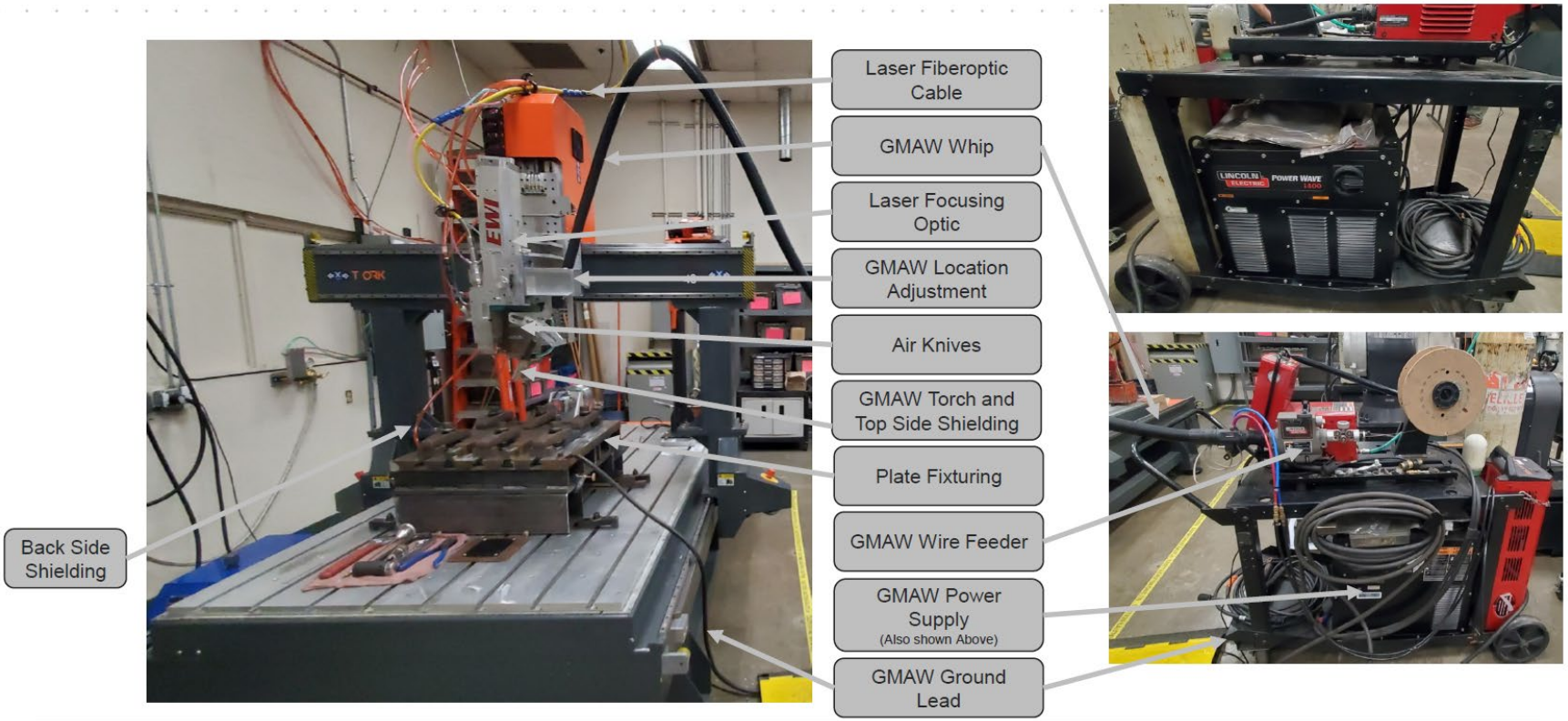

Figure 55. Laser Controls, Power Supply, and Fixturing to Weld Head

Laser	IPG YLS-20000
Optics	EWI Custom B3
Fiber Diameter	200 µm
Focal Length	800 mm
Theoretical Spot Size	400 µm
Laser Beam Angle	0 Degree (normal)
Measured Spot Size	401 µm
Measured Beam Quality	7.994 mm-mrad

Laser Fiberoptic Cable

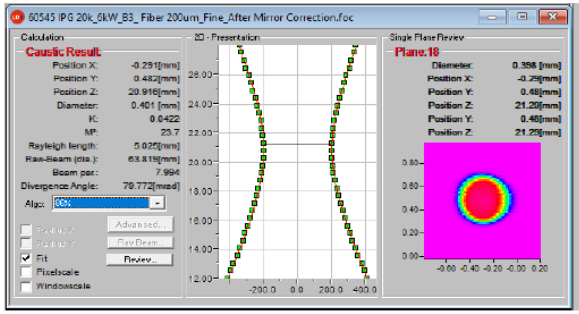

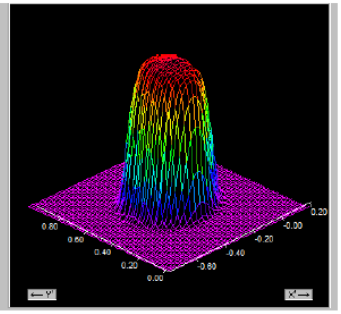

PRIMES Laser Beam Characterization Measurement

- Expected spot size and beam quality measured for this setup

EWI
We Manufacture Innovation

There are numerous variables that can be controlled for a HLAW weld procedure. EWI varied (1) travel speed, (2) laser power, (3) beam-to-wire distance, (4) wire feed speed, (5) wire trim, (6) wire stickout, and (7) gas cushion mixture and volume. EWI performed many weld trials to refine and improve the weld results. They started with simple Bead on Plate (BOP) welds, as seen in Figure 56, before attempting welds on joints, as shown on Figure 57. Sharing all weld trials is beyond the scope of this final report. Instead, see Figure 58 for cross-sections of early flawed welds and later refined welds. The remainder of the joint was later filled with a GMAW capping pass; this step is not shown here.

Figure 56. Bead On Plate Trials to Approximate HLAW Parameters

Figure 57. HLAW Trial #3A on U-Groove Joint – Above View (Top), Below View (Bottom)

Figure 58. HLAW Joints – Early (Left) and Refined (Right) Trials

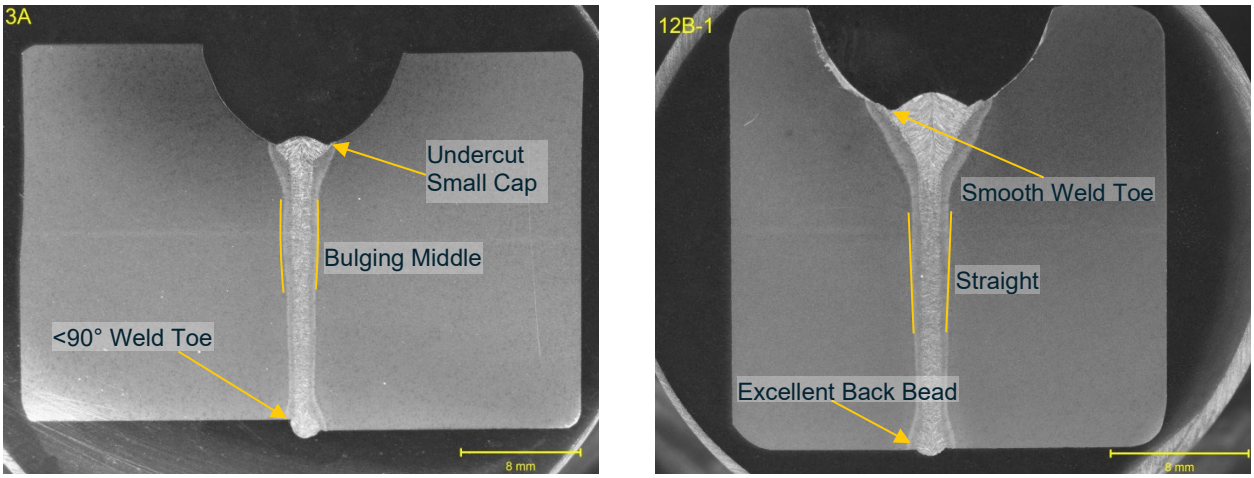

Keystone toured EWI's facilities in Columbus, Ohio. During that visit, Keystone welding engineers asked EWI to attempt a double-sided HLAW weld. The preliminary trial proved potentially successful. The HLAW back beads were proving difficult to control and a double-sided HLAW would permit: (1) increased control of the weld reinforcing cap, (2) a taller square land, and (3) overall thicker weld joint. A successful demonstration of a Two-sided HLAW joint is given in Figure 59.

Figure 59. Cross-Section of Final Two-Sided HLAW Weld

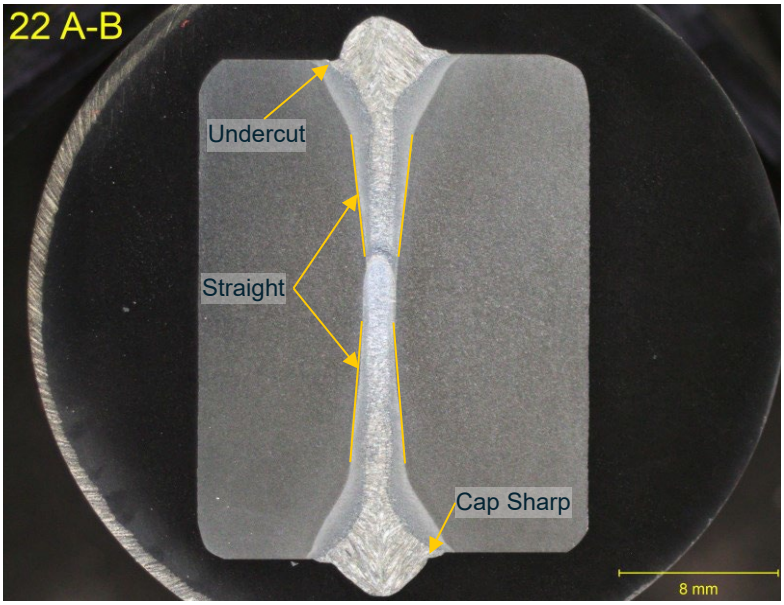

5.1.2 HLAW Joint Inspection and Mechanical Tests

As EWI developed the weld procedure, they also performed non-destructive testing to inspect for weld quality. Early welds exhibited surface visible flaws as well as flaws locked in the quickly recrystallized mixture of filler and base metal within the weld joint. EWI took X-rays to non-destructively examine the weld joint quality. Images are shared in Figure 60 and Figure 61 of a low quality and high quality weld, respectively.

Figure 60. VT (Above) & X-ray (Below) of Sample 9A Cross-Correlated

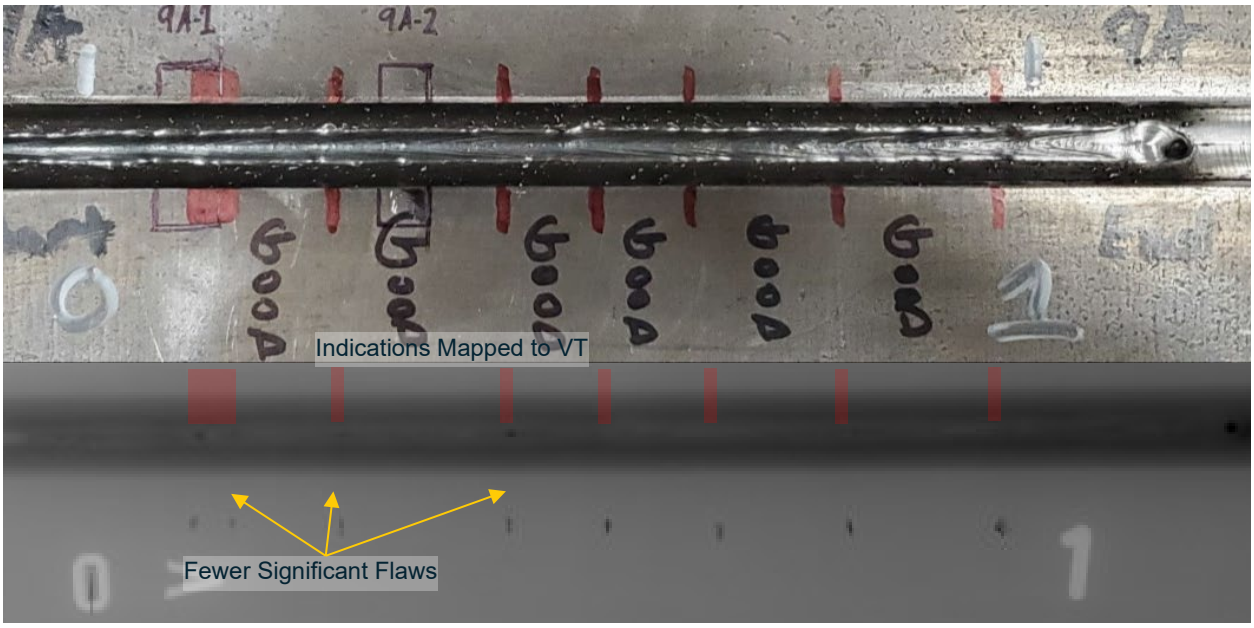

Figure 61. VT (Above) & X-ray (Below) of Sample 12B – Few Discontinuities

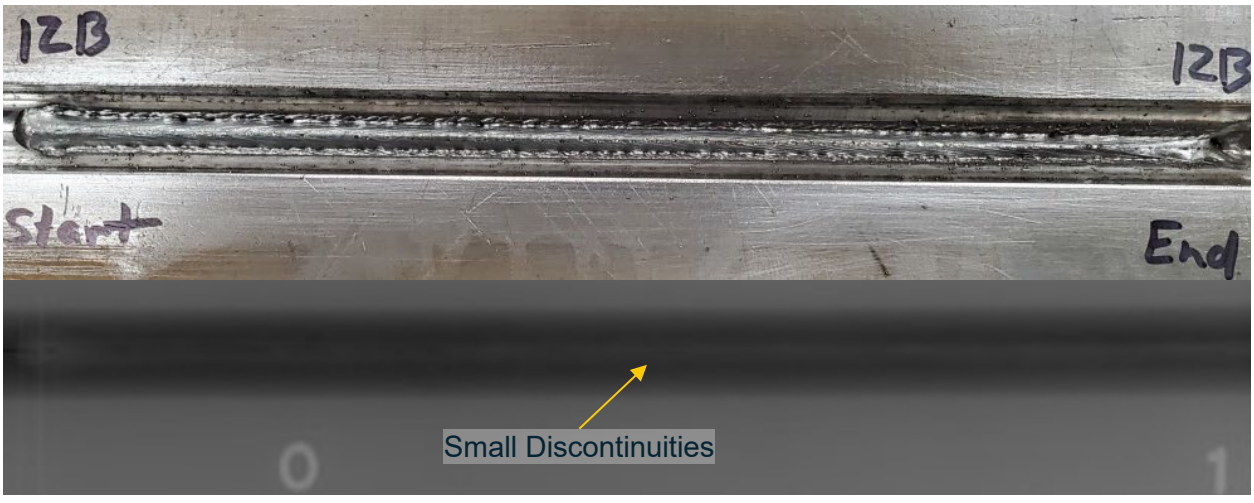

EWI's Analysis of the defect rate in Sample 12A and 12B established that this weld procedure passes the acceptance criteria established in ASTM D1.1 for statically loaded non-tubular connections. Keystone deemed this an acceptable threshold to prove viability of the HLAW technology to enhance the automated spiral-welded manufacturing of heavy-walled towers. Further refinement of weld parameters will be needed to reduce discontinuities even further to ASTM D1.1 criteria for cyclically loaded connections.

Destructive mechanical testing of the welds were also performed by EWI. The material tests included (1) Microindentation Hardness, (2) Tensile, (3) Notch Toughness, and (4) Bend Ductility. All samples were taken from a single HLAW weld joint, as detailed in Figure 62.

Figure 62. Machining Plan for Mechanical Test Coupons

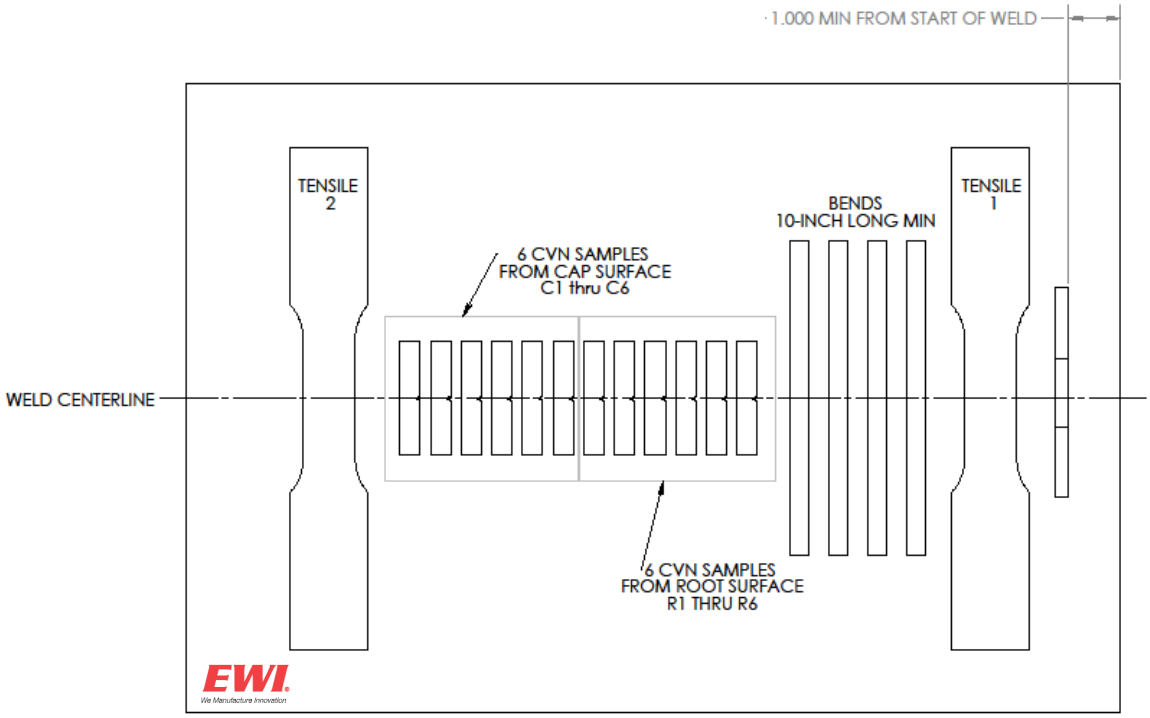

Hardness was tested following ASTM E384 for micro-indentation. Test points are located as in Figure 63 with results shared in Figure 64. The average hardness reading is 204gf/mm2 with a maximum reading of 246gf/mm2 whereas Keystone required a maximum hardness of 380gf/mm2 or less. The hardest region was the GMAW capping pass and the HLAW weld did not exhibit hardness that was readily distinguishable from the base material. All readings are well under Keystone's acceptance criteria of 380gf/mm2 and are satisfactory.

Figure 63. Micro-Indentation Hardness Test Pattern

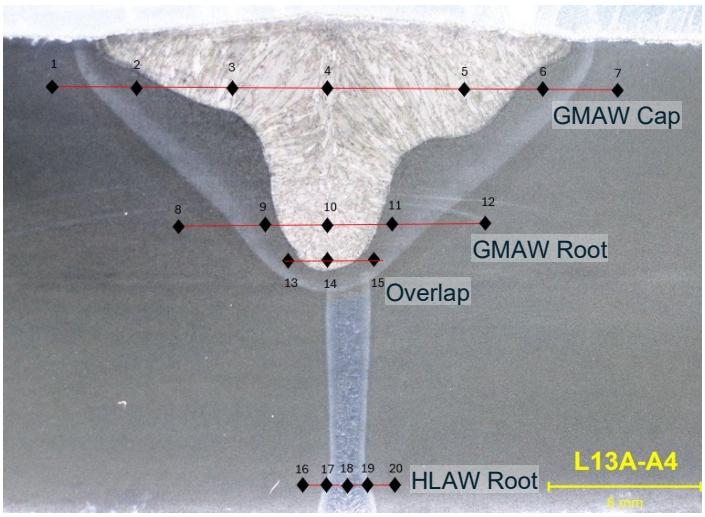

Figure 64. Micro-Indentation Hardness Test Results

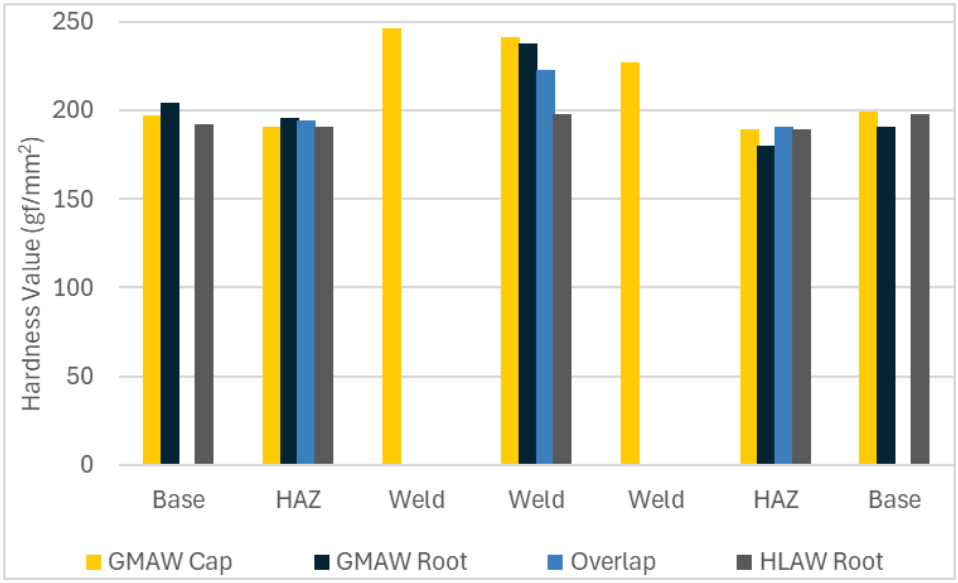

Tensile tests were performed by EWI. The resulting material properties are provided in Table 21. The material was specified as ASTM A572 Grade 50 and it met the requirements of that specification.

Table 21. Tensile Test Results

Property	Requirement	L14A-A5-T1	L14A-A5-T2	Disposition
Yield Point (ksi), min	50.0	60.2	63.3	Pass
Tensile Strength (ksi), min	65.0	72.0	75.1	Pass
Elongation (%), min	21.0	36.0	36.8	Pass

Toughness describes the ability of a material to absorb energy while plastically deforming without fracturing. The material property is tested by the Charpy V-Notch test. The perform the test, a sample is machined with a sharp notch, cooled to a low temperature, and struck with a standard hammer on the back-side of the notch. The energy absorbed by the sample is recorded – a more ductile material will tear and dissipate energy more than a brittle material that readily cleaves. EWI tested the (1) Centerline of the GMAW cap, (2) Heat Affected Zone (HAZ) of the GMAW cap, (3) Centerline of the HLAW root weld, and (4) HAZ of the HLAW root weld as depicted in Figure 65.

Figure 65. CVN Notch Location Test Plan Depicted on Welded Cross-Section

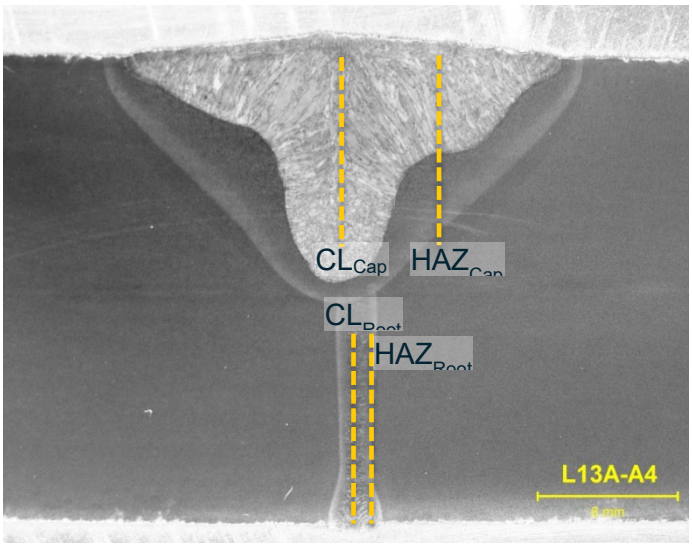

Test results are collated in Table 22. The HLAW weld was sufficiently tough. The centerline of the GMAW cap did not exhibit high enough energy absorption; however, the GMAW cap weld is outside the scope of the project and is acceptable.

Table 22. CVN Test Results

Specimen #	Test Region	Required Abs. Energy (J)	Absorbed Energy (J)	Avg. Absorbed Energy (J)	Disposition
1	CL_{Cap}	27	25	31.7	Fail
2			21		
3			49		
4	HAZ_{Cap}		222	203.7	Pass
5			229		
6			160		
7	CL_{Root}		274	302.0	Pass
8			290		
9			342		
10	HAZ_{Root}		310	305.0	Pass
11			313		
12			292		

Ductility was tested with a side-bend test. The side-bend test was introduced in Section 4.4.2 when Keystone tested weld ductility of the multi-layer fatigue test panels. Figure 66 shows the result of a weld bent around a 1.5inch diameter bar at 180°. This bend geometry yields a 20% elongation of the weld cross-section. There are *no visual defects*; the welds *pass the bend test*.

Figure 66. No Visible Defects on Bend Samples

In summary, EWI developed a HLAW weld procedure that:

1. Passes acceptance criteria of ASTM D1.1 for *statically loaded* non-tubular connections.
2. Has the HLAW pass travel at 80IPM (33.9mm/sec)
3. Exhibits low hardness, consistent with values measured for the base material.
4. Complies with tensile requirements of ASTM A572 Grade 50 material.
5. Demonstrates high energy absorption, as measured by CVN testing
6. Is highly ductile without visible defects in a bend test.

The weld development efforts by EWI demonstrated that HLAW welding can achieve high quality welds with minimal flaws while rapidly joining thick plate material. EWI worked with 25mm (1") thick plate. They developed (1) single-sided HLAW joints of 19mm square lands and (2) two-sided HLAW joints of 25mm square lands. To perform the two-sided joints on 25mm thick material, EWI reduced the laser power 40% as compared to the single-sided 19mm land. Keystone believes these two joint weld procedures give a strong indication that HLAW could be used to form a two-sided 34mm square joint at full power with a 6mm GMAW (or SAW) trailing capping pass; thus, a joint with a total thickness of 40mm that can be formed in approximately the same time as a traditional single-pass SAW weld.

6 Factory Details

This section provides an overview of Keystone Tower Systems' integrated factory design, process optimization, and economic analysis for spiral-welded wind turbine towers. The content outlines the key manufacturing stations, the underlying throughput models that govern production rates, and the cost implications of applying advanced Hybrid Laser Arc Welding (HLAW) technology

Keystone developed a quayside factory for manufacturing offshore wind towers. The factory design is described by the flow of material through the factory, the layout of the factory, and how the tower products are handled throughout the forming process.

Keystone placed additional emphasis on developing a robust weld-timing model to inform a spiral-mill throughput model. SAW and HLAW weld technologies were considered in the models. Feedstock material ranged from 1.8m to 3.0m wide. This spiral-mill throughput model became a key method of evaluating the relative value proposition of single-wrap or multi-wrap tower and monopile designs.

The integrated tower design – spiral-mill – factory *system* is vital to evaluating the costs to manufacture various tower and monopile designs. Keystone demonstrated that significant material savings are achievable with improved manufacturing Tolerance Quality Class capabilities. Keystone can further improve costs with optimized designs that maximize throughput and reduce conversion costs associated with labor and fixed capital expenditure costs.

6.1 Key Station Descriptions

A brief description of each major tower manufacturing process is provided below. These major processes represent physical stations/bays within a factory where specific activities take place and serve as the basic building blocks of an integrated factory model. The equipment used, space requirements, and staffing needs of each station are known and form the basis for the factory economic model.

Plate Processing: Trapezoidal plate material processing will be vertically integrated into Keystone's product line. Plate processing includes (1) cutting lengths from coil stock, (2) final cold-rolling to specified thicknesses, (3) cutting final trapezoidal shapes, (4) surface preparation, and (5) beveling edges for welding operations. Currently, Keystone uses third-party processors for all steps prior to beveling. In-house plate processing will improve control over material properties, reduce costs, and simplify logistics.

Spiral Mill: The spiral mill is the backbone of every Keystone tower factory. The spiral mill consists of a trapezoid infeed table with automated cross-weld gantry, a set of push and bend roller banks, helical weld heads, and a tower section runout table.

The factory is sized according to the throughput limits of the spiral mill. Keystone does not have operator experience with such heavy wall thicknesses that are required in offshore towers. Therefore, Keystone improved a weld-timing model that realistically sets the pace for throughput in the spiral-mill.

Black Fabrication: Tower sections pay-out of the spiral mill into black fabrication. "Black fab" is where the overall structure quality is measured, repaired as needed, and qualified. Processes include Non-Destructive Evaluation (NDE) of welds, geometric verification of the structure, flanging of the section, and door installation in base sections.

Blast, Metalize, and Paint: Surface treatment of tower sections is necessary to ensure a long service life, especially in saline offshore environments. The "black" surface (internal and external) is blasted with abrasives to remove any layers of mill scale, dirt, oils, or oxidation. Flanged ends are metalized with a rugged corrosion resistant layer of zinc or aluminium. Finally, a series of engineered paints is layered and dried to totally seal the steel from corrosive agents. These processes are rather repetitive and lend themselves to automation.

Internals Install: Personnel access platforms, cable trays, ladders, HVAC systems, and all other components internal to the tower shell are installed. This is the final process a tower section goes through prior to being moved to site storage and eventually shipped to the customer.

The preferred factory layout is depicted in Figure 67. Raw plate arrives at the factory, or may be processes on-site from coil, and is placed in storage. The plate then flows through infeed and is formed into a spiral-welded tower on the spiral-mill. The tower pays-out of the spiral-mill and arrives in black-fab where it is inspected, repaired if needed, internal bosses and flanges (and doors) are welded to the section. The section is then blasted, metalized, painted, and internals kits are added. The factory footprint, including section egress, is approximately 9 sections wide (with clearance margin) and 4 section length long. This factory layout, with north and south egress, permits sections to be removed or added back to any process at any time.

Figure 67. Preferred Factory Layout

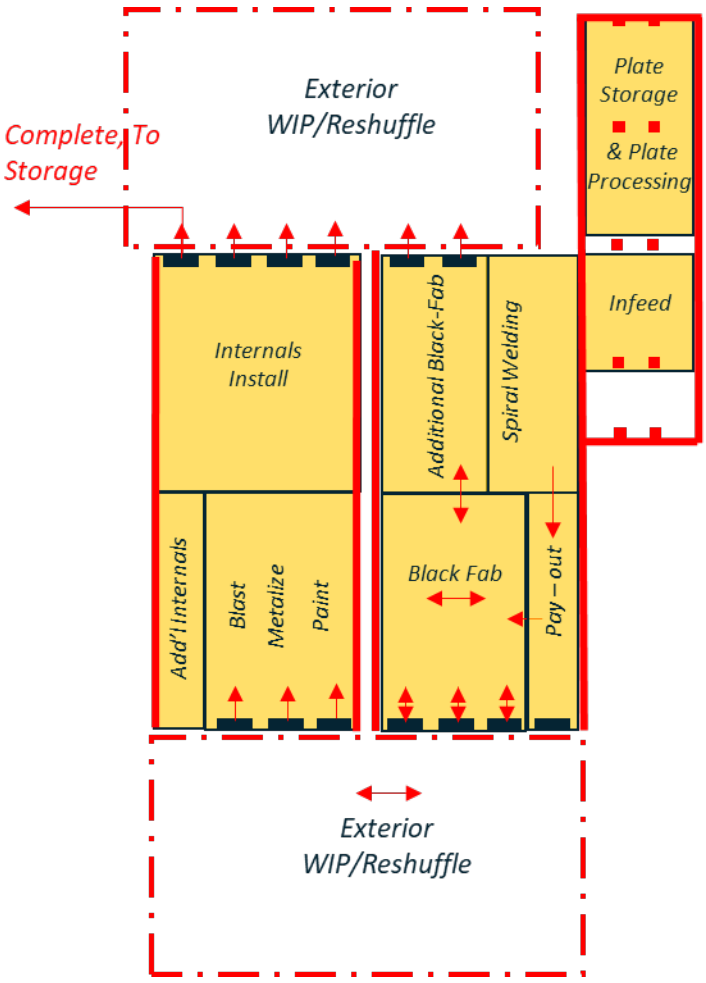

6.1.1 Spiral-Mill Throughput Analysis

Keystone developed a set of crossweld timing models that were based on bevel geometries and weld procedures deployed in the Pampa, TX onshore tower factory. Keystone's current cross weld procedures consist of a 4G MIG root pass followed by SAW welds in the flat position. Timing studies were conducted by observing workers performing the weld procedures. Additionally, weld models were extended to a HLAW bevel geometry developed by research partner EWI, as discussed in Section 5.1.1. The (1) current 4G MIG & SAW weld procedure and (2) HLAW weld procedure models were then extrapolated out to large thicknesses.

A simplified depiction of the crossweld timing model is shown in Figure 68. Each cross-weld is characterized by the number of passes to complete the joint. Each pass can have unique filler material deposition rates and travel speeds. Accounting is also done for the time spent between welds; this time is

used for inspection, flux cleanup, equipment realignment, etc. The weld timing model takes the form of a helical weld velocity that can be achieved given crossweld timing and geometry, as stated in Eq 1.

Figure 68. Crossweld Timing and Balance with Helical Weld

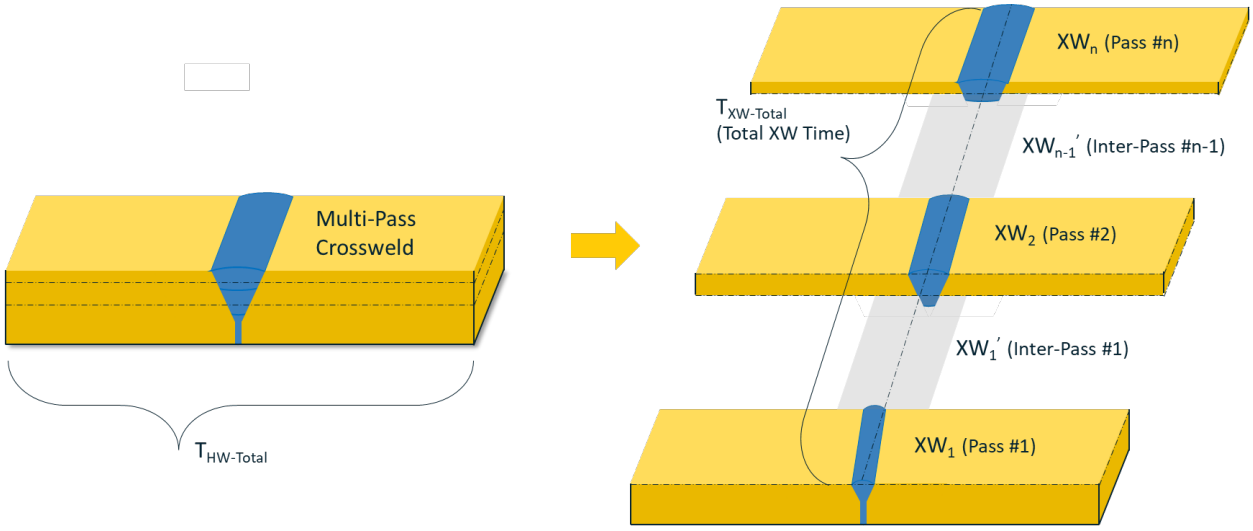

$$\min V_{HW} \leq \begin{cases} \dfrac{L_{HW}}{T_{Setup} + \sum_{i=1}^{n} \dfrac{L_{XW_i}}{V_{XW_i}} + (n-1)T_{IP}} \\ 910 \end{cases} \qquad \text{Eq 1}$$

The crossweld timing model was used for Keystone's existing SAW procedure over a range of thicknesses with feedstock material from 1.8m to 3.0m widths and while considering single-wrap or two-wrap configurations. The relative mass flowrates for these conditions are compared in Figure 69. Observe that, for SAW welds, (1) mass throughput is maximum for 24mm thick material, (2) wider plate increases throughput at all thicknesses, (3) and that, if forced to use coil feedstock with a thickness limit of 26mm, multi-wrap productivity actually decreases in the range of 26-32mm thicknesses.

Figure 69. Mass Flow Rate – Single Wrap & Multi-Wrap of Varying Widths

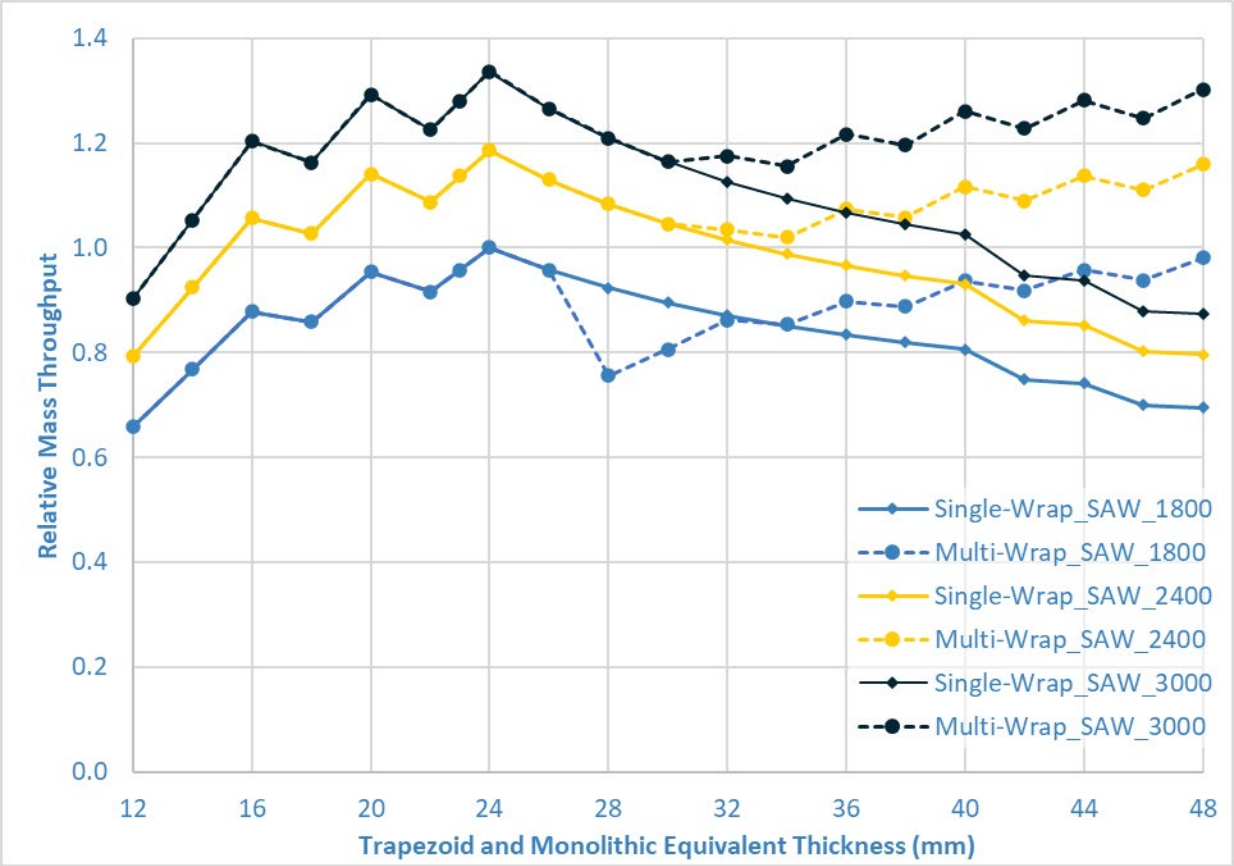

A similar exercise was performed, but for crosswelds completed with HLAW technology. The HLAW joint considered is a theoretical extension from the work performed by EWI in Section 5.1.1. The theoretical HLAW joint consists of square land of up to 34mm; for thicknesses beyond 34mm, a U-groove is placed above the square joint. Relative mass throughput is plotted in Figure 70.

For all trapezoid widths and for thicknesses 22mm or beyond, HLAW increases spiral-mill productivity when compared to any previous SAW analyses. Maximum HLAW throughput is observed for trapezoid widths of 3,000mm at a thickness of 40mm. Maximum HLAW throughput is approximately 400% of the maximum achievable SAW productivity when using coil feedstock. For thicknesses applicable to the 12MW reference wind towers (approximately 24-44mm), maximum productivity of the spiral-mill using HLAW instead of optimized SAW technology is increase by approximately 80% to 220%.

Figure 70. Mass Flow Rate –HLAW of Varying Widths Relative to Maximum SAW Productivity

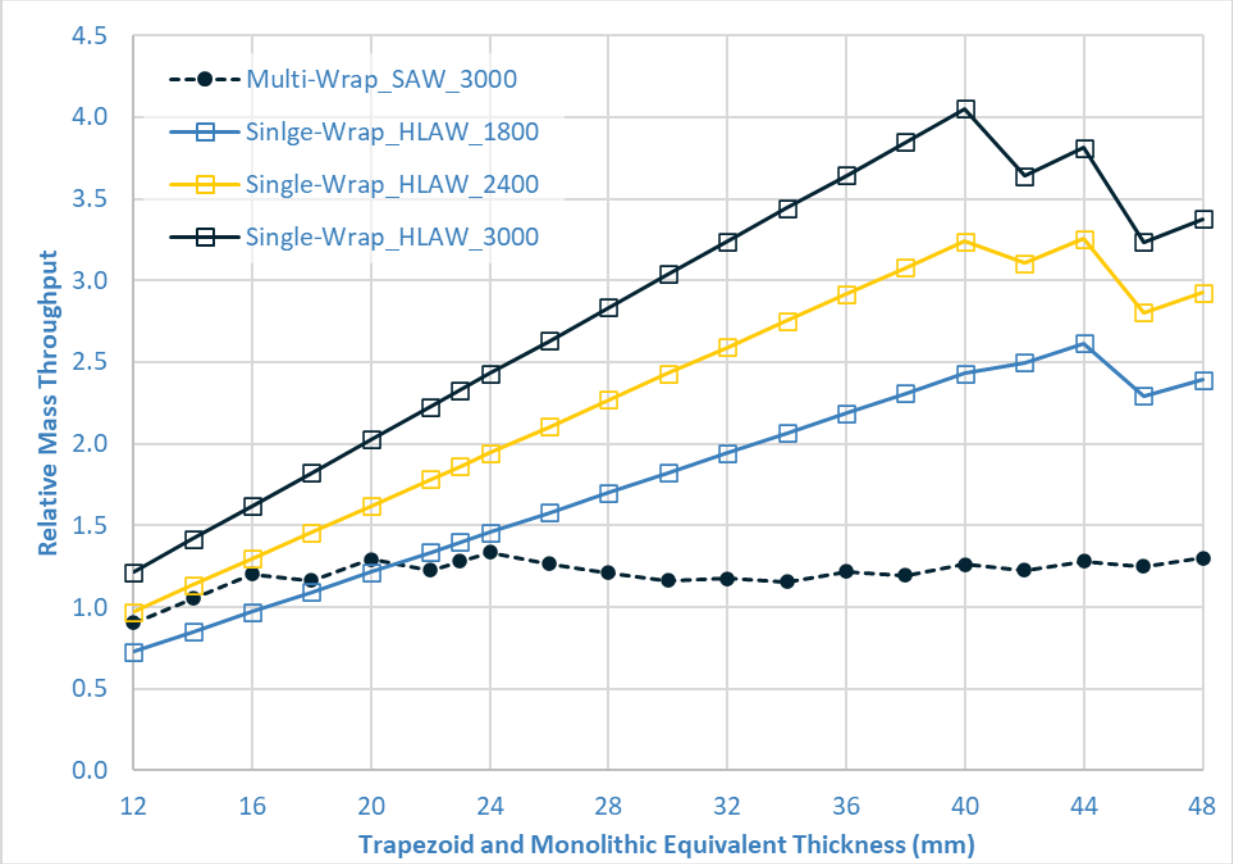

These mass throughput models were applied to the actual Bill of Materials (BoM) for the three-section drop-in replacement (TQC-B) spiral-welded tower designed by Keystone. The BoM in all cases is for a single-wrap design. The design with the 1.8m wide feedstock was previously shown in Figure 2(b) and the 3.0m wide feedstock design was provided as Figure 2(c). Relative mass throughput for each BoM and welding technology are plotted in Figure 71. Clearly, the use of HLAW weld technology increases spiral-mill throughput relative to SAW crosswelds. Throughput is further increased when using wider plate feedstock.

Figure 71. Increase Productivity with Plate Feedstock Width and HLAW

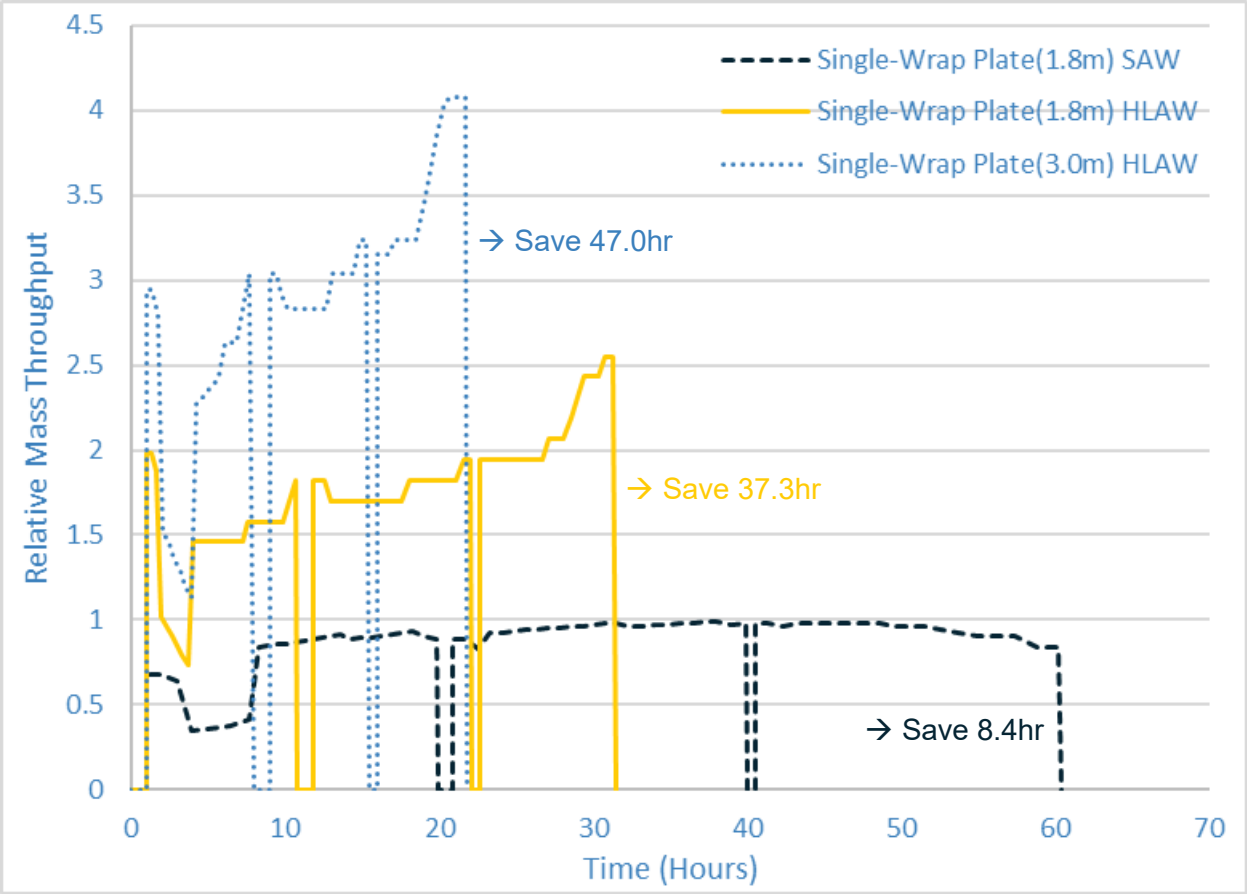

6.1.2 Economic Considerations

Keystone fed several versions of tower designs through a full factory economic model. Equipment and labor requirements are quantified for each factory station based on spiral-mill throughput. Results in the conceptual factory analysis demonstrated several value propositions that Keystone brings: (1) spiral-forming is more efficient than can tower production and costs are saved just by using Keystone, (2) minor savings may be achieved with unique designs such as specified clearance heights or single-section towers, (3) Keystone can achieve tighter manufactured tolerances (TQC-A) and shave steel out of the design. The trends are observable in Figure 72 and Figure 73.

Figure 72. Tower Cost Components using Fit-for-Purpose Factory Designs

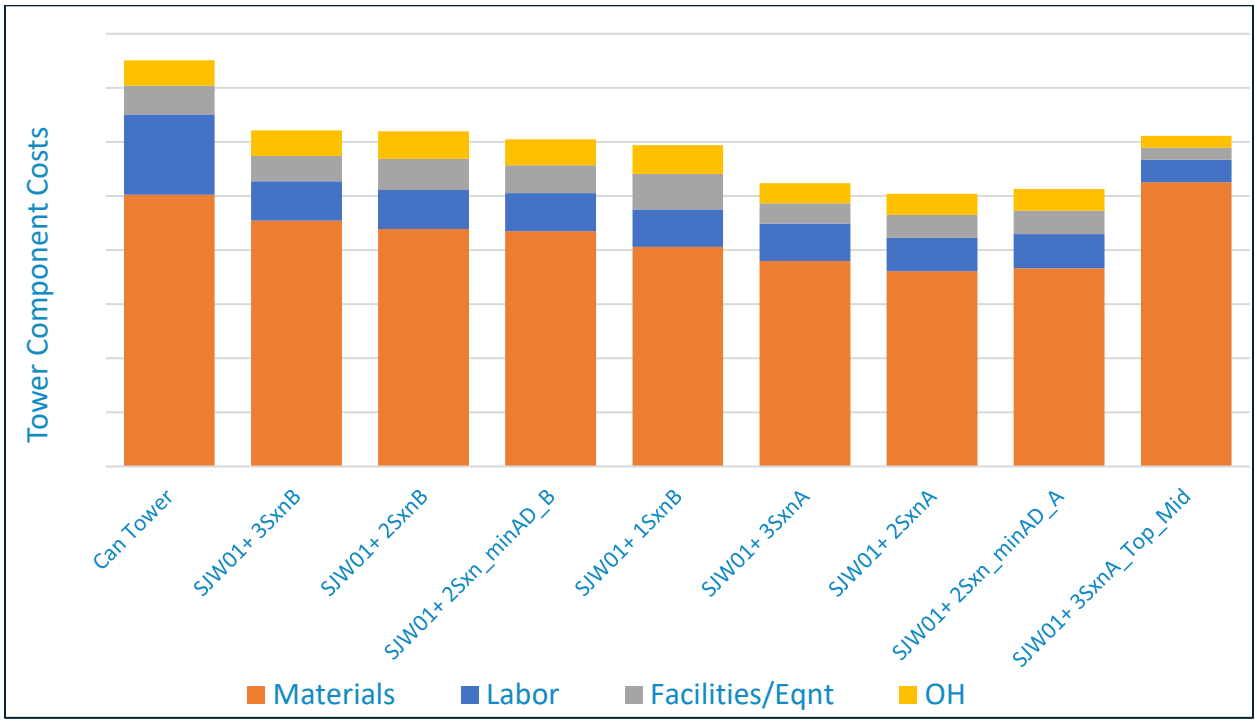

Figure 73. Relative Benefits of Keystone Technologies

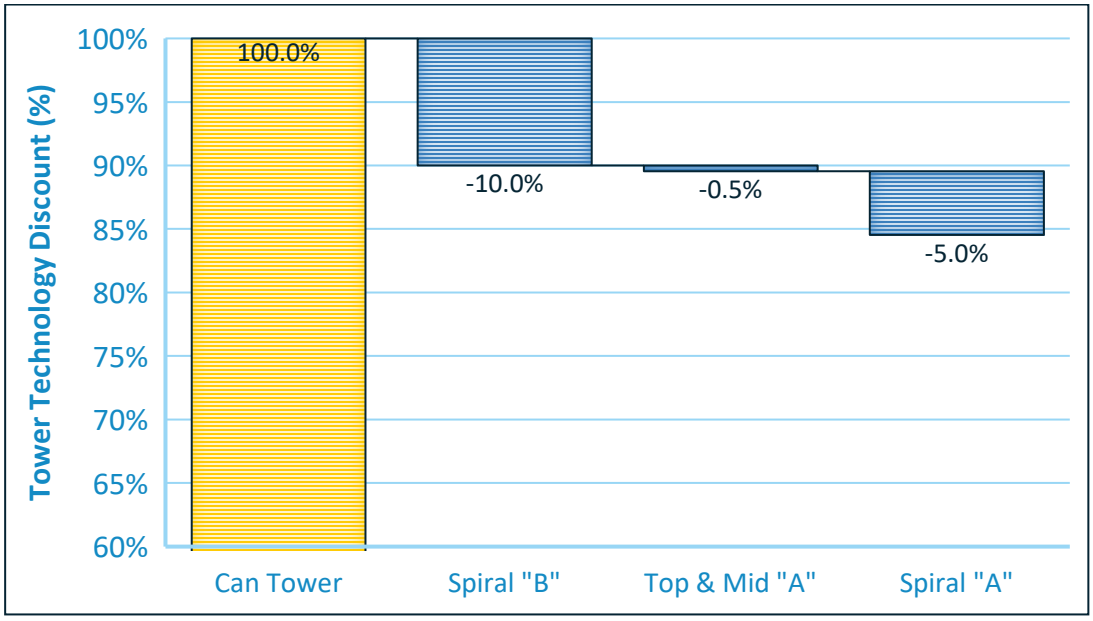

A more thorough analysis of the 3-section spiral-welded direct drop-in replacement design – Figure 2(b) and Figure 2(c) shows relative costs between the multi-wrap concept and optimized single-wrap designs. The HRC material costs for the multi-wrap concept are cheaper than plate; however, the more efficient

use of labor and capital equipment more than makes up the cost difference, in this scenario. Additionally, 170% *more* production is achievable with the optimized HLAW design. Thus, even with conversion costs to Keystone that are near parity (< 2% savings with optimized design), Keystone can be more competitive on margin when more product is produced from the factory each year. Relative total tower costs are provided in Figure 74. A detailed analysis of labor costs for each factory station is shared in Figure 75 to demonstrate the much more efficient deployment of labor resources for the optimized tower – spiral-mill – factory *system*.

Figure 74. Fabrication Costs for Various 12MW Reference Tower Designs

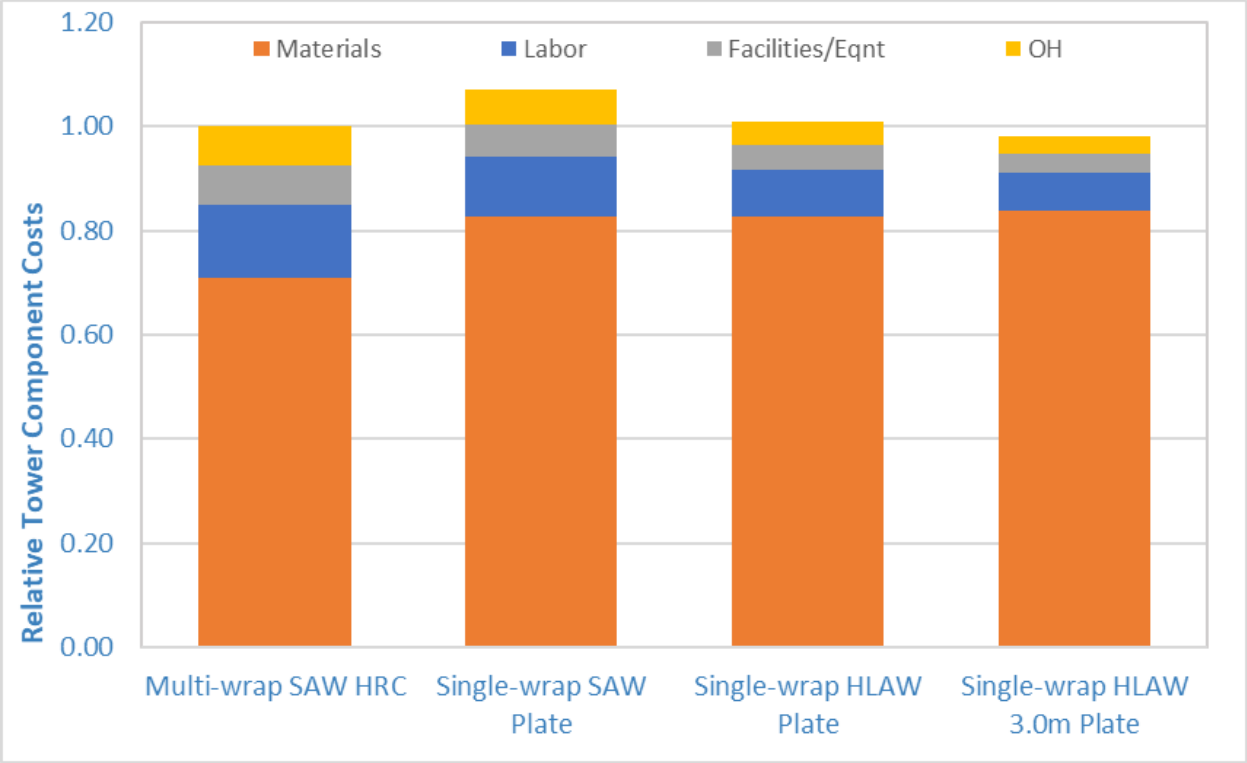

Figure 75. Per Tower Labor Demand for Factory Stations for Various 12MW Reference Towers

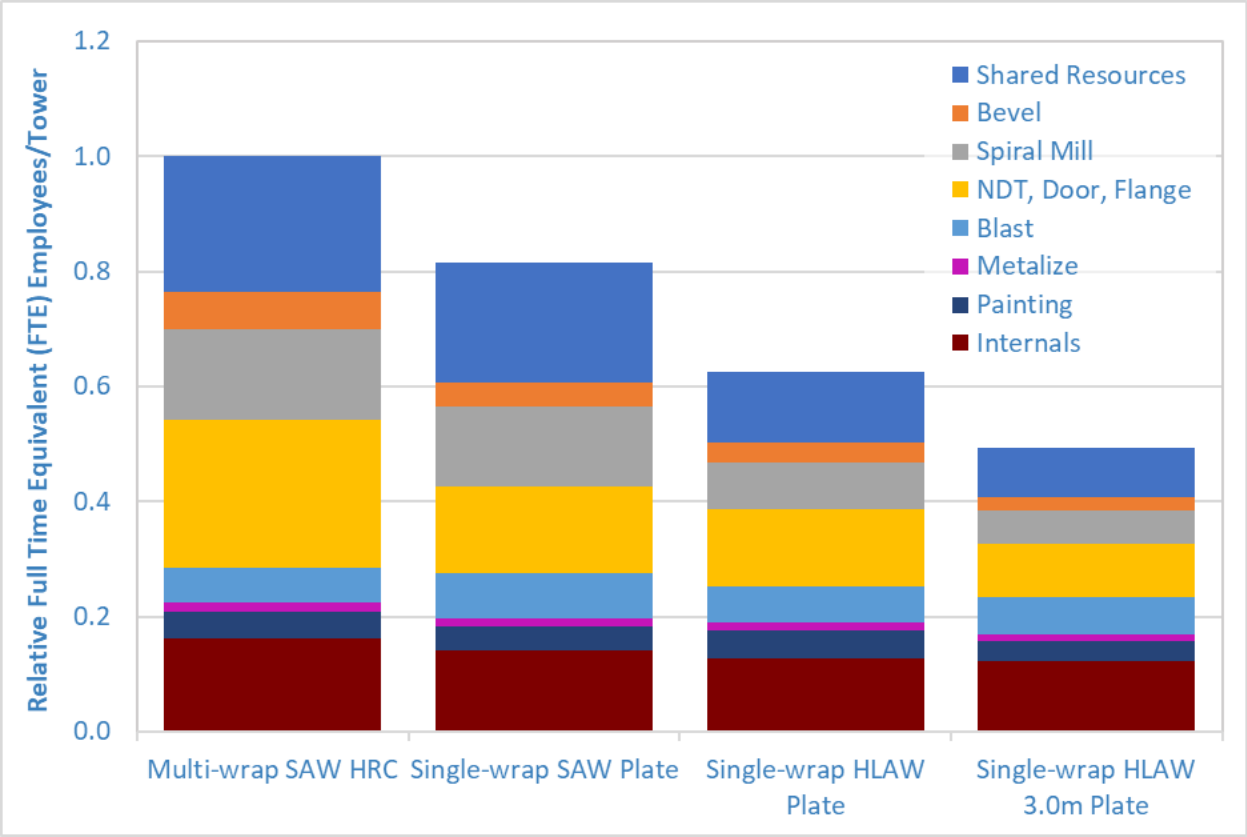

Keystone performed an LCOE analysis for potential cost savings when supplying spiral-welded shell structures. The approximate LCOE savings ($/MWh) are provided in Figure 76, with their source of savings, for 12MW towers, 18MW monopiles, and XXXL (25MW) monopiles.

Figure 76. LCOE Savings for Spiral-Welded Shell Structures

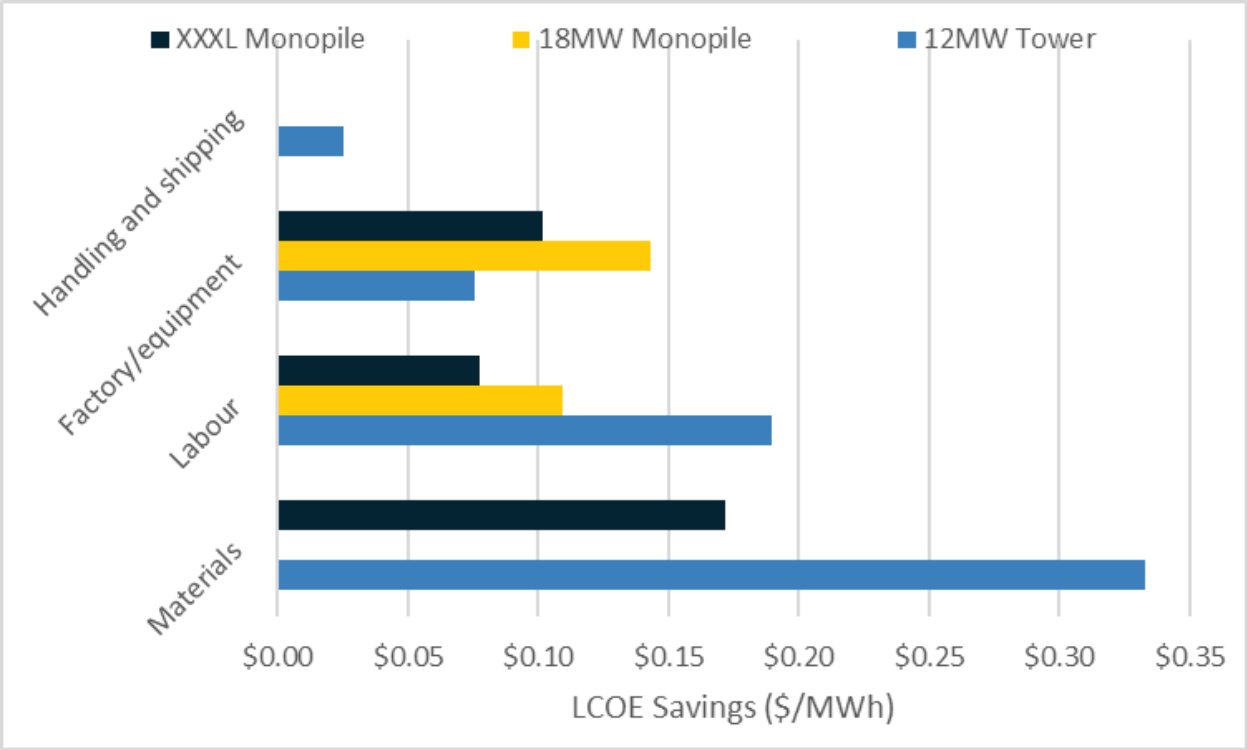

7 Conclusions, Recommendations, Impacts

This research, sponsored by NOWRDC, has been wide ranging and impactful. The researched areas range from highly technical fundamental research, gathering market research, and growing a commercial network, refining commercial offerings. The research is summarized here with a handful of conclusions. Recommendations are made for future continuing research. Keystone also prepared an impact statement to provide the reader with an understanding of how this project affected Keystone, the offshore wind industry, and the state of fundamental research.

7.1 Conclusions

This project marks a major milestone in advancing spiral-welded shell structures into the offshore wind tower and monopile scales. Collaborations with GE Vernova, Northeastern University, Johns Hopkins University, Edison Welding Institute (EWI) and BVG Associates, enabled critical progress in manufacturing optimization, structural validation, and cost reduction strategies. The following conclusions summarize the technical and economic outcomes of the study:

1. Keystone's spiral-welded manufacturing method demonstrates superior scalability, material efficiency, and cost-effectiveness compared to traditional can-tower fabrication.
2. Fully bonded multi-wrap shells achieved structural equivalence with single-wrap shells in buckling confirming the viability of multi-layer construction.
3. Multi-layer samples in fatigue perform similarly, also affirming viability of the multi-layer concept.
4. Multi-layer designs offer key mechanical advantages, including reduced bending forces, improved weld productivity, and access to more economical steel feedstock.
5. Hybrid Laser Arc Welding (HLAW) provided transformative improvements in fabrication efficiency, meeting ASTM standards while reducing weld time.
6. Throughput analyses indicated HLAW can deliver up to 400% greater productivity than SAW for large-thickness sections, particularly using 3.0 m wide plate.
7. Multi-wrap monopile configurations achieved ~27% higher throughput with <1% cost increase and significantly lower bending force requirements.
8. The optimized spiral-welded factory design yields approximately 25% lower fabrication costs, 55% staffing reduction, and 47% smaller facility footprint.
9. Keystone's ability to produce higher Tolerance Quality Class (TQC-A) towers translates to 12% steel mass reduction and improved cost.
10. Single-section tower fabrication offers an additional $12,500/MW savings through simplified logistics and reduced flange requirements, though port and vessel constraints limit implementation in the U.S.

11. The optimized tower–spiral-mill–factory system supports cost-effective scaling of the spiral-forming process to 18–25 MW turbine classes, enhancing industry competitiveness and sustainability.

7.2 Recommendations

The benefits of the multi-wrap concept of reducing (1) weld delays and (2) bend stresses are still acknowledged. The thickness threshold where these benefits can be realized, though, is thicker than expect at the onset of this project. The thickness at which multiple wraps should be considered appears to be in the range of 55-60mm instead of 25mm. So, instead of seeking to continue using coil feedstock, Keystone must consider plate material.

Keystone shall continue to work with OEMs and hold discussions with Developers. Keystone can be a key collaborative partner and can rapidly prototype tower and monopile conceptual designs. Direct collaboration can reduce the design cycle time which brings clarity to development plans - a key value proposition to offshore Developers. Keystone also notes that large offshore developments often have varying water depths and soil conditions – Keystone could provide value by enabling unique monopile designs to each monopile (or a set of monopiles). Soil-structure interaction means there is often not a conservative monopile design; therefore, it may already be necessary to vary the design across a large offshore wind farm.

Continue researching the buckling capacity of multi-layered shell structures. Scaling effects of multi-layer shells is not well understood – variables of interest are (1) achievable gap sizes when forming production scale tower sections, (2) effective mechanical properties for structural adhesives at production scales tower sections. Weld imperfection size and shape for multi-layers structures was not explored thoroughly. The welds of multi-layer structures are smaller then their monolithic equivalents; it is possible the smaller weld imperfections will not impact capacity as dramatically.

Additional fatigue tests should target variables not well captured by the testing completed for this project. The multi-layer fatigue samples tested for this project appear to be limited by the DC80 detail of the surface-breaking welds. Future testing should improve the weld quality to DC90 to see if the surface-breaking weld continues to be the failure point. Consider grinding the surface-breaking welds to see if performance continues to mimic monolithic samples.

Continue to refine the HLAW weld procedures to achieve fatigue requirements from ASTM D1.1. Perform tests to better mimic industrial settings and throughput requirements of a full-production facility. Consider (1) in-plane offsets, (2) out-of-plane offsets, and (3) quality of the joint.

7.3 Project Impacts

This project had significant impact in three primary area: (1) the state of fundamental research on multi-layer shell structures, (2) the offshore wind industry and market participants around the globe, and (3) Keystone's commercial and technical readiness level.

Like any good research, the buckling work kicked-off between Keystone, Johns Hopkins University, and Northeastern University with a literature review. The primary finding of that literature review was that there was a dearth of previous research in the area of compressive buckling of multi-layer shell structures with or without periodic fasteners. The multi-layer fatigue details are similarly unique and there is no such detail codified in fatigue analysis standards. The work contributed significantly to both areas (buckling and fatigue) of research. Furthermore, the results of the investigations appear to point in a positive direction – that properly designed and manufactured multi-layer shell structures may achieve buckling and fatigue capacities consistent with traditional single-layer (monolithic) shell structures of similar total wall thicknesses.

A tangible result of this study for the offshore wind industry is a quantified LCOE savings when utilizing Keystone's spiral-welded towers and/or monopiles for developments. Along the way, numerous parties were engaged directly, or indirectly, in this research and gained less tangible benefits. Some of the parties most involved in this research include: GE Vernova, several researchers from Johns Hopkins University, several researchers from Northeastern University, Edison Welding Institute, BVG-Associates, Sike adhesive supplier, Nordfab HVAC supplier, Orsted, Equinor, GustoMSC, Pema, SurfacePrep, DTA, and Vestas. There were also countless informal conversations at trade conventions and business planning that spun-off from those conversations.

Lastly, Keystone obviously benefitted greatly. Some of the lessons learned are already being implemented into the design of Keystone's second spiral-mill, which is currently under development. Keystone formed new partnerships. A new understanding of the multi-wrap concept capability is vital, as well as realizing the limitations to its applicability. Limitations to the value of the multi-wrap concept also forced a better understanding of the non-coil supply chain. The welding research can be immediately leveraged to bring immediate value to Keystone, even for onshore factories. The numerous benefits Keystone gained from

the research is captured well in Figure 77 to easily demonstrate the commercial and technical readiness improvements made by Keystone throughout this project.

Figure 77. TRL & CRL Before (Top) and After (Right) this Project